

https://dspace.org/

Epigenetic regulation profile in uninfected and TB-HIV infected Patients

Mamabolo, Katlego

2025
University of the Witwatersrand, Johannesburg
https://hdl.handle.net/10539/50044
Mamabolo, Katlego . (2025). Epigenetic regulation profile in uninfected and TB-HIV infected Patients [Master's dissertation, University of the Witwatersrand, Johannesburg]. WIReDspace. https://hdl.handle.net/10539/50044

Downloaded from a DSpace repository. https://dspace.org/

Epigenetic regulation profile in uninfected and TB-HIV infected Patients.



WITS
UNIVERSITY

Katlego Mamabolo

A dissertation submitted to the Faculty of Health Sciences, University of the Witwatersrand, in the fulfilment of the requirements for the degree

Of

Master of Science in

Medicine

Johannesburg, 2025

Declarations

I, Katlego Mamabolo, hereby declare that this dissertation is my own original work, all sources of information or data used in this dissertation have been properly acknowledged and cited in accordance with the University of Witwatersrand standards and guidelines.

The dissertation has not been submitted at the University of Witwatersrand or any other University before. It is now being submitted for the degree of Masters of Science in Medicine at the University of Witwatersrand, Johannesburg.



Signature: …_____……

Date: …**25 September 2025**……..

Dedication

“To all Humanity’’

—Research for the betterment of society

Peer- Reviewed Conferences

1. **University of the Witwatersrand Biennial Health Sciences Research Day and Postgraduate Expo**, 22 September 2022, Wits University, Johannesburg, South Africa. *Poster: Katlego Mamabolo, Musa Marimani. Determining the level of DNA methylation in HIV-1 positive patients and healthy controls* (*MCB-P-06*)

2. **University of the Witwatersrand, Department Of Physiology, Integrated Molecular**

   Physiology Research Initiative (IMPRI), 22 June 2023**.** *Oral presentation:*

   Katlego Mamabolo. The Epigenetic regulation profile in uninfected and TB-HIV co-infected patients

List of Publications

1. **Katlego Mamabolo**, Reubina Wadee, Yvonne Perner, Pumza Magangane, Saneliwe Thinasonke Duze, Musa Marimani (2024). Differential Epigenetic Regulation in Uninfected and Tuberculosis–Human Immunodeficiency Virus Co-Infected Patients. *Microorganisms journal* 12 (**5**): 1001. https://doi.org/10.3390/microorganisms12051001

Abstract

INTRODUCTION:

Devastatingly, both public and private health institutions in sub-Saharan Africa are burdened by the high prevalence of TB-HIV co-infections. Epigenetics involves changes in gene activity, occurring independently of alterations in the underlying DNA sequence. Epigenetic modifications, such as aberrant methylation, acetylation, phosphorylation, and ribosylation, are introduced by HIV and *Mtb* to evade host immunity, leading to microbial infection.

This study aimed to detect the degree of epigenetic modifications in the TB-HIV co-infected cohort and the uninfected control subjects.

METHOD:

We obtained t issue samples from the lymph nodes of 45 TB-HIV co-infected patients and 45 TB-HIV uninfected individuals which were fixed in formalin and embedded in paraffin between 2017 and 2019 from the Charlotte Maxeke Johannesburg Academic Hospital, Republic of South Africa. TB-HIV co-infection was confirmed using conventional Polymerase chain reaction (PCR) targeting the *Mtb rpoB* and HIV *gag-pol* genes. To unravel the genetic identity of the HIV and *Mtb* strains in the TB-HIV cohort. Sanger sequencing and phylogenetic analysis were performed. Reverse Transcription quantitative PCR (RT-qPCR) was utilized to compare the degree of DNA methylation, histone acetylation, and histone methylation by analyzing the expression of corresponding target genes: *DNA Methyltransferase 1(DNMT1), histone acetylation (HAT), Class II transactivator (CIITA), histone lysine methyl transferase (KMT),* and *SET domain bifurcated histone lysine methyltransferase2* (*SETDB2).* Subsequently, the H3 modification assay was used to detect and quantify patterns of histone methylation, acetylation and phosphorylation. Finally, the associated between age, gender and race in the observed epigenetic expression as well as H3 modification were assessed using statistical based methods.

RESULTS:

TB-HIV co-infection was confirmed among the TB-HIV tissue samples through the successful amplification and sequencing of the *Mtb rpoB* and HIV *gag-pol* genes, respectively. HIV-1 sequencing predominantly aligned with the intersubtype 07 BC strain,

while the *Mtb* sequencing showed high identity with an *Mtb* strain with an accession number CP085590.1, revealing distinct phylogenetic clustering. Gene expression profiling via RT-qPCR demonstrated significant upregulation of the *DNMT1*, *HAT*, *CIITA*, *KMT*, and *SETDB2* in the TB-HIV co-infected group. Histone modification analysis revealed widespread chromatin remodelling, including increased methylation (H3K4me1, H3K27me3), acetylation (H3K9ac, H3K27ac), and phosphorylation (H3S10ph, H3S28ph). Race and gender specific differences in gene expression and histone modification were observed, with race exerting a stronger influence on the expression of the *CIITA* and *SETDB2* genes in the TB-HIV group.

CONCLUSION*:*

The disparities in the expression profiles of our candidate genes between the TB-HIV cohort and the non-TB-HIV cohort highlight the important role played by various TB and HIV strains in regulating the host gene expression landscape. Importantly, our findings reveal the potential of epigenetic modifications to be used as valuable biological markers that may, in the long run be applied for diagnostic procedures and for the synthesis of new and effective vaccines and therapeutics.

Acknowledgements

It gives me great pleasure to offer my sincere gratitude to everyone who supported me throughout my research process and helped me to successfully complete this dissertation. I want to start by expressing my gratitude to my family for their unwavering love and support along this journey. Their support, compassion, and understanding have been the pillars that have helped me persevere throughout the hard times. They have always believed in me, and I owe them for being a constant source of motivation. I want to sincerely thank my friends for being by my side throughout this journey. Their encouragement and direction have been crucial in helping me to maintain my positive attitude and focus. I also want to express my deepest gratitude to my supervisors and the research committee, their insights and expertise facilitated the process of ensuring my research is of a good quality, worthy of contributing to knowledge in my field.

It also a great pleasure to acknowledge funding received from the National Research Foundation (NRF) for their Thuthuka research grant and the Carnegie DTA research grant, which assisted in the purchase of lab equipment and reagents and ensuring that the research project is completed successfully

Finally, I would like to express my appreciation to all those who have contributed to this project in different ways. Your assistance, encouragement, and feedback have been invaluable, and I am truly grateful for your support.

Above all, I thank God who is the source of my strength, wisdom and competence.

—glory be to God—

Table of Contents

Declarations ii
Dedication iii
Peer- Reviewed Conferences iv
List of Publications v
Abstract vi
Acknowledgements viii
Table of Contents ix
List of Abbreviations xv
Chapter 1: Introduction and Literature Review 2
Part A: The Human Immunodeficiency Virus 2
1.1 The Origin of the Human Immunodeficiency Virus 2
1.2 HIV-1 and HIV-2 Diversity 2
1.3 Morphology and Biology of HIV-1 3
1.4 Molecular Biology of HIV-1 5
1.5 HIV-1 Mode of Transmission 6
1.6 HIV Pathogenesis and Replication Cycle 7
1.7. Phases of HIV-1 Infection 9
1.8 HIV-1 Diagnosis 10
1.9. HIV-1 Treatment Regimen 12
1.10. HIV-1 Curative Strategies 14
Part B: Review of Mycobacterium tuberculosis 15
1.11 The Origin of Mycobacterium tuberculosis 15
1.12 The Morphology of *Mtb* 15
1.13 Mechanisms of TB Transmission 16
1.14 The Target Cells and Host Environment of *Mtb* 17
1.15 *Mtb* Replication Process 17
1.16 Epidemiology of *Mtb* 18
1.17 Diagnosis of *Mtb* 18
1.18 Active and Latent TB 19
1.19 Mechanism behind LTBI 19
1.20 Biomarkers that Differentiate Active and Latent TB 19
1.21 TB Prevention and Vaccination 20
1.22 Treatment of TB 20

Part C: Review of TB-HIV Co-Infection 22
1.23 HIV, TB Co-Infection, and Immunity 22
1.24 Genetic Susceptibility to TB and HIV Infection 22
1.25 Host Antiviral Genes 23
1.26 Treatment of HIV, TB Co-Infected Patients 24
Part D: Review of Epigenetic Mechanisms in the Context of TB-HIV Co-Infection 25
1.27 The Concept of Epigenetics 25
1.28 Histone Modifications 26
1.29 DNA Methylation 28
1.30 Epigenetic Regulation and Resistance to TB in HIV Patients 31
1.31 The Effect of Epigenetic Modification in TB-HIV Co-infection and Immune Response 31
1.32 The Roles of Epigenetic Mediators 32
Chapter 2: Materials and Methods 34
2.1 Ethics Consideration 34
2.2 Sample Size and Collection 35
2.3 Total RNA Extraction from the Infected and the Control Human Tissues 37
2.4 Synthesis of Complementary DNA 38
2.5 Amplification of cDNA by PCR, DNA Sequencing and Phylogenetic Analysis 38
2.6 Evaluation of target gene expression level by RT-PCR 41
2.7 Protein Isolation and Analysis for the TB-HIV co-infected and control group 43
2.8 Determination of Protein Levels in TB-HIV co-infected and control groups using the Histone H3 Modification Multiplex Assay 43
2.9 Statistical Analysis 44
Chapter 3: Results 46
3.1. Demographic characteristics of the tissue samples from the TB-HIV co-infected and the control cohort 46
3.2. Conventional PCR to confirm TB-HIV co-infection 47
3.3 Sequence and phylogenetic analysis 48
3.3.1 HIV-1 sequences 48
3.3.2 *Mtb* sequences 52
3.4. RT-PCR to detect the expression of genes associated with DNA methylation, histone acetylation, and histone methylation. 54
3.5 Association of gene expression with demographics 57
3.5.1 Correlation of age and gene expression in the TB-HIV co-infected cohort 57
3.5.2 Association of gene expression with gender in the TB-HIV co-infected cohort 58
3.5.3 Association of gene expression with race 59
3.6 H3 multiplex assay to detect epigenetic modification patterns 60
3.7 Correlation of protein markers with demographics 61

3.7.1 Association of age with protein markers in the TB-HIV co-infected group 61
Chapter 4: Discussion 67
4.1. Conventional PCR, DNA Sequencing, and Phylogenetic Analysis for HIV and TB 67
4.2 Epigenetic Modifications in the TB-HIV Co-Infected Tissue Samples 68
4.3 Histone modification patterns 70
Chapter 5: Conclusion 75

List of Figures

Figure 1.1 The Structure of HIV-1. A schematic representation of the morphology of the HIV virion and associated proteins. 3
Figure 1.2. HIV-1 Transcripts. An overview of the structure and organization of the HIV-1 genome 4
Figure 1.3. The Replication Cycle of HIV-1. 9
Figure 1.4. An Illustration Depicting the Transmission of *Mtb*..... 16
Figure 1.5. A Schematic Illustration Demonstrating the Concept of Epigenetic of Epigenetic Modification. 27
Figure 1.6. DNA Methyltransferases. 29
Figure 2.1. Experimental Design to Interrogate Epigenetic Mechanisms in TB-HIV and Non-infected Individuals. 34
Figure 3.1: Amplification of HIV *gag-pol* gene by conventional PCR 47
Figure 3.2: Amplification of *Mtb rpoB* gene by conventional PCR 48
Figure 3.3 Multiple sequence alignment of the 10 HIV-1 sequences from this study alongside reference sequences for HIV-1 subtypes A, B, and C obtained from the LANL HIV Sequence Database HIV Sequence Database 50
Figure 3.4. Multiple sequence alignment of the 10 HIV-1 sequences from this study alongside reference sequences for HIV-1 subtypes A, B, and C obtained from the LANL HIV Sequence Database, as well as 10 HIV-1 sequences from the NCBI database 50
Figure 3.5. Maximum likelihood tree constructed using RaxmlGUI 2.0 with a bootstrapping stringency of 1000. 51
Figure 3.6: Multiple sequence alignment of 10 *Mtb* sequences from this study alongside nine *Mtb* reference sequences from the NCBI database 53
Figure 3.7. Maximum likelihood tree constructed using RaxmlGUI 2.0 with a bootstrapping stringency of 1000. 54
Figures 3.8. *DNMT1* and *HAT* Gene Expression in the TB-HIV HIV co-infected cohort relative to the Control group. 55
Figures 3.9. *CIITA* and *KMT* gene Expression in the TB-HIV co-infected cohort relative to the Control group. 56
Figures 3.10. *SETDB2* gene Expression in the TB-HIV co-infected cohort relative to the Control group. 57

Figure 3.11. Association of age with the gene expression of epigenetic markers, *DNMT*, *HAT*, *KMT*, *CIITA*, and *SETDB2* in the TB-HIV co-infected cohort. 58
Figure 3.12. The association between gender and expression levels of five genes based on the Wilcoxon rank-sum test results in the TB-HIV co-infected cohort. 59
Figure 3.13. Target Protein Production in TB-HIV co-infected and Control groups. 61
Figure 3.14. Image showing the association of age, methylation, acetylation, and phosphorylation markers in the TB-HIV co-infected cohort. 62

List of Tables

Table 1.1. Overview of HIV-1 genes, their corresponding proteins, and functional roles. Retrieved from Transfus Med Hemother, (2016), p. 204. 5
Table 1.2. Classes of anti-HIV drugs approved for clinical use. 13
Table 1.3. Classes of anti-TB drugs. 21
Table 1.4. Summarized description of the histone modifications at different amino acid residues within the histone tail. 26
Table 2.1. The primer sequences of HIV *gag-pol* and *Mtb rpoB* gene were used in cDNA amplification by conventional PCR 40
Table 2.2. Sequences of primers used in RT-qPCR to amplify target candidate genes and to determine gene expression. 41
Table 3.1: Demographic characteristics for the TB-HIV and the control group 46
Table 3.2. Summary of HIV-1 BLAST results for ten isolates queried against the LANL HIV Sequence Database 49
Table 3.3. Summary of *Mtb* BLAST results for ten isolates queried. 52
Table 3.4. Association of age with the gene expression of epigenetic markers, DNMT, HAT, KMT, CIITA, and SETDB2 in the TB-HIV co-infected cohort. 58
Table 3.5. Association of race with gene expressions in control and TB-HIV co-infected groups. 59
Table 3.6. Spearman's correlation coefficients for the association of age with methylation, acetylation, and phosphorylation markers in the TB-HIV co-infected cohort 63
Table 3.7. Statistical associations of histone modification markers with gender and race in the TB-HIV co-infected and control groups. 66

List of Abbreviations

Abbreviations	Definitions
AARMS	Academic Affairs and Research Management System
AIDS	Acquired Immunodeficiency Syndrome
ART	Antiretroviral Therapy
ATP 10A	Adenosine Triphosphate 10A
APOBEC 3G	Apolipoprotein B mRNA- Editing Enzyme, Catalytic Polypeptide-like 3G
BCG	Bacillus Calmette-Guérin
HAT CBP	Histone Acetyl Transferase CBP
CCR5	C-C Chemokine Receptor Type 5
CD38	Cluster of Differentiation 38
CD4	Cluster of Differentiation 4
CD8	Cluster of Differentiation 8
CIITA	Class II Transactivator
COVID	Coronavirus Disease
CRF	Circulating Recombinant Forms
CXC4	C-X-C Chemokine Receptor 4
CXCL10	C-X-C-L Chemokine Receptor 10
CXCR4	C-X-C-R Chemokine Receptor 4
DNA	Deoxyribonucleic Acid
DNMT	DNA Methyltransferase
DNMT1	DNA Methyltransferase 1
ELISA	Enzyme Linked Immunosorbent Assay

FFPE	Formalin Fixed Paraffin Embedded
FOXP3	Foxhead Box Protein 3
GAPDH	Glyceraldehyde 3-Phosphate Hydrogenase
HAT GCNS	Histone Acetyltransferase GCNS
HAT	Histone Acetyltransferase
HDAC	Histone Deacetyltransferase
HIV	Human Immunodeficieny Virus
HLA	Human Leukocyte Antigen
HMT	Histone Methyltransferase Enzyme
IGRA	Interferon Gamma Release Assay
KMT	Histone Lysine Methyltransferase
LPA	Line Probe Assays
LTBI	Latent Tuberculosis Infection
MDR	Multidrug- Resistant
HAT MOF	Histone Acetyl Transferase MOF
MTB	Mycobacterium Tuberculosis
MTBC	Mycobacterium Tuberculosis Complex
NCBI	National Centre for Biotechnology Information
NHLS	National Health Laboratory Service
NNRTI	Non-nucleoside Reverse Transcriptase Inhibitor
NRTI	Nucleoside/Nucleotide Reverse Transcriptase Inhibitor
NSP	South Africa's National Strategic Plan
P17	Matrix Protein 17

P24	Matrix Protein 24
P3	Matrix Protein 3
HAT PCAF	Histone Acetyl Transferase PCAF
PCR	Polymerase Chain Reaction
RIF	Rifampin
RNA	Ribonucleic Acid
SAM	S-Adenosylmethianine
SETDB2	Histone Lysine Methyltransferase 2
SIV	Simian Immunodeficiency Virus
TB	Tuberculosis
TET1	Ten–Eleven Translocation Methylcytosine Dioxygenase 1
TLR6	Toll-like Receptor 6
TRIM 5a	Tripartite Motif-Containing 5 Alpha Protein
WHO	World Health Organization
XDR	Extensively Drug-Resistant TB

Chapter 1: Introduction and Literature Review

Part A: The Human Immunodeficiency Virus

1.1 The Origin of the Human Immunodeficiency Virus

The human immunodeficiency virus (HIV) is a retrovirus that attacks the cells of the immune system, predominantly the CD4+ cells that participate in both the innate and acquired immune defense mechanisms (1). Over time, this culminates in full-blown acquired immunodeficiency syndrome (AIDS), which is characterized by profound immunosuppression, development of secondary neoplasms, emergence of opportunistic infections, and manifestation of neurological conditions (1). Several studies have suggested that HIV originated from the simian immunodeficiency virus (SIV), which targets non-human primates, including species such as monkeys and chimpanzees (2). SIV is a blood-borne pathogen that infects mucous epithelial cells in non-human primates; therefore, it is speculated that the virus may have crossed the species barrier several times in sufficient quantities and established infection in humans (2). This may have been facilitated by bites and scratches from non-human primates during hunting. Two strains of SIV, namely SIVsm from sooty mangabeys and SIVcpz from chimpanzees, mutated to result in two types of HIV strains, namely HIV-2 and HIV-1, respectively, upon crossing the species barrier (2).

1.2 HIV-1 and HIV-2 Diversity

HIV-1 is the most virulent type of HIV strain compared to HIV-2, and it is responsible for the global AIDS pandemic due to its highly transmissible nature (3). Phylogenetic studies have classified HIV-1 into four separate groups based on variations in the envelope gene: M group (major group), O group (outlier), P group (newest group), and N group (non-M, O, or new) (4). Additionally, within Group M of HIV-1 isolates, genetic recombination has led to the emergence of variants and subtypes, intra-subtypes, and the circulating recombinant forms (CRFs) that are responsible for the global pandemic and are classified as A-D, F-H, J, and K (4). CRF81 cpx and CRF99 BF1 are examples of CRFs that were identified in Central Western Brazil (5). Further differentiation of the HIV-1 isolates is based on their unique interactions with the host cell's core-receptors, CCR5 and CXCR4 (1). The HIV-1 isolates that use CCR5 are referred to as the R5 strains, whereas the ones that use the CXCR4 are referred to as the X4 strains, and some strains are dual-tropic (R5X4). The R5 strain normally

infects cells of the monocyte lineage and is described as being M-tropic, while X4 strains infect cells of the T-lymphocyte and are referred to as being T-tropic (1). Figure 1.1. Presents the morphological details of HIV-1. HIV-2 is classified into eight distinct groups (A-H), and only groups A and B are known as sources of epidemics (2). The C-H groups are closely related to the SIVsm strains identified in the sooty mangabey species of monkeys.

1.3 Morphology and Biology of HIV-1

HIV is a spherically shaped virus with a complex morphology that is comprised of an electron-dense core, which is cone-shaped and contains two copies of the RNA strands (Figure 1.1). HIV has the following components: the envelope, capsid, genome, reverse transcriptase, integrase, and protease, which collectively contribute to the structure and function of the virus. The HIV envelope is a lipid bilayer, formed from the host cell membrane during budding. It comprises the viral glycoproteins, including gp120 and gp41, the components that facilitate viral attachment and entry.

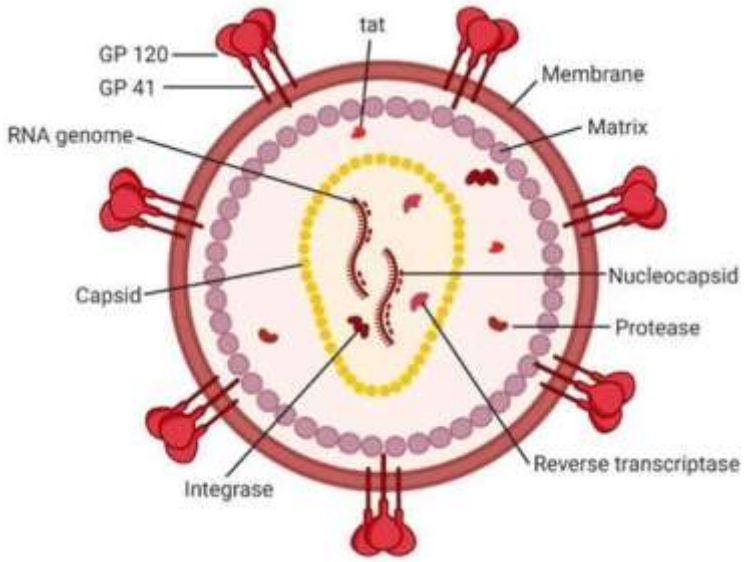


FIGURE 1.1 THE STRUCTURE OF HIV-1. A SCHEMATIC REPRESENTATION OF THE MORPHOLOGY OF THE HIV VIRION AND ASSOCIATED PROTEINS.

These viral proteins: protease, reverse transcriptase, and integrase are crucial for viral infection, survival, and replication. The diagram has been adapted from Rossi et al., 2021 (6).

Underneath the envelope is the capsid, which is a viral structure composed of repeating units of protein p24. It contains the viral genomic RNA and its associated proteins. The HIV genome is formed by the single-stranded, positive-sense RNA genome, which has three overlapping reading frames that code for the gag, pol, env, vif, vpr, tat, rev, vpu, and nef proteins that give rise to the HIV architecture. Furthermore, the virus has essential HIV enzymes that play a crucial role in the replication cycle, and they include:

- The reverse transcriptase, an enzyme essential in the virus life cycle and responsible for the conversion of RNA genome to DNA upon invading the host cell.
- Integrase aids in integrating the HIV DNA into the viral host genome.
- Protease enzyme is implicated in the processing of immature precursor proteins into mature functional proteins that facilitate assembly of new viral particles.

The complete and matured structure of the virion is crucial for pathogenesis and HIV virulence (7). The complex structure of the virus plays a role in its life cycle and interaction with the immune system. The assembly and maturation of the virion involve a series of complex steps that contribute to its pathogenicity. Upon merging of the virus with the host cell's membrane, the viral RNA genome and its enzymes are discharged into the host cell's cytoplasm. This leads to conversion of the viral RNA to double-stranded complementary DNA or proviral DNA, which is subsequently integrated into the host genome, catalyzed by the integrase enzyme (1).

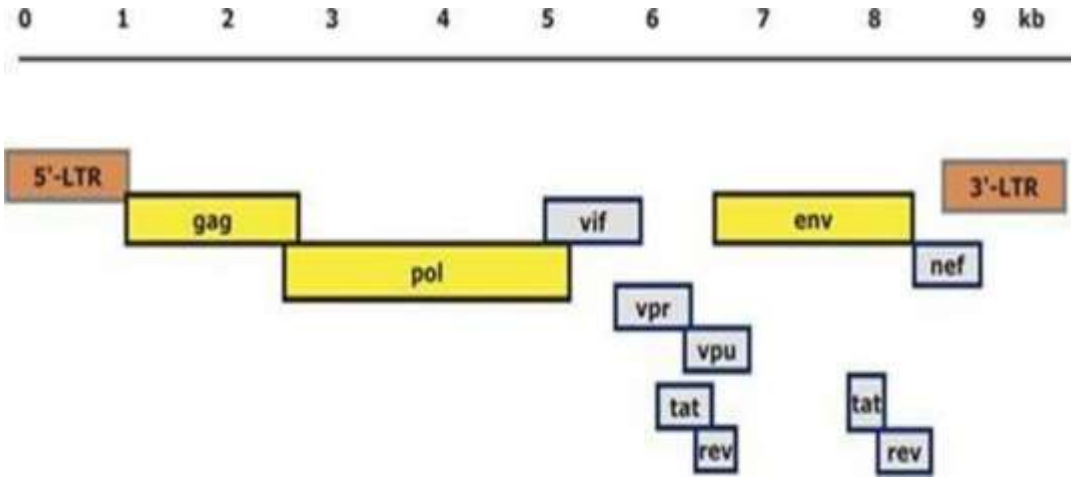


FIGURE 1.2. HIV-1 TRANSCRIPTS. AN OVERVIEW OF THE STRUCTURE AND ORGANIZATION OF THE HIV-1 GENOME.

The illustration shows the reading frames of the gene coding for structural and regulatory proteins: LTR= Long terminal repeat; gag= group-specific antigen; pol= polymerase; env=envelope. The diagram has been adapted from Transfus Med Hemother (2016) (8).

1.4 Molecular Biology of HIV-1

Several key genes play a crucial role in shaping the virus into its unique structure (Table 1.1); the *gag*, and *env* genes encode the viral structural proteins, which give the HIV virion a unique structure. These proteins are first synthesized as immature long proteins that are cleaved by the viral protease enzyme into mature and functional protein molecules (5).

TABLE 1.1. OVERVIEW OF HIV-1 GENES, THEIR CORRESPONDING PROTEINS, AND FUNCTIONAL ROLES. RETRIEVED FROM TRANSFUS MED HEMOTHER, (2016), P. 204.

Gene	Protein	Function
gag	**Capsid Protein (CA)**	Forms the viral capsid, a protein shell that encases the viral RNA.
	Matrix Protein (MA)	Forms the inner membrane layer, providing structural integrity and mediating interactions between the viral envelope and core
	Nucleocapsid Protein (NC)	Packages the viral RNA genome into the nucleocapsid, facilitating viral particle assembly
pol	**Protease (PR)**	Catalyzes proteolytic cleavage of precursor proteins Gag (Pr55) and Gag-Pol (Pr160Gag-Pol), releasing structural proteins and viral enzymes
	Reverse Transcriptase (RT)	Converts HIV RNA into proviral DNA, essential for viral replication and integration into the host genome.
	Integrase (IN)	Integrates proviral DNA into the host cell genome, establishing productive infection
env	**Surface Glycoprotein (SU)**	Facilitates viral attachment to the target cell by binding to specific cell surface receptors.
	Transmembrane Protein (TM)	Anchors gp120 and mediates fusion of the viral envelope with the host cell membrane, enabling viral entry.
vpu	**Virus Protein Unique**	Modulates efficient release of virions from the infected host cell
tat	**Trans Activator Protein**	Activates transcription of viral genes.
rev	**RNA Splicing Regulator**	Regulates transportation of non-spliced and partially spliced viral mRNA.
nef	**Negative Regulating Factor**	Enhances viral infectivity and downregulates CD4 on target cells
vpr	**Virus Protein R**	Facilitates virus infectivity

1.5 HIV-1 Mode of Transmission

HIV is only transmitted through specific activities, and the viral particle solely resides in certain bodily fluids. Consequently, all individuals need to be aware not only for protection but also to reduce stigmas associated with people living with HIV (6). The virus is found in the bodily fluids of infected people, and these include blood, semen, vaginal fluids, rectal fluids, and breast milk of an HIV-infected mother (7). The virus can also be transmitted vertically, from mother to child during gestation or delivery. Previous studies suggest that HIV infection is associated with risky behaviours, which are defined according to the literature (9) as involving the following:

(a) The sharing of syringes and needles among intravenous drug users (10)

(b) Drug addiction (11,12),

(c) Multiple sexual partners (8–11),

(d) Unprotected sex (8–12),

(e) Casual sex (10,11), and

(f) Practicing sex under the influence of alcohol (9–11).

These factors encourage the spread of resistant strains and promote the occurrence of superinfection even while on antiretroviral therapy (ART) (13). Additionally, individuals with haemophilia face an increased risk of contracting HIV infection through exposure to contaminated blood products or donated blood that contains HIV (13). Superinfection has also been observed in high-risk individuals exposed through sexual practices or intravenous drug use (14,15). Studies conducted in various African countries have identified risky behaviour associated with HIV infection (16). The risky behaviours were defined according to literature as involving sexual intercourse with two or more sexual partners or inconsistent use of a condom or no condom use; moreover, previous studies indicate that a change in the risky behaviours can lead to a reduction in HIV infection by approximately 20% (16). For the virus to successfully infect an individual, an HIV-containing bodily fluid has to come in contact with the mucous membrane, i.e., the vagina, mouth, rectum, damaged tissue, or be directly injected into the blood circulation (17). Therefore, apart from these, it is rare that the virus can be transmitted between individuals.

1.6 HIV Pathogenesis and Replication Cycle

HIV has tropism for tissues of the immune system as well as the central nervous system. However, for the virus to establish infection, its surface glycoproteins—gp120 and gp41 must first interact with the host receptors and core-receptor of the target cells (1). The HIV gp120 interacts with the CD4 receptor and the gp41 interacts with the CCR5 or CXC4 core receptor. Nevertheless, polymorphism in the CCR5 core-receptor makes some individuals resistant to HIV infection (18). HIV-1 mainly attacks and destroys the lymphocytes, specifically the CD4+ T cells that play a crucial role in both the innate and adaptive immune responses (1). The virus hijacks the cells and uses its biosynthetic machinery to replicate and produce more viral copies that spread throughout the body (Figure 1.3). The life cycle of the virus includes the following stages (1):

(a) Attachment

HIV has a specific affinity for cells that express the CD4 molecule, which includes the T helper cells, macrophages, and microglial cells. The virus gp120 and gp160 proteins specifically bind to the CD4 cell surface receptor. This binding process is mediated through the interaction between gp41/gp160 and the core-receptors, primarily CCR5 or CXCR4.

(b) Fusion and entry

The HIV envelope fuses with the CD4+ cell membrane, thus allowing the virus to enter the host cell. During entry, HIV interacts with both the CD4 receptor and a core-receptor, either CCR5 or CXCR4 core-receptor. This molecular interaction stabilises the binding of the virus and alters the shape of the gp41, facilitating fusion with the cell membrane and entry into the host cell cytoplasm (19).

(c) Reverse transcription

HIV and other retroviruses have the capacity to convert their genomic RNA to cDNA after invading the cell. This mechanism is mediated by the viral reverse transcriptase (RT) enzyme, which catalyzes the conversion of the single-stranded RNA into a double-stranded cDNA referred to as the provirus. This is then followed by the degradation of the RNA template through the action of the RNase H enzyme (19).

(d) Integration

Subsequent to the process of reverse transcription, the Vpr protein (20,21) facilitates the entry of HIV cDNA into the host cell nucleus as the pre-integration complex (PIC). Once inside the

nucleus, the viral integrase enzyme within the PIC facilitates the incorporation of the HIV DNA copy into the host chromosome. Once integrated, the provirus may remain latent for months or years or it may immediately be transcribed, resulting in the synthesis of viral proteins (1).

(e) Transcription

During transcription the integrated provirus serves as a template for the transcription of both viral messengers and genomic RNA catalyzed by the cellular Pol II polymerase. Proviral transcription is initiated by the viral promoter located in the U3 region of the 5' LTR. The cellular transcription factors such as NF-kB and NFAF facilitate viral gene expression. Tat protein mediates the process of transcription by binding on the R region of the 5'LTR referred to as the trans-acting response (TAR) element. The interaction of the Tat protein with TAR results in the synthesis of HIV transcripts and the generation of more than 25 different mRNAs by alternative splicing. The mRNAs fall into three size classes:

(1) Unspliced RNA(9kb) used as genomic RNA or to synthesize the Gag and Gag-pol precursors.

(2) Singly singled RNA (4kb) encoding Vif, Vpr, Vpu, and Env

(3) Fully spliced RNA (2 kb) expressing Tat, Rev, and Nef

(f) Translation and assembly

Fully spliced RNA produces the Tat, Rev, and Nef proteins, each of which plays various roles in the HIV life cycle. The synthesis of Tat and Rev facilitates the production of full-length unspliced mRNA that expresses the Gag and Gag-pol precursor, which is then processed to major structural and enzymatic proteins (22).

(g) Budding

During budding, the viral protease enzyme cleaves the Gag and Gag-Pol polyproteins to form functional proteins, resulting in new viral particles referred to as progeny virions, which are then released from the infected cells. This is also facilitated by the late domain located in the p6 part of the viral Gag protein as well as the Tsg101 protein (22).

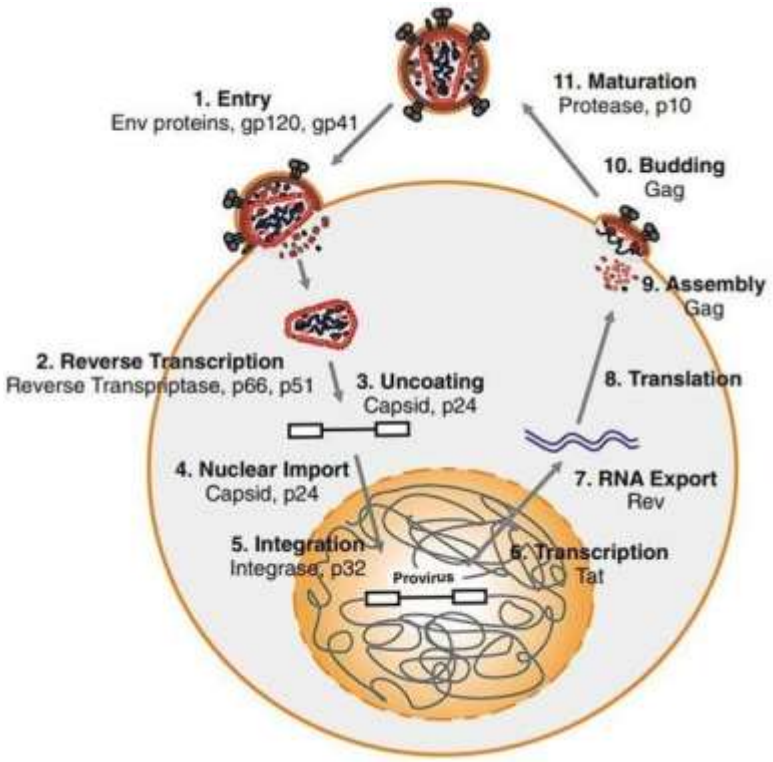


FIGURE 1.3. THE REPLICATION CYCLE OF HIV-1.

A schematic representation of the HIV-1 life cycle from entry into the host CD4+ cells to integration into the host genome (provirus). Subsequent viral replication cycles lead to the formation of immature virion progeny, which escape from the host cell as mature infectious virions. The diagram has been adapted from Kirchhoff (2013) (22).

1.7. Phases of HIV-1 Infection

Progressive viral replication cycles lead to the development of full-blown AIDS through a series of steps, a deleterious process that involves the destruction of immune cells (1). The virus typically enters the human body after invading mucosal surfaces, followed by entry into the host cells to initiate acute infection. In the acute phase of the infectious process, the integrity of the gut mucosal immunity is damaged, and there is the manifestation of cytopathic effects resulting in a compromised gut mucosal barrier (1). This causes unhindered entry of microbial products and dysbiosis (17). The virus thrives within lymphoid tissues and there is activation of the local innate and adaptive immune responses against the virus. The persisting infection and sustained activation of immune cells result in damage to the lymphoid tissue structure by inducing the formation of scar tissue, which blocks essential homeostatic products from reaching these cells. Thus, this results in the manifestation of two hazardous events: loss of immune cells.

Within 3 to 6 weeks of the infection, the body exhibits a series of symptoms referred to as acute HIV syndrome; they include fever, loss of weight, sore throat, and fatigue, among others. These clinical manifestations occur following the significant spread of the virus and an increase in viremia, which is ultimately contained after host immune intervention (1). Over time, the infectious process progresses to a chronic phase that is marked by clinical latency. However, early in infection, the HIV genome becomes latent within various types of cells and tissues, and more importantly, viral persistence is suggested to be the main reason for inadequate viral eradication (17).

In the chronic HIV phase, there is no manifestation of disease symptoms, though there is still a presence of the virus within the CD4+ cells. The progressive destruction of these cells and other critical immune cells over the years leads to exceptionally low CD4+ cell counts in the blood circulation (23). As such, this renders the immune system compromised, resulting in AIDS phase that is marked by a significantly increased viral load in the circulation, opportunistic infections such as salmonella infection, candidiasis, and tuberculosis, various AIDS-defining cancers such Kaposi sarcoma and cervical cancer, and many other life-threatening illnesses (1,18,19).

1.8 HIV-1 Diagnosis

In the year 2018, multiple countries worldwide were aware of their HIV status, and fortunately, a significant fraction of the infected individuals were on HIV treatment and showing improved viral load suppression (20). Nonetheless, despite all the promising progress, there are still millions of people living with HIV who remain unaware of their status (21), and a larger portion of these individuals contribute significantly to new cases. This is supported by evidence that suggests that roughly 60% to 80% of new cases were caused by people who were undiagnosed and unaware of their status in studies conducted in the USA and the UK (22,23).

In the context of South Africa, the dynamics of undiagnosed cases have demonstrated variability over time, specifically, the prevalence of undiagnosed cases decreased from 29.3% in 2005 to 15.8% in 2011, increased to 18.9% in 2016; however, in 2017, this decreased to 14.0% (23,24), indicating a fluctuation of undiagnosed cases over time within the community. South Africa's National Strategic Plan (NSP) has initiated an HIV testing programme that aims to encourage all people to know their HIV status (24). This is important

for reducing the number of new HIV and TB cases from 270 000 HIV cases per year to less than 100 000 cases and from 450 000 TB cases per year to less than 315 000 cases (24,25). In most clinical settings, HIV infection is routinely tested using the following techniques:

(a) ELISA is the gold standard procedure which detects the secretion of anti-HIV antibodies.

(b) Western blot is used to survey and validate the presence of viral proteins

(c) Nucleic acid-based techniques, such as reverse transcription quantitative polymerase chain reaction (RT-qPCR), is also used to detect the presence of HIV RNA or DNA molecules of these diagnostic techniques, ELISA is the most preferred test due to its high sensitivity and specificity (25).

The ELISA test detects the presence of antibodies specific for HIV. The procedure involves coating the plate with HIV antigens from the patient's serum. Thereafter, the antibody-captured HIV antigens are detected by a secondary antibody linked to an enzyme, which produces a visible colour change indicating the presence of HIV antibodies (151). Additionally, the P24 test detects the presence of the HIV antigen P24 protein in the blood. The presence of this protein in the serum is one of the first markers of HIV infection. The test involves utilizing antibodies specific for the P24 protein coated on a solid plate. The captured P24 protein is detected using a secondary antibody linked to an enzyme and emits a measurable signal (150).

Methods such as RT-qPCR and western blot are generally used as confirmatory tests to validate ELISA results. In addition to the routine HIV testing service, HIV self-testing is a novel approach that was recommended by the World Health Organization (WHO) to supplement the existing HIV screening tools (26). HIV self-testing is still in its infancy regarding implementation; however, it has been proven to be effective, safe, confidential, and increases the rate of human participation and HIV testing. Additionally, this strategy does not compromise condom use and/or enhance social harm (27). In the self-testing procedure, the individual withdraws their own specimen, conducts the assay, and subsequently interprets their own results (26–28). Relative to the standard approach of HIV testing, self-testing was observed to have an advantage of overcoming the fear of social stigma and social rejection as it is performed privately (29,30). During barriers of quarantine, social distancing, and other barriers put in place to prevent the spread of the new Coronavirus disease of 2019 (COVID-

19); home-based HIV self-testing allowed individuals to know their status even during the pandemic (31,32).

These HIV self-testing kits have already been made available for purchase in various countries like the United States of America, United Kingdom, France, South Africa and Kenya. Encouragingly, these tests have recently been made available in countries like Zimbabwe, Malawi and Zambia (39). This is crucially important for reducing global HIV cases, particularly in high endemic locations like sub-Saharan Africa, which also has an exceptionally high tuberculosis (TB) burden. Therefore, provision of self-testing kits and timely enrolment into the ART program is one of the key strategies required to enhance the lifespan of infected individuals as well as to decrease the HIV burden.

1.9. HIV-1 Treatment Regimen

Existing studies suggest that the average lifespan of people living with HIV is approximately 9-11 years, depending on HIV strain virulence and the host's immune competence (33). Nevertheless, the introduction of ART has significantly improved the life expectancy of people living with HIV, to the extent that they can live as long as HIV-negative individuals (41). ART refers to the lifelong use of a combination of three or more antiretroviral drugs for treating HIV infection. Even though there is increased access to ART globally with 28.7 million people globally who accessed ART at the end of December 2021 (21), the HIV burden remains substantial, and this can among other reasons be attributed to the fact that 28% of eligible patients are not yet on ART, while 35% of those on ART do not display efficient viral suppression. Additionally, the persistence of undiagnosed cases exacerbates the situation (23,24,34).

Previous studies have shown that poor adherence to antiretroviral agents and drug resistance are some of the reasons that viral replication and plasma viral load are unable to be suppressed to undetectable levels, thus preventing viral transmission (35,36). Specifically, ART drugs fall into five classes as described in Table 1.1. These are:

(a) Nucleoside Reverse Transcriptase Inhibitors (NRTI)

(b) Non-Nucleoside Reverse Transcriptase Inhibitors (NNRTI)

(c) Protease Inhibitors (P I)

(d) Integrase Strand-Transfer Inhibitors (INSTI), and

(e) Entry Inhibitors.

TABLE 1.2. CLASSES OF ANTI-HIV DRUGS APPROVED FOR CLINICAL USE (37).

Antiretroviral drug classes	Names	Mode of Action
(a) Nucleoside analog of HIV-reverse transcriptase inhibitors	Zidovudine; Stavudine; Lamivudine; emitricitabine.	Competes with natural deoxyribonucleotides for incorporation into the forming HIV DNA
(b) Nucleotide analog of HIV-reverse transcriptase inhibitors	Tenofovir, adefovir	Compete with natural deoxynucleotides for incorporation in the forming HIV DNA
(c) Non-nucleoside HIV-reverse transcriptase inhibitors	Efavirenz, nevirapine, delavirdine, etravirine, rilpivirine, doravirine	Hamper the function of HIV-reverse transcriptase by binding to its allosteric sites
(d) Integrase strand transfer inhibitors	Eviltegravir, dolutegravir, Raltegravir	Bind to the active site of HIV integrase, thereby inhibiting its function
(e) HIV-protease inhibitors	Saquinavir, indinavir, ritonavir, darunavir and nelfinavir	Mimic the substrate of HIV protease
(f) CXCR4 Antagonists	AMD3100	Compete either HIV or CXCL12 binding to CXCR4

The benefits of ART include prevention of mother-to-child transmission during or after pregnancy, during breastfeeding, reduction of HIV transmission to serodiscordant sexual partners, and prevention of viral infection after exposure (post-exposure prophylaxis) (38).

Even though ART has an immense positive impact on people living with HIV, previous studies have highlighted the challenges and limitations of ART, which include drug-induced and transmitted resistance, difficulty in adhering to the daily regimens, and drug-to-drug interactions, among other challenges (39).

1.10. HIV-1 Curative Strategies

Although HIV infection is well managed by ART, there is still ongoing research to ultimately produce a cure for HIV. In the long run, this will alleviate the need for lifelong ART application. Existing studies have divided HIV cure into functional cure and sterilizing cure. Progress has been achieved in developing the functional cure (40), which is defined as the control of viral load to undetectable levels or low levels without the use of antiretroviral Drugs, and this includes early treatment initiation, shock-and-kill, block-and-lock strategies. By contrast, the sterilizing cure is a treatment that allows complete eradication of the virus from its hidden latent reservoirs in infected individuals (40).

To date, the sterilizing cure remains an ambitious goal to be achieved. There have been several research attempts to develop cellular or gene therapy strategies to silence the HIV viral genes. This approach is known as the Kick and Kill regimen (41,42) and acts by triggering apoptotic death of the HIV-infected cells while simultaneously preventing new infections through cART. This therapeutic method attempts to create curative therapy. Additionally, the block and lock strategy involves the use of therapeutic agents to inhibit the transcription of HIV proviruses and induce their permanent silencing (43) while the shock and kill reactivates latent HIV and then eliminates it (44). The procedure of eliminating latent reservoirs has been proven to be possible from studies on both the Berlin and London patients who were cured from HIV infection through allogenic stem cell transplants with homogenous delta-CCR5 bone marrow, and chemotherapy, radiation, and immunotherapy (45,46).

Part B: Review of *Mycobacterium tuberculosis*

1.11 The Origin of *Mycobacterium tuberculosis*

The origin of *Mycobacterium tuberculosis* (*Mtb*) in terms of its relationship with humans is poorly understood; however, phylogenetic data suggest the bacterium diverged from a common ancestor 15000 years ago (47). Moreover, the tuberculosis disease (TB) is caused by more than one mycobacterial agent; a group of *Mycobacteriaceae tuberculosis* strains collectively referred to as the Mycobacterium Tuberculosis Complex (MTBC) is responsible for the disease. This group is comprised of: bovis (*M. bovis*) canettii (*M. canettii*), africanum (*M. africanum*), microti (*M. microti*), pinnipedii (*M. pinnipedii*), orygis (*M. orygis*), caprae (*M. caprae*), mungi (*M. mungi*), suricattae (*M. suricattae*), and the Dassie and Chimpanzee bacilli. Therefore, the strains that humans are most susceptible to are *M. africanum*, *M. canettii*, *M. bovis,* and *M. tuberculosis* (38,48). Previously, it was hypothesized that *Mtb* evolved from *M. bovis*, which typically infects cattle, and that it later infected humans through livestock domestication. This hypothesis was recently revised when sequences revealed the reverse to be the case (49).

1.12 The Morphology of *Mtb*

The tubercle bacillus, are thin, straight rod measuring about 0.4 × 3 μm (50). *Mtb* does not always maintain the typical rod shape, but has been observed to exhibit various morphological shapes including: the granular rod, coccid, round, filament, Y, V, ovoid, and club shapes. Typically, the V-forms of M. tuberculosis arise by any of the three different methods (51):

(a) Germination of adjacent coccoid elements

(b) Subpolar germination (budding) of rods

(c) Snapping post-fission movements

The various shapes could potentially play a role in virulence, defence against the immune system, and cell division (52).

1.13 Mechanisms of TB Transmission

Mtb is typically transmitted from one infected host to a new susceptible host through transportation by an infectious droplet. Typically, the droplet contains approximately 1-10 *Mtb* bacilli and the droplets are generally 1–5 μm in diameter (55). Three things are required in order for transmission to occur; namely, a source case, a susceptible new potential host, and a passage of the pathogen (Figure 1.4). The bacilli escape the respiratory tract of the infected individual, i.e., through sneezing and coughing, and subsequently survive the rigors of the outside environment, including ultraviolet light. The bacterium is ultimately inhaled into the lungs of the susceptible healthy host and evades immune recognition and defense to establish infection (53).

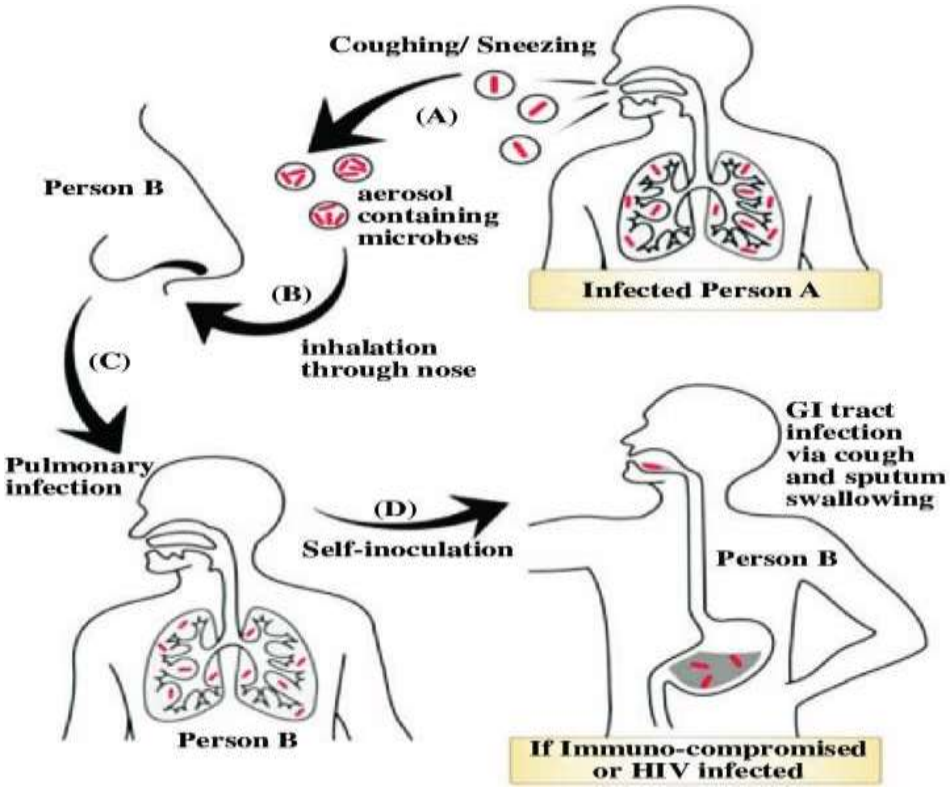


FIGURE 1.4. AN ILLUSTRATION DEPICTING THE TRANSMISSION OF *MTB*.

Bacterial infection is transmitted from an infected individual to a susceptible host through infectious droplets. These infectious droplets, which contain 1-10 TB bacilli, are typically transmitted when an infected person coughs or sneezes. The droplets are then inhaled by the susceptible host through the nasal or mouth cavity and subsequently infect the alveoli, resulting in pulmonary TB infection. Image has been adopted from Bhunia et al., 2015 (54).

1.14 The Target Cells and Host Environment of *Mtb*

During *Mtb* invasion, the bacilli target the macrophages. Upon inhalation, *Mtb* gets phagocytosed by alveolar macrophages in the lungs. These immune cells play a role in defence against the infection and can also be exploited as a reservoir for the replication of *Mtb*. Dendritic cells also phagocytose the *Mtb* and is involved the antigen presentation of the pathogen. The Alveoli comprised of type 1 and type II epithelial cells, in conjunction with alveolar macrophages, dendritic cells and neutrophils, serve as a dynamic environment for Mtb upon infection (55).

1.15 *Mtb* Replication Process

Intracellular invasion: Upon inhalation, *Mtb* reaches the alveoli in the lungs. Alveolar macrophages which play a key role in the immune defense, phagocytose *Mtb*, leading to the formation of phagosomes. Alveolar macrophages also provide an environment for *Mtb* growth through increased access to iron and fatty acids (56).

Phagosomal maturation: *Mtb* resides within the phagosome, which undergoes maturation and acidification, and antimicrobial molecules accumulate. However, Mtb has evolved the mechanism to evade phagosomal degradation (57).

Replication: During this phase, *Mtb* replicates within phagosomes. The bacteria exploit effectors that contribute to the ability of the *Mtb* to replicate in macrophages (58).

Immune invasion: *Mtb* uses several strategies to evade host immune response including inhibiting phagolysosome fusion, modulating cytokine production, and altering antigen presentation (59).

Migration to lymph nodes: Infected cells migrate to local draining lymph nodes, promoting dissemination of the infection (60).

Granuloma formation: *Mtb* triggers granuloma formation, whereby macrophages, T cells, and other immune cells aggregate to contain the infection (61).

Caseous necrosis: In some cases, granulomas undergo caseous necrosis, leading to further destruction of tissues and formation of cavities in the lungs (62).

1.16 Epidemiology of *Mtb*

Devastatingly, *Mtb* is the primary cause of high death rates in HIV-infected people and TB patients (54,55). In 2021, an estimated 10 million people worldwide were diagnosed with *M. tuberculosis* infection, and more than 300,000 HIV-positive patients died from TB-related causes in the same year (63). The countries of India, China, Indonesia, the Philippines, Pakistan, Nigeria, Bangladesh, and South Africa account for more than 60% of the world's TB cases (63). Patients who have active TB infection exhibit common clinical symptoms such as coughing, night sweats, lethargy, nausea, and chest pains. Individuals with LTBI, however, continue to be asymptomatic. Despite having *Mtb*, these patients cannot spread the pathogen to other people.

1.17 Diagnosis of *Mtb*

The sputum smear microscopy method, which is used to detect *Mtb* in sputum samples, is the traditional approach for diagnosing tuberculosis. The drawback of this approach is that it can only identify half of TB infections, cannot distinguish drug-resistant strains, and is unable to identify paucibacillary TB in HIV patients. Positively, new developments in diagnostics have resulted in the development of molecular-based detection techniques like GeneXpert MTB/RIF (102), which has better sensitivity, specificity, and turnaround time than conventional diagnostic techniques and can identify both active tuberculosis and strains of *Mtb* resistant to rifampicin. The GeneXpert *Mtb*/Rif test is a nucleic acid detection method that detects mycobacterium DNA and resistance to rifampicin. It uses a cartridge-based system to purify, concentrate, amplify and detect the DNA sequences and mutation on the *rpoB* gene associated with rifampicin resistance (149). Additionally, line probe assays (LPAs) are utilized to identify extensively drug-resistant (XDR) organisms as well as multidrug-resistant (MDR) strains that are resistant to rifampicin and isoniazid treatment (102). Staining tests such as Ziehl-Neelsen are also used to detect acid-fact bacteria like Mycobacteria. The test involves the bacterial waxy cell wall, which is penetrated by the carbol fuchin dye. Subsequent to staining, the smear is decolorised with acid- alcohol, removing the dye from the non-acid-fast cells and retaining it in mycobacteria. A counterstain is then applied for contrast (148).

1.18 Active and Latent TB

Latent *Mtb* infection is a condition whereby there is no manifestation of clinical symptoms associated with TB, and the infected individual cannot spread the infection. However, without anti-TB treatment, there is a 50-10% chance that the infection will progress into active TB disease within the first two years of the initial infection. Individuals with weaker immune defences, such as those co-infected with HIV, have a significantly higher risk of developing active TB disease (66).

1.19 Mechanism behind LTBI

During infection, the alveolar macrophages contain the *Mtb* tubercle in a structure called a granuloma which is a key pathological mechanism behind LTBI. The granuloma effectively limits the spread of the *Mtb*, thus establishing a state of persistent immune response to *Mtb* antigens without clinical TB manifestation (67). The onset of active TB disease exhibits significant variability among individuals, and this is influenced by several factors, including immune status, Age, the presence of underlying conditions such as diabetes, and lifestyle factors, for example, substance abuse (68).

1.20 Biomarkers that Differentiate Active and Latent TB

Gene expression studies conducted by Lu et al., 2011 (69) in patients who had active TB and those latently infected suggest several biomarkers with the potential to differentiate between active TB and LTBI. The study revealed that the expression of interferon-gamma (IFN-γ), which is the biomarker used in Interferon Gamma Release Assay (IGRA), was not significantly different between the TB active group and the latently infected cohort. Thereafter, it showed a combination of three genes that distinguish the two states of TB, namely:

(a) CXCL10 (Chemokine C-X-C motif ligand 10),

(b) ATP 10A (ATPase, class V, type 10A), and TLR6 (Toll-like receptor6).

In contrast, the biomarkers identified by Wu et al., 2007 (70), aimed at distinguishing active TB from LTBI include:

(a) IL-8 (Interleukin 8),

(b) FOXP3 (Fork head box P3), and

(c) IL-12B (Interleukin 12 Beta).

The discrepancies between the two studies could be attributed to differences in genetic background. Genetic variability between the different study populations may contribute to the different gene expression patterns and biomarker profiles. Nevertheless, the gene expression biomarkers serve as potential indicators of active TB, and they also represent a more sensitive approach, capable of accurately detecting LTBI (71).

1.21 TB Prevention and Vaccination

Following the recommended treatment plan, covering the mouth when coughing or sneezing, cleaning hands after coughing or sneezing, avoiding crowded public spaces and transportation, and ensuring adequate ventilation can all help to prevent or reduce the spread of TB (72). The Bacillus Calmette-Guérin (BCG) vaccine consisting of attenuated live mycobacterium bovis is widely used to prevent and control the spread of TB illness (73,74). Unfortunately, it has been shown that this prophylactic agent differs in its ability to provide sustained immune protection in investigations carried out across diverse geographic regions, because of factors such as variations in manufacturing methodologies, co-infection and genetic factors, and age at the time of vaccination (75). As a result, the development of a new, improved, and efficient vaccination to prevent TB infection is required.

1.22 Treatment of TB

A patient may receive first-, second-, or third-line anti-TB drugs for treatment, depending on the *Mtb* virulence, drug susceptibility/resistance profile, and host immunological competence. Isoniazid, rifabutin, ethambutol, pyrazinamide, rifapentine, and rifampicin are among the first-line anti-TB medications (76). Capreomycin, amikacin, and kanamycin are among the second-line therapies, while linezolid, clofazimine, amoxicillin, clarithromycin, and clavulanate are among the third-line medications (77). To treat pulmonary TB in adult patients, bedaquiline is given along with other TB drugs (78). Importantly, careful and constant adherence to drug prescription is necessary for complete TB clearance and symptom relief. In general, the antibacterial medication must be taken for about 6 months to 2 years, depending on diagnosis (79), moreover, as per the guidelines provided by the South African

National Guideline for the treatment of tuberculosis, the standard treatment for adults and children who weigh 30 kg or more involves following up with patients every two weeks after the start of treatment. During these follow-up visits, the patient's TB symptoms are evaluated, their weight is recorded, and the dosage is adjusted accordingly. Adherence is evaluated through pill counts and review of their treatment cards, side effects are evaluated, HIV status is tested if it is unknown, and co-morbidities, including HIV, are managed. The re-establishment of *Mtb* infection is caused by improper adherence to the medication treatment plan, which also jeopardizes safety and effectiveness by encouraging the growth of strains that are resistant to the drugs (80). Table 1.3 shows the different categories of anti-TB drugs.

TABLE 1.3. CLASSES OF ANTI-TB DRUGS (81).

TB Drug	Category	Mechanism of Drug Action
Group 1		
Amikacin	First Line	Prevents protein synthesis by binding to the 30S ribosomal subunit
Ethambutol	First Line	Prevents synthesis of essential metabolites, impairing metabolism and causing cell death
Isoniazid	First Line	Interrupts synthesis of mycolic acid, leading to bacterial cell wall disruption
Pyrazinamide	First Line	Inhibits translation by interrupting ribosomal protein S1 (RpsA) production and prevents fatty acid synthesis
Rifampicin	First Line	Interrupts RNA polymerase activity required for chain initiation
Streptomycin	First Line	Inhibits protein synthesis by disrupting the 30S ribosomal subunit
Group 2		
Bedaquiline	Second Line	Disrupts energy production by inhibiting ATP synthase
Capreomycin	Second Line	Binds to the 70S ribosomal subunit, preventing protein synthesis
Clofazimine	Second Line	Binds to Mtb guanine bases, impairing bacterial growth
Cycloserine	Second Line	Alters D-alanine function, disrupting cell wall synthesis and decreasing growth
Ethionamide	Second Line	Interrupts synthesis of mycolic acid, causing bacterial cell wall disruption
Levofloxacin	Second Line	Interferes with DNA gyrase and topoisomerase IV, essential for DNA replication, transcription, recombination, and repair
Moxifloxacin	Second Line	Binds and interacts with the A subunit of DNA gyrase, disrupting DNA replication and transcription

PASER	Second Line	Disrupts folic acid synthesis and causes iron deficiency by inhibiting mycobactin synthesis
Group 3		
Rifabutin	Third Line	Antagonizes RNA polymerase activity, disrupting the elongation step of DNA replication

These anti-TB treatment regimens are chosen through a systematic process focusing on efficacy, safety and cost considerations. Moreover, they are chosen based on the specific form of drug-resistant tuberculosis (DR-TB) being treated (82). Drug-susceptibility testing outcomes play an essential role as they guide the selection process and determine the most appropriate drugs for the treatment regimen (82). These drugs are divided into three lines based on their effectiveness against *Mycobacterium tuberculosis*. The first-line drugs are utilized to treat the drug-susceptible *Mycobacterium tuberculosis*, while the second-line drugs target the multidrug-resistant Mycobacterium tuberculosis, and the third line targets the extensively drug-resistant *Mycobacterium tuberculosis* (83). The drug-susceptible *Mycobacterium tuberculosis* is treated with only first-line anti-TB drugs, whereas the drug-resistant *Mycobacterium tuberculosis* is treated with a combination of both second-line drugs and a few first-line drugs (84). To control the transmission of the infection, quarantine is limited to necessity and adhering to ethical principles (85).

Part C: Review of TB-HIV Co-Infection

1.23 HIV, TB Co-Infection, and Immunity

HIV infection results in immune system dysfunction, and this significantly increases the risk of contracting TB in TB-endemic areas, culminating in increased mortality (59,60). The co-existence of TB and HIV in an infected host synergistically accelerates the decline of CD4 count, and other immune cell populations, specifically Th17 and Th22 cells, while also increasing HIV viral load. Moreover, infection impairs the immune defence toward M. tuberculosis, potentially culminating in a rapid progression to AIDs (88).

1.24 Genetic Susceptibility to TB and HIV Infection

Studies documented in various parts of the world suggest that polymorphisms in the Human Leukocyte Antigen (HLA) can potentially predispose individuals to both HIV and TB infection (89). Specifically, the HLA-B, HLA-C, and KIR genotypes have been associated

with TB, HIV-1 infection and the onset of immune reconstitution inflammatory syndrome (IRIS) among TB-HIV co-infected individuals (90). Moreover, certain genetic variants have also been implicated in the progression of the HIV disease and are associated with TB development (63), for instance, genetic variants: ANAKRD39; LOC105378523 and GTF3C3 genes have been significantly associated with HIV-1 progression (91). In contrast, genome-wide association studies report on some genes that can protect from HIV disease progression (64–67).

1.25 Host Antiviral Genes

Evidence indicates that some host genes can predispose individuals to infection, while other genes play a crucial role in defence against HIV-1 infection and potentially influence the immune response. These include:

(a) The Virus Restriction Factor TRIM 5a

The Tripartite motif-containing 5 alpha protein, composed of 493 amino acids, is suggested to contribute to defence mechanisms in humans and non-human primates against various retroviruses (92). The protein acts during viral uncoating and binds to recognized and specific motifs within the viral capsid. This interaction interrupts the process of viral uncoating and inhibits reverse transcription. Nevertheless, the antiviral activity of TRIM5a protein against HIV-1 is hindered by two recognized polymorphisms, namely H43Y and R136Y in the TRIM 5a protein. These mutations weaken the antiviral activity of the protein to neutralize the virus (92).

(b) APOBEC 3G

The apolipoprotein B mRNA-editing enzyme, catalytic polypeptide-like 3G, is a host antiviral agent that plays a role as a potent post-entry inhibitor of HIV-1 in naïve CD4 T cells (93). Its mechanism of action involves altering the genetic code of the virus by catalyzing the conversion of cytidine to uridine, a process is referred to as cytidine deamination. This enzymatic activity results in the introduction of a mutation into the viral genome, which hinders its replication (92,94). While a significant portion of the human population has lost the antiviral activity of the protein due to polymorphism, evidence suggests that the African population still retains the effectiveness of the protein against HIV (92). Despite the high incidences of HIV cases in the African continent, which are influenced by various factors

including inadequate health care, lack of prevention education, and poverty among other reasons (95,96).

(c) SAMHD1

SAMHD1 is a protein synthesized from the SAMHD1 gene. It is a cellular enzyme that interferes with the replication of HIV within various immune cells. Particularly, SAMHD1 interferes with replication in antigen-presenting cells such as dendritic cells, phagocytes including macrophages, and other immune cells, like resting CD4+ T cell lymphocytes. The enzymes exhibit the ability to hydrolyze phosphates, converting deoxynucleoside triphosphate (dNTPs) to inorganic phosphate(iPPP) and a 2' deoxynucleoside. In doing so, SAMHD1 depletes a pool of dNTPs available to a reverse transcriptase for viral cDNA synthesis and thus prevents viral replication (97).

(d) Tetherin

Tetherin is a lipid raft-associated protein that in humans is encoded by the BST2 gene, and it is part of the interferon (IFN) dependent antiviral response pathway and inhibits a broad range of enveloped viruses, including HIV by physically tethering nascent particles to the plasma membrane of infected cells. Evidence from prior studies done on mice suggests that tetherin-deficient mice were more susceptible to viral infection, which indicates that tetherin plays a direct antiviral role in vivo (98).

1.26 Treatment of HIV, TB Co-Infected Patients

The treatment of HIV and TB co-infection is much more complex, relative to treating the pathogens HIV or TB separately. Nevertheless, a study by Lawn et al., (2011) indicated that HIV treatment and strict adherence to antiretroviral therapy significantly reduce the risk of developing active TB among TB-HIV co-infected patients and consequently produce CD4+ cell count that is above 500 μl/ml, thus leading to lower TB incidences in HIV-infected patients (99).

Part D: Review of Epigenetic Mechanisms in the Context of TB-HIV Co-Infection

1.27 The Concept of Epigenetics

The term is formed by the prefix “Epi,” meaning above, and the word “genetics” referring to the genome. Therefore, it is the study of reversible and heritable changes in gene expression induced by specific chemical groups that bind to the DNA molecule (100). These changes occur without altering the DNA sequence. In the nucleosome, there are positively-charged proteins called histones that have an exposed N-terminal tail that can be subjected to various posttranscriptional modifications (103). These modifications lead to alterations in the chromatin accessibility that result in either up-regulation or down-regulation of a specific gene (103). The three major modifications include: histone acetylation, histone phosphorylation; and histone methylation (129–131).

The table below presents a comprehensive overview of the Histone modification patterns occurring at various positions on the histone tail. The patterns as depicted in Figure 3.2 have implications on the expression of the target genes and other cellular pathways. This table is a summarized description of the results indicated in Figure 3.2. It was compiled with aid of the histome database and several prior studies (132–134).

TABLE 1.4. SUMMARIZED DESCRIPTION OF THE HISTONE MODIFICATIONS AT DIFFERENT AMINO ACID RESIDUES WITHIN THE HISTONE TAIL.

Notes: Methylation, acetylation and phosphorylation positions=H3K (Histone 3 and K-lysine position). H3Ser (Histone 3 and Ser-Serine position).

Histone Positions	Modifications/degree of modification	Implications
Histone Methylation		
H3K4me1	Mono-methylation	Mono-methylation of histone H3K4 is linked to transcriptional activation.
H3K4me2	Di-methylation	Di-methylation of histone H3K4 is linked to transcriptional Activation.
H3K4me3	Tri-methylation	Tri-methylation of H3K4 is associated with transcriptional activation of the Major Histocompatibility complex class II—Human Leukocyte antigen (**HLA-DR**) genes, expressed in antigen presenting cells, such as dendritic cells, Macrophages and B cells.
H3K9me1	Mono-methylation	Mono-methylation of Histone H3K9 is associated with transcriptional repression.
H3K9me2	Di-methylation	Di-methylation of Histone H3K9 is typically a mark of transcriptional repression.
H3K9me3	Tri-methylation	Tri-methylation of Histone H3K9 is characterised as a mark of transcriptional repression.
H3K27me1	Mono-methylation	Mono-methylation of Histone H3K27 is a mark of active transcription at active promoters.
H3K27me2	Di-methylation	Di-methylation of Histone H3K27 is linked to transcriptional repression

1.28 Histone Modifications

Histone acetylation is well studied among the three epigenetic modifications, and it is catalyzed by two enzymes namely: histone acetyltransferases (HAT) and histone deacetylase enzyme (HDAC); these enzymes have opposite functions (104). The HAT enzyme increases accessibility to the chromatin structure and promotes interactions with the RNA-polymerase,

transcription factors and DNA molecule to induce gene expression (102,103). On the other hand, the HDAC induces down-regulation of gene expression (103).

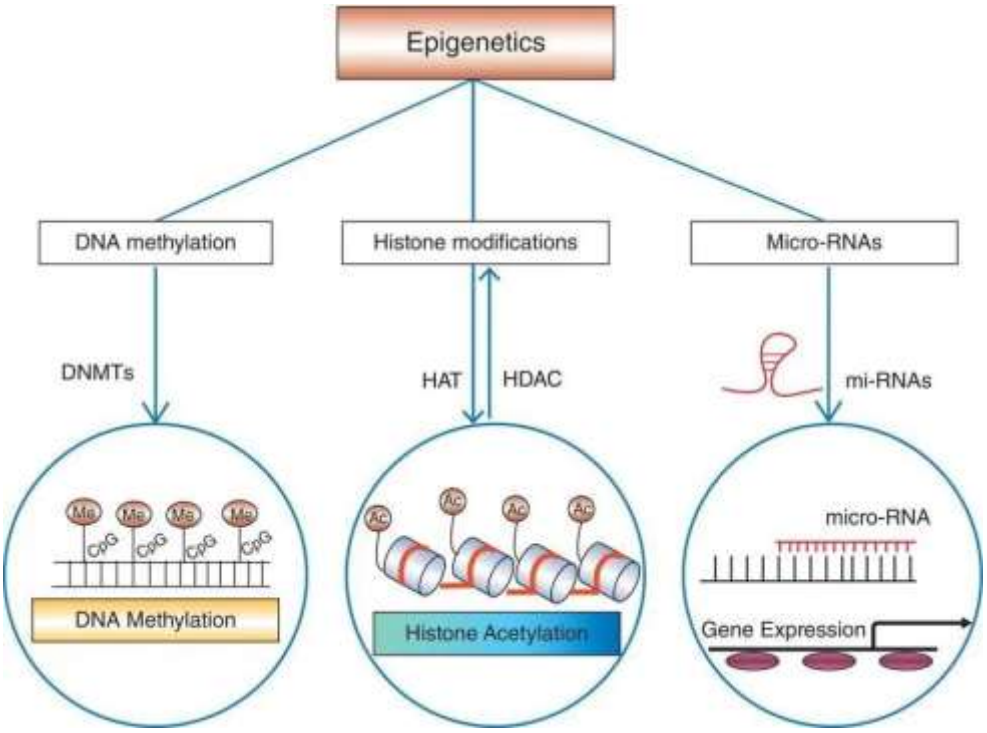


FIGURE 1.5. A SCHEMATIC ILLUSTRATION DEMONSTRATING THE CONCEPT OF EPIGENETIC OF EPIGENETIC MODIFICATION.

Histone modification via acetylation and methylation, DNA methylation, and microRNA-mediated posttranscriptional regulation are examples of epigenetic mechanisms. Gene methylation involves methyltransferase. The processes of chromatin remodelling and histone acetylation are mediated by HAT and HDAC. MicroRNAs play a role in the post-transcriptional regulation of genes. Image has been adopted from Chaturvedi and Tyagi, 2014 (101).

Several HATs have been identified as co-activators; these include GCNS; PCAF, CBP, P300, Tip60, and MOF (104). Based on phylogenetic analysis, HDACs are suggested to be evolutionarily conserved from yeast to human, and four classes of human HDACs have been identified, and they include (104):

(a) Class I: (HDAC 1, 2, 3, and 8 with a homology to Rpd3)

(b) Class II: (HDAC 4, 5, 6, 7, 9, and 10 with a homology to Hda1)

(c) Class III: (Sirt 1, 2,3,4,5,6, and 7 with a homology to Sir 2) and

(d) Class IV: (HDAC 11).

Histone methylation is regulated by the histone methyltransferase enzyme (HMT), and gene expression can be activated or repressed depending on the histone protein and the amino acid residue that is modified (103). The last of the histone modifications, referred to as histone phosphorylation, has an indirect effect on the regulation of gene expression (103).

1. **Transcriptional activation**

Phosphorylation of specific histone residues can promote transcriptional activation by facilitating the recruitment of transcription factors and RNA polymerase II to gene promoters (105).

2. **Enhancer function**

Phosphorylated histone can also associate with enhancer regions, which are regulatory elements that enhance gene expression. These enhancers may be located far from the gene they regulate (106).

3. **DNA repair**

In response to DNA damage, phosphorylated histone recruits repair factors to damage sites, ensuring proper DNA repair before gene expression resumes (107).

1.29 DNA Methylation

DNA methylation is a biological process whereby the methyl group is transferred from the S-adenosylmethionine (SAM) (Figure 1.4) to the fifth-carbon of a cytosine ring, resulting in the formation of 5-methylcytosine (121). This modification occurs in the CpG region, which is defined according to literature as the site where a cytosine nucleotide is in close proximity to the guanine nucleotide (108). This epigenetic mechanism is catalyzed by the enzyme called DNA methyltransferase (DNMT), and it typically results in transcriptional silencing of target gene(s) (121). The majority of CpG regions are methylated throughout the genome, except for the germline and near promoter regions (67). Three major DNMTs catalyze the

methylation processes and are as follows: DNA methytransferase1 (DNMT1); DNMT 3A and DNMT 3B (Figure 1.4) (121).

The DNMT1 facilitates the maintenance of methylation after every replication cycle of the DNA molecule; while the DNMT3A and 3B are known for their de novo or repetitive methylation activity, whereby the methyl group is added on sites that were not previously methylated (121). Patterns of methylation can be inherited into daughter cells when the cells divide, and this process is catalyzed by the DNMT1 enzyme that acts on the CG- sequences that are base-paired with the methylated CG sequences. As a result, the parent strand serves as the template for the formation of a new daughter strand, thus transmitting methylation to the next generation (128) (Figure 1.4). Even though methylation can be maintained in differentiated daughter cells, as shown in Figure 1.4, the methylation patterns often change during mammalian development.

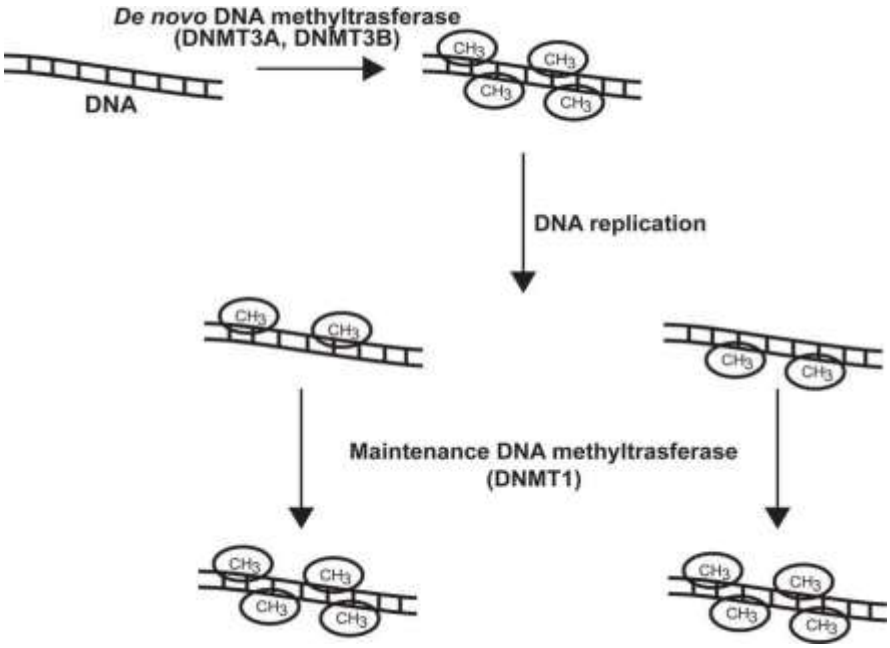


FIGURE 1.6. DNA METHYLTRANSFERASES.

A schematic overview of the different roles of DNMTs: The de novo DNMTs (3A and 3B) and the maintenance function of DNMT 1. The DNMTs catalyze the transfer of the methyl moiety to genomic DNA. Significant changes in the amount of DNA methylation cause a change in gene expression, function, and protein synthesis. Image has been adopted from Thuy et al., 2017 (128).

This is because shortly after fertilization, there is genome-wide demethylation, whereby the methyl-groups are lost from the DNA sequence either through suppression of the maintenance DNMT1 function or the methyl-groups are removed by the demethylating enzyme (128). However, at a later stage in mammalian development the DNMT 3A and 3B; the *de novo* methyltransferases, establish new methylation patterns essential for resetting the epigenetic landscape of the zygote, thus allowing for proper gene expression patterns and developmental potential during early embryogenesis (128). They are maintained and passed on by the DNMT1 enzyme. This is crucial for the maintenance of methyltransferase following DNA replication (121).

Methylation has key roles, namely: regulation of gene expression and ensuring genomic stability. The more methylated a region of DNA is, the more the activity of that particular gene is going to be down-regulated, and vice versa. Methylation plays a key role in cell differentiation and normal mammalian development (137); therefore, a correct methylation level is essential for parental imprinting and X-chromosome inactivation mechanisms. Previous studies also found that methylation can affect gene expression by interfering with the function of transcription factors (138). Genome stability is maintained by methylation of the CpG regions, which keep repetitive DNA elements such as retrotransposons highly silenced, thus preventing destabilization of the genome and disturbing the cellular transcriptome (139). A large body of scientific evidence suggests that methylation on the promoter regions induces silencing of transcription (140).

Although methylation is generally known to activate transcriptional silencing, in some cases, it can induce gene expression (121). Generally, methylation patterns are the same throughout a gene, particularly in lowly expressed genes. In contrast to this, in highly expressed genes, the level of methylation is low from the promoter site and increases towards the end of the gene; thus, implying that there is a possible connection between methylation and gene expression (135). Other investigations suggest that two possible mechanisms might link DNA methylation with gene regulation (128,136):

(a) The methyl groups on the methylated cytosine ring adhere to DNA sequences where they interfere with the ability of transcription regulators and transcription factors to bind and initiate transcription.

(b) An indirect influence associated with changes in DNA properties (i.e., a change in the binding affinity of transcription factors or DNA methylation changing the chromatin structure).

1.30 Epigenetic Regulation and Resistance to TB in HIV Patients

A study by Catherine et al., 2020 reported that resistance and susceptibility to active TB in TB-HIV co-infection is influenced by epigenetic marks in conjunction with the host's genetic variants. This was reported after the genome-wide analyses revealed methylation as a marker that prevented the development of active TB in some HIV-infected patients. Moreover, the study also demonstrated that epigenetic regulation of T cells, B cells, and monocytes can influence protection from the development of active TB (141).

1.31 The Effect of Epigenetic Modification in TB-HIV Co-infection and Immune Response

Previous studies have unravelled the epigenetic mechanism by which HIV and TB thrive in a study conducted by Marimani et al.,2020 (102); it has been shown that co-infection with *Mtb* and HIV induces epigenetic modification, as evidenced by the expression profiles of seven candidate genes: *Dicer, DNMT1, HAT, HDAC, PtkA; ptpA* and *TET1*. These modifications have been found to weaken the potent defense mechanisms of the innate and adaptive immune response, furthermore, the investigations have also demonstrated that epigenetically modified proteins influence *Mtb* resistance to antibiotics, virulence, and replication (102). Additionally, a prior study also suggests that increased expression of *DNMT* 1 post-infection with HIV-1 in 78 Hut lymphoid cells can potentially affect the functionality of the immune system (142). Moreover, hypermethylation at specific CpG sites in TB patients affects *TLR2* gene expression, which controls innate immunity against TB infection (143).

Epigenetic mechanisms play a crucial role in influencing the immune system. Only a few studies in the literature report on the role of epigenetic modifications in the control of immune system mediators (102).

1.32 The Roles of Epigenetic Mediators

The *DNMT1* gene is implicated in methylation and maintenance of methylation patterns, thus its role could potentially affect the immune response and pathogenesis resistance in TB-HIV co-infection (102). *SETDB2* and *KMT* are involved in histone methylation, and they can either repress or activate gene expression; therefore, investigating these genes could yield valuable insights into how histone modification could influence disease progression and immune response (144). *CIITA* is crucial for the expression of Major Histocompatibility Complex genes (MHC) class II genes involved in antigen presentation and immune response and *HAT*s through mediation of acetylation promote expression of genes implicated in immune defense (102,117), therefore, investigating these genes in the context of TB-HIV co-infection could elucidate how epigenetic changes affect immune competence and pathogen control. Accordingly, the novelty of our study was to evaluate the expression level of *histone acetyltransferase* (*HAT*), *SET domain bifurcated histonelysin methyltransferase2* (*SETDB2*), *histone lysine methyltransferase* (*KMT*), *Class II transactivator* (*CIITA*), and *DNA methyltransferase1* (*DNMT1*) target genes in the context of TB-HIV co-infection in Sub-Saharan Africa. These genes were selected as their role and expression levels have not been vigorously elucidated in TB-HIV co-infected patients following microbial infection and epigenetic programming. The demographic makeup, genetic variability, and the TB and HIV drug-resistant profile in Sub-Saharan Africa is unique and different from other geographical locations. These features may be important as they may significantly affect the epigenetic processes leading to a significant change in gene expression. In contrast to most previous studies, our investigation utilised human lymph node FFPE biopsies as a source of *Mtb* and HIV microbial agents. Additionally, compared to other studies using FFPE tissues, our study utilized a large sample size to enhance data reproducibility and reliability.

Study Aim

This study aimed to compare the degree of epigenetic modifications in the TB-HIV co-infected patients and the non-infected subjects.

Objectives

1. To confirm TB-HIV coinfection in the tissue samples by conducting conventional polymerase chain reaction (PCR) targeting the HIV *gag-pol* and *Mtb rpoB* genes.

2. To determine the evolutionary relationships between the infecting HIV and TB strains, respectively using DNA sequencing and phylogenetic analysis of the HIV *gag-pol* and *Mtb rpoB* genes.

3. To evaluate the expression of *DNMT1*, *SETDB2*, and *KMT* genes involved in DNA methylation in non-TB-HIV and HIV co-infected FFPE tissue samples by reverse transcription quantitative polymerase chain reaction (RT-qPCR).

4. To examine the expression profile of *CIITA* and *HAT* genes implicated in histone acetylation in TB-HIV co-infected and non-TB-HIV human biopsies by RT-qPCR.

5. To determine the degree of histone methylation, acetylation, and phosphorylation in infected and non-TB-HIV tissue samples by applying the Histone H3 modification multiplex assay.

Chapter 2: Materials and Methods

2.1 Ethics Consideration

Ethical clearance to conduct this study was obtained from the Human Research Ethics Committee (HREC) of the University of Witwatersrand, protocol no: M220614 (Appendix 6.2). Before the commencement of the project, the study was registered with the National Health Laboratory Service (NHLS) under the Academic Affairs and Research Management System (AARMS) and permission to retrieve patient clinical information, such as age, gender, the status of diagnosis, CD4 counts, history of surgical procedures, allergies, or AIDS-defining cancers, was granted (Appendix 6.3).

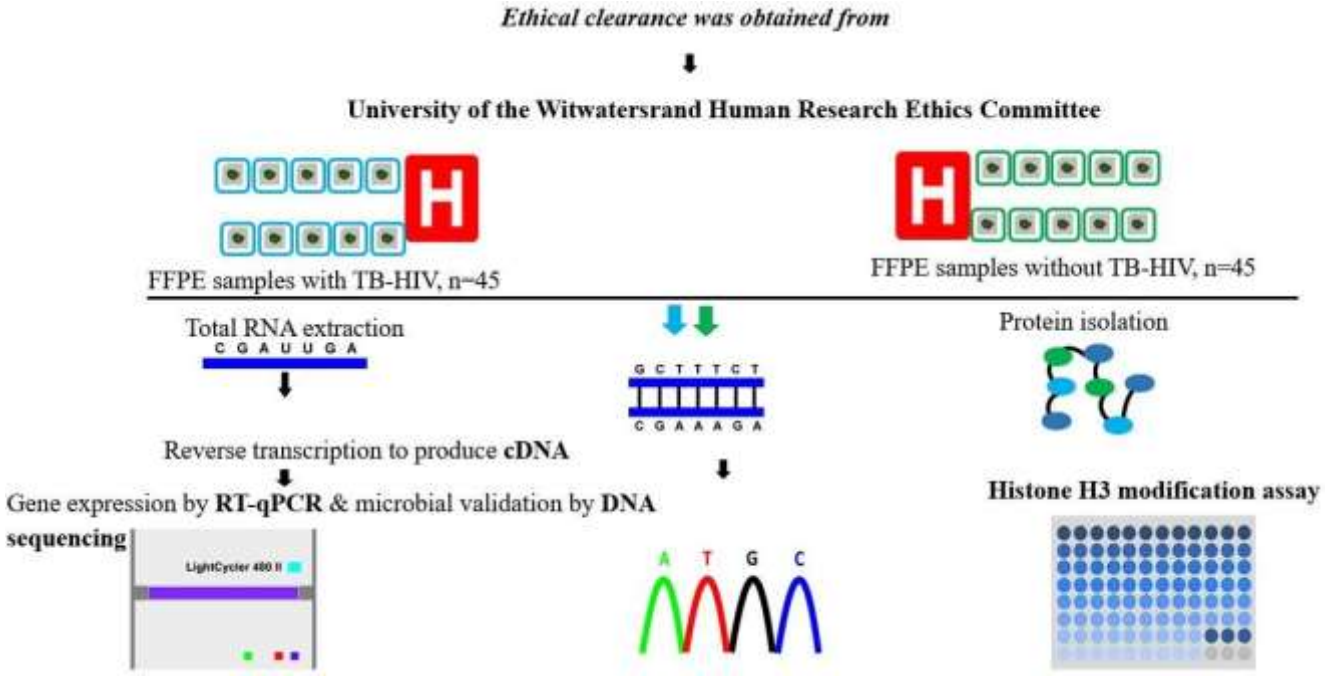


FIGURE 2.1. EXPERIMENTAL DESIGN TO INTERROGATE EPIGENETIC MECHANISMS IN TB-HIV AND NON-INFECTED INDIVIDUALS.

Human biopsy samples were collected from patients co-infected with TB-HIV and individuals without TB-HIV co-infection and subjected to total RNA and protein extraction. Total RNA was reverse transcribed to produce cDNA and subjected to amplification by RT-qPCR to assess gene expression profiling. The generated cDNA was also utilized for DNA sequencing to determine the evolutionary relationship of the infecting *Mtb* and HIV strains. Protein molecules were utilized to evaluate their respective production levels by H3 modification

2.2 Sample Size and Collection

The Systemized Nomenclature of Medicine (SNOMED) search was conducted to search for patient cases with TB-HIV coinfection and control samples without TB-HIV infection. A total of forty-five (45) TB-HIV human lymph node tissue samples collected from the Charlotte Maxeke Academic Hospital in Johannesburg were from patients who were on ART treatment for less than six months, as evidence from prior studies indicates that patients undergoing ART for more than 6 months typically exhibit competent immunity against the virus (118). As such, their immune function may be comparable to that of healthy subjects. In addition to TB-HIV co-infection, the experimental group was comprised of patients presenting with Kaposi sarcoma, palatal ulcers, erythema, induratum, lupus panniculitis, or necrotizing granulomas at the time of tissue collection.

Unfortunately, information relating to viral load, CD4 counts, bacterial load, ARV drug type, and TB regimen is not available in most data sheets. This data was not captured by the requesting clinician. Furthermore, the 45 control tissue samples from the same hospital as the test group (without TB-HIV and with no clinical history of cancer, high blood pressure, diabetes, allergies or any other major underlying clinical conditions) were obtained. The control tissue biopsies were from patients who did not have cancer, hypertension, diabetes, allergies, or any other major underlying clinical conditions. However, these patients presented with chest pain, cough, headache, fatigue, nausea, weight loss or fever at the time of tissue excision. The FFPE samples were retrieved from 90 individuals, consisting of 45 TB-HIV co-infection patients and 45 non-TB-HIV patients, who were matched according to age, race, and gender. We used human lymph node tissues as surrogate specimens to study the impact of TB-HIV co-infection in regulating epigenetic processes. Although crude extraction of tissues from lymph node tissues cannot truly represent the immune system of an individual, these tissues were used, as it is very challenging to extract human immune cells from FFPE samples due to extensive crosslinking. This negatively affects the anatomical, physiological, and cellular properties of the cells and generally produces inaccurate and irreproducible data. Moreover, the protocols used to isolate immune cells from human tissue specimens are technically demanding, and the isolation of tissue-derived immune cells is challenging. As such, the use of human lymph nodes was a viable option for our research project as they are a rich source of *Mtb* and HIV pathogens. Moreover, the extraction of nucleic acids and proteins from FFPE lymph node tissues is relatively easy, less labour-

intensive and cost-effective compared to working with human immune cells from FFPE specimens.

In selecting our sample size (n=45; TB-HIV cases and n=45; non-TB-HIV cases), we used our prior investigation (102) as a benchmark since it is related to this research project. Specifically, in the previous study, we observed statistical significance in gene expression and protein production levels between the TB-HIV co-infected cohort (n=10) and the uninfected cohort (n=10) (102). This investigation focused on evaluating and comparing the expression levels of *Dicer, DNMT, HAT, histone deacetylase (HDAC), protein tyrosine kinase (PtkA), protein tyrosine phosphatase* (*PtpA*), and *ten-eleven translocation methylcytosine dioxygenase* (*TET1*) genes in blood samples collected from TB-HIV patients and healthy individuals (102). For this reason, the sample size (n=45; TB-HIV samples and n=45 non-TB-HIV cases) was utilized to enable effective management of the project and to enhance the cost-effectiveness of the study budget. Notably, the lymph node tissues are reported to be a rich source of TB-HIV cases from diagnoses performed by Pathologists in our Department (i.e., Department of Anatomical Pathology, University of the Witwatersrand). Therefore, the lymph node tissues were used for the extraction of RNA, DNA, and protein from individuals with TB-HIV co-infection and the non-TB-HIV cohort. Additionally, the lymph node tissues are a reliable source for retrieving tissue samples invaded by microbial pathogens. The Pathologists aided and facilitated the selection and retrieval of tissue blocks and clinical data such as age, gender, the status of diagnoses and documented history of surgical procedures, allergies, or AIDS-defining cancers as they have access to the NHLS TrackCare system. We randomly selected the TB-HIV co-infected cases and matched the age and gender of this cohort with that of the control cohort. These cases in our study were collected from patients diagnosed from 2017 to 2019. These samples were subjected to histopathological, histochemical, and molecular evaluations as part of the NHLS diagnostic work-up in the Department of Anatomical Pathology.

In particular, HIV infection was diagnosed using the P24 staining and ELISA, while TB infection was detected after applying the Ziehl-Neelsen staining and GeneXpert MTB/RIF tests. The experimental design for the current research project is shown in Figure 2.1.

2.3 Total RNA Extraction from the Infected and the Control Human Tissues

The total RNA was extracted from the 45 TB-HIV and 45 non-TB-HIV lymph node biopsies using the PureLink FFPE total RNA isolation Kit (Thermo Fisher Scientific, MA, USA). The collected human tissue blocks were sectioned using the rotary microtome (RM2152 RTS, Leica) set at 10 μm, and five (5) tissue sections from each tissue block were placed into sterile, RNase-free 1.5 ml Eppendorf tubes. The removal of paraffin from the tissue blocks was accomplished by adding 300 μl melting buffer into each tube. The melting buffer was composed of chemicals like tuelene or xylene, which have an affinity for paraffin. These chemicals break down paraffin into a liquid that can be separated from the tissues. The tubes were then centrifuged (Microfuge®16 centrifuge, Beckman Coulter, CA, USA) at a maximum speed of 13 000 × g for 20 seconds and followed by incubation for 10 minutes at 72°C with intermitted mixing. To enhance protein digestion, twenty microlitres (20 μl) of proteinase K was aliquoted to each tube, which acts by cleaving peptide bonds within proteins resulting in digestion. The reaction mixture was incubated at 60°C overnight and centrifuged at a maximum speed of 13 000 × g for 1 minute to segregate the lysate from the paraffin. The segregated lysates were transferred into separate new RNase-free Eppendorf tubes. Thereafter, each sample tube was treated with 400 μl binding buffer and 800 μl 100% ethanol to remove impurities. The binding buffer binds to nucleic acid molecules, while ethanol precipitates the molecules. Seven hundred microliters (700 μl) from each sample were transferred to a spin column contained in a 2 ml collection tube (In these tubes the positively charged silica in spin column binds to the negatively charged RNA). The tubes were then centrifuged at 800 × g for 1 minute. The resulting flow-through was discarded and the remaining sample was transferred to the spin cartridge in the collection tube and centrifuged at 800 × g for 1 minute. The flow-through was discarded and the genomic DNA was removed by the addition of 80 μl DNase which cleaves phosphodiester linkages in the DNA resulting in degradation. The sample tubes were then incubated at room temperature for 15 minutes.

Five hundred microliters (500 μl) wash buffer solution as aliquoted to each sample tube and centrifuged at 13 000 × g for a minute (this step was repeated twice), followed by discarding the flow through and reinserting the tubes back into the 2ml collection tube. The sample tubes were further centrifuged at 13 000 × g to eliminate any residual wash buffer. The resulting flow through was discarded, and the spin column were transferred into new 1.5 ml Eppendorf tubes. For eluting the total RNA, nuclease free water pre-heated at 65°C was applied to the

centre of each spin column, incubated for 1 minute at room temperature and centrifuged at 13 000 × g for 1 minute. The new sample tubes containing total RNA were stored at -80°C until used for synthesis of complementary DNA by reverse transcription.

2.4 Synthesis of Complementary DNA

The extracted total RNA was subjected to complementary DNA (cDNA) synthesis by utilizing the Revert Aid kit (Thermo Fisher Scientific, MA, USA) in a final volume of 20 µl. The reaction mix contained: 4 µl of 5× reaction mix, 20 U/µl Ribo Lock RNase inhibitor, 100 µM random primer, 10 mM dNTP mix, 200 U/µl of RevertAid M-MuLV RT, 1 µg total RNA template and nuclease free water to make up a total volume of 20 µl. The initial step was priming whereby the primer binds to the RNA to initiate reverse transcription. This step involved incubation at room temperature for 5 minutes, followed by reverse transcription at 42°C for 1 hour and the final step was the termination of reverse transcription at 70°C for 5 minutes. The samples were incubated on ice for 5 minutes and the purity and concentration of the cDNA was determined by measuring the absorbance at the ratio A260/280 nm on the Nanodrop instrument (NanoDrop ONE, Thermo Fisher Scientific, MA, USA).

2.5 Amplification of cDNA by PCR, DNA Sequencing and Phylogenetic Analysis

Conventional PCR and DNA Sequencing were performed to confirm TB-HIV co-infection as well as to determine the evolutionary relationship between the infecting HIV and *Mtb* strains in the experimental group. Specifically, the qualitative conventional PCR technique was used to confirm the quality, purity, and integrity of cDNA samples collected from experimental and control groups. As DNA, RNA, and protein molecules isolated from FFPE samples are known to degrade over time due to fixation and cross-linking, conventional PCR was used to verify the quality of the generated cDNA samples. This is important for obtaining accurate results, precise data analysis, and maintaining experimental validity and data reproducibility. Unlike RT-qPCR, which is a quantitative procedure and contains fluorescent dyes and allows visualization of DNA amplification in real-time, conventional PCR is a qualitative method and does not contain fluorescent dyes. For this reason, it necessitates to use of agarose gel electrophoresis to confirm DNA amplification. Conventional PCR consists of three stages namely:

(a) Denaturation, where the double-stranded DNA is separated into two single DNA strands following heating at 95°C

(b) Annealing, where each primer binds to the complementary sequence on the single-stranded DNA and initiates amplification. The annealing step of PCR is typically performed between 50-65°C, depending on the primer GC content.

(c) Elongation, this step is catalyzed by the enzyme Taq polymerase, which uses the DNA template strand to synthesize the new complementary DNA strand. This is achieved by adding dNTPs to complementary DNA strands.

The elongation step is generally conducted at 72°C, which is the optimum temperature for the Taq polymerase enzyme. Conventional PCR amplification usually involves 30-35 cycles (i.e. denaturation, annealing, and elongation) of amplification to obtain a sufficient number of amplified DNA molecules. This procedure was utilized for the amplification of cDNA from ten TB-HIV samples. The reaction mix included the 2× PCR master mix (Thermo Fisher Scientific, MA, USA),10 pmol of each primer pair specific to the HIV *gag-pol* or *Mtb rpoB* gene, and 2 µl cDNA (100 ng/µl). The primer sequences targeting the *gag-pol* and *rpoB* genes are illustrated in Table 2.4. The no template control (NTC) was used as a negative control to monitor cross-contamination. The T100 thermal cycler PCR device (Bio-Rad, CA, USA) was used and the thermal cycling conditions for amplification were set as follows: one cycle of initial denaturation at 95°C for 3 minutes, 35 cycles of denaturation at 95°C for 30 seconds, annealing at 51°C for 30 seconds (*rpoB*) or 53°C for 30 seconds (*gag-pol*), extension at 72°C for 1 minute and the final extension step was performed at 72°C for 10 minutes. To verify the quality of the amplified DNA, 15 µl the amplicons were mixed with 5 µl 6× loading dye and loaded into the gel lanes (Thermo Fisher Scientific, MA, USA). Five microliters of the 100 bp DNA ladder (Thermo Fisher Scientific, MA, USA) was loaded in the first and final lanes. The DNA ladder was used to determine the size of the amplified DNA samples. All samples were electrophoresed on a 2% agarose gel stained with 3 µl of 3% ethidium bromide (Thermo Fisher Scientific, MA, USA) at 100 volts for 45 minutes. The bands were visualized using the Gel Doc System (Syngene G: Box, UK) UV transilluminator equipment.

TABLE 2.1. THE PRIMER SEQUENCES OF HIV *GAG-POL* AND *MTB RPOB* GENE WERE USED IN CDNA AMPLIFICATION BY CONVENTIONAL PCR.

Primer name	Orientation	Primer Sequence	PCR DNA Fragment size
*Mtb_rpoB*_F	Forward	5'-GTCGACGAGTGCAAAGACAA-3'	110 bp
*Mtb_rpoB*_R	Reverse	5'-TGGTCTCGTCGAAGTACACC-3'	
HIV_gag-pol_F	Forward	5'-CCAGCGGCTACACTAGAAGA-3'	120 bp
HIV_*gag-pol*_R	Reverse	5'-CCTGCAATTTCTGGCTGTGT-3'	

To determine the evolutionary relationship between the infecting HIV and TB strains, the 10 PCR amplicons of HIV *gag-pol* and *Mtb rpoB* genes, respectively, were sent to Inqaba Biotechnical Industries (Inqaba, Biotech Industries, South Africa) for DNA sequencing. This technique utilized the forward and the reverse primers shown in Table 2.4. These primers are specific to the template to initiate DNA synthesis. The process involves the incorporation of deoxynucleotide triphosphates (dNTPs) and special chain-terminating molecules called dideoxynucleotide triphosphates (ddNTPs). These chain-terminating molecules halt the elongation of DNA strands at specific positions, resulting in DNA fragments of varying lengths. These DNA fragments are then separated by size, revealing a sequence of nucleotide bases in the original DNA molecules. The resulting DNA sequences were edited using the FinchTV 1.4.0 software (Geospiza, WA, USA). The subtype classification of HIV-1 *gag-pol* gene sequences was determined using Basic Local Alignment Search Tool (BLAST) analysis performed using the Los Alamos National Laboratory (LANL) HIV Sequence Database. The LANL BLAST interface was accessed via the online portal on https://www.hiv.lanl.gov/content/sequence/BASIC_BLAST/basic_blast.html. In this particular database, the viral sequences were submitted against the curated HIV-1 reference database. The BLAST was run against all subtyped sequences. The percent identity, alignment score, and E-value were used to assess sequence similarity. In addition, metadata such as subtype, country of origin, and year of isolation were also recorded. For subtype classification, the top BLAST hit was selected. The *Mtb* sequences were compared with GenBank reference sequences deposited in the National Center for Biotechnology Information (NCBI, https://blast.ncbi.nlm.nih.gov/Blast.cgi) database using BLASTn. The BLAST parameters included default settings optimised for highly similar sequences (megablast). The top BLAST hit, which was an alignment with the highest combination of

identity, the lowest E-value, and the highest query coverage, was selected to assign species identification.

To examine the relationship between the 10 HIV-1 sequences from this study and those in public databases, three reference HIV-1 sequences representing subtypes (A, B, and C) were randomly selected from the LANL HIV sequence database (https://www.hiv.lanl.gov/components/sequence/HIV/search/search.comp). In addition, 10 reference HIV-1 sequences from the NCBI database were randomly selected for phylogenetic analysis. The phylogenetic analysis for the *Mtb* sequences was performed using the 10 *Mtb* sequences from this study, as well as nine *Mtb* reference sequences from the NCBI database. Multiple sequence alignment was performed using ClustalW through the BioEdit Sequence Alignment Editor (164). Thereafter, a maximum likelihood (ML) phylogenetic tree was constructed using RaxmlGUI 2.0 (165) with optimized model parameters and branch length for the given tree and 1000 bootstrap replicates. The phylogenetic tree was visualized and edited on iTOL (166).

2.6 Evaluation of target gene expression level by RT-PCR

The RT-qPCR molecular test was utilized to assess the levels of gene expression using cDNA molecules derived from the 45 co-infected and 45 non-TB-HIV infected tissue specimens. The reaction cocktail was comprised of 2× iTaq Universal SYBR Green Supermix (Bio-Rad,CA, USA), 10 pmol of each candidate gene-specific primer (Integrated DNA Technologies, IA, USA) and 2 µl cDNA (100 ng/µl). All the primers utilized in our study were designed using Primer3 software and were purchase from Integrated DNA technologies. The primer sequences used for RT-qPCR experiments are depicted in Table 2.3. The Light Cycler® 480 II (Roche Diagnostics, Germany) was used for cDNA amplification.

TABLE 2.2. SEQUENCES OF PRIMERS USED IN RT-QPCR TO AMPLIFY TARGET CANDIDATE GENES AND TO DETERMINE GENE EXPRESSION.

Primer name	Orientation	Primer sequence
Human CIITA F Human CIITA R	Forward Reverse	5’-AGAAGTCCAAGGTTAGGGGC-3’ 5’-GGGTTGTCGTGGGAGTAAGA-3’

Human HAT F Human HAT R	Forward Reverse	5'-CCCGTGGTGACTGTTTTTCT-3' 5'-ATGCCCTTACCTCACACCTG-3'
Human DNMT1 F Human DNMT1 R	Reverse Forward	5'-GTGGGGGACTGTGTCTCTGT-3' 5'-AGGAGCACTCGTCCTTTTCA-3'
Human SETDB2 F Human SETDB2 R	Forward Reverse	5'-AAATGACTGGCTTGCCAAGG-3' 5'-TAACACACTGCTCGGGAAGT-3'
Human KMT F Human KMT R	Forward Reverse	5`-TCAACCTGCTCTCCTTCCAG-3` 5`-AAGGGAAGAACAGGGATGGG-3`
Human GAPDH F Human GAPDH R	Forward Reverse	5'-CCCTAGTCCCCAGAAACAGG-3' 5'-ATTTCCTTCCCGGTTGCAAC-3'

The cycling conditions were programmed as follows: hot start at 95°C for 30 seconds, followed by 40 cycles of denaturation at 95°C for 15 seconds, annealing at 53°C for 30 seconds, and extension at 72°C for 30 seconds. The real-time mastermix or supermix that we applied to detect target gene expression contained SYBR Green dye. SYBR Green is an intercalating dye or a fluorescent dye that binds to DNA during the elongation step of PCR in a sequence-independent manner. This allows fluorescent detection and quantification of amplified DNA molecules. A high intensity indicates high level of DNA, while a low fluorescent intensity corresponds to low levels. With regard to gene expression, a high SYBR Green fluorescence intensity implies high target gene expression. Conversely, a low SYBR Green fluorescent intensity indicates low expression levels. To compare the rate of gene expression, a reference gene *glyceraldehyde 3-phosphate dehydrogenase* (*GAPDH*) was exploited as a positive control. No-template samples and water blanks were included to validate each RT-qPCR reaction. The level of gene expression was analyzed using the crossing-point analysis, which determines the amount of DNA at threshold, and the specificity of the amplification was determined using the melting curve analysis, which examines DNA after temperature-dependent separation of the strands into single strands. Data were surveyed from 45 samples representing TB-HIV co-infected and 45 non-TB-HIV controls, and the level of expression was calculated using the formula:

$$\Delta Cq = Cq_{target} - Cq_{reference}$$

Cq represents the average Cq value of the target gene minus the *GAPDH* reference gene in the same sample

2.7 Protein Isolation and Analysis for the TB-HIV co-infected and control group

Proteins were isolated from lymph node specimens using the Qproteome FFPE Tissue Kit (Qiagen, GmbH, Germany), with minor modifications. The FFPE samples were cut using a rotary microtome set at 10 µm. Thereafter, five (5) tissue sections were transferred into 1.5 ml Eppendorf tubes and paraffin was removed by aliquoting one milliliter (1 ml) of xylene into each tube. The mixture was vortexed for 10 seconds and incubated for 10 minutes at room temperature. All the samples were centrifuged at a maximum speed of 13,000 × g for 2 minutes, and the supernatant was discarded. The graded alcohol solutions of 100% ethanol, 96% ethanol, and 70% ethanol, respectively, were used to remove xylene and hydrate the tissues, followed by centrifuging at 13,000 × g for 2 minutes. The samples were incubated for 10 minutes at room temperature, and the supernatant was removed. Proteins were extracted by adding 100 µl of the extraction buffer supplemented with β-mercaptoethanol into each tube containing the pellet and mixed by vortexing. The samples were incubated on ice for 5 minutes and subjected to heating at 100°C on a heating block for 20 minutes using a thermomixer (Thermo Fisher Scientific, MA, USA). An additional incubation step was conducted at 80°C for 2 hours with agitation at 750rpm. Subsequently, the sample tubes were placed on ice for a minute and centrifuged for 15 minutes at 13,000 × g to ensure the protein extracts were free from contaminants. The supernatant containing the extracted proteins was transferred to a new and sterile 1.5 ml Eppendorf tube. Protein purity was assessed by measuring absorbance at 280 nm using a NanoDrop, and the isolated protein samples were stored at -20°C. (The procedure has antibodies that have high affinity and specificity for the target proteins).

2.8 Determination of Protein Levels in TB-HIV co-infected and control groups using the Histone H3 Modification Multiplex Assay

The histone3 (H3) modification multiplex assay kit (LifeSpan Biosciences, WA, USA) was utilized to determine the degree of histone methylation, acetylation, and phosphorylation in human lymph node biopsies retrieved from 45 TB-HIV co-infected and 45 non-TB-HIV individuals. The purpose of performing the H3 multiplex assay was to investigate and quantify the degree of protein acetylation, methylation and Phosphorylation on the histone 3 protein. These modifications were assessed from protein samples extracted from TB-HIV patients and control subjects. For this experiment, we utilized the histone3 (H3) modification multiplex assay kit comprised of anti-acetylation, anti-methylation and anti-phosphorylation

antibodies. As such, the kit allows simultaneous detection of 21 different protein modification patterns present on histone3 following binding of anti-acetylation, anti-methylation, and anti-phosphorylation antibodies to protein samples. We evaluated these protein modifications on histone3 as it is one of the primary proteins that are highly susceptible to microbial-mediated epigenetic regulation.

Briefly, the protein molecules were diluted to a final concentration of 100 ng/µl with 1× wash buffer, and 4 µl of this sample was mixed with 46 µl antibody buffer and transferred to a corresponding well in a 96-well microtiter plate. The control wells were comprised of 49 µl antibody buffer and µl assay control proteins diluted to 5 and 25 ng/µl (The low concentration along with high concentration control samples were used to generate proportional concentration-intensity) diluted to 5 and 25 ng/µl. The microtiter plate was covered with an adhesive film and incubated at 37°C for 2 hours, resulting in the binding between the antibody buffer and the H3 histone proteins (The blank controls contained 49 µL and only two replicates were used). The solution was removed from each well by aspiration and washed three times with 150 µl of 1× wash buffer. For antibody binding and signal enhancing, 50 µl detection antibody (1:1000 in 1× wash buffer) was dispensed to each well, covered with adhesive film, and incubated for 1 hour at room temperature. The detection antibody was removed by aspiration and subjected to three washing cycles with 1× wash buffer. To improve signal detection, 100 µl developer solution was transferred to each sample well, followed by a 10-minute incubation step in the dark at ambient temperature. Finally, the reaction was inactivated by the addition of 100 µl stop solution, which prevents binding between the detection antibody and developer solution. The degree of H3 histone acetylation, methylation, and phosphorylation was quantified by measuring the absorbance at 450 nm using the iMarkTM microplate reader (Bio-Rad, CA, USA). The relative change in H3 modification between the TB-HIV co-infected and control samples was calculated using the formula:

$$\frac{(Sample\ OD - Blank\ OD) \div S}{(Assay\ Control\ OD - Blank\ OD) \div P} = \times 1000$$

2.9 Statistical Analysis

The gene expression data and protein results were analysed using the GraphPad Prism software version 7 (GraphPad Software Inc., CA, USA) by applying the non-parametric

student t-tests. Data were considered statistically significant when $p < 0.05$. The RT-qPCR and histone3 (H3) modification multiplex assay data was collected from two independent experiments, and all replicates were pooled for analysis. Descriptive statistics were used to summarize demographic data. Numerical variables were assessed for normality using the Shapiro-Wilk test, with a P-value >0.05 indicating a normal distribution. Normally distributed variables were summarized as mean ± standard deviation (SD), while non-normally distributed variables were presented as median and interquartile range (IQR). Categorical variables were summarized using frequencies and percentages. Comparative analyses were performed between 45 control cases and 45 TB-HIV co-infected cases. Statistical significance was defined as $p < 0.05$. The Wilcoxon rank-sum test was used to assess the association between gender and gene/protein expression levels, as gender is a binary categorical variable and the expression data were non-parametric. The Kruskal-Wallis test was used to evaluate the association between race (a categorical variable with more than two groups) and gene/protein expression. The Spearman's rank correlation was used to assess the relationship between age and gene/protein expression.

Chapter 3: Results

3.1. Demographic characteristics of the tissue samples from the TB-HIV co-infected and the control cohort.

A total of 90 FFPE tissues were included in the study, comprising 45 TB-HIV co-infected and 45 non-TB-HIV samples. The HIV-TB co-infected tissue samples had other clinical conditions such as Kaposi sarcoma, palatal ulcers, erythema induratum, lupus panniculitis, and necrotizing granulomas. In contrast, the control group comprised tissue samples without TB, HIV or any documented history of cancer, hypertension, diabetes, allergies, or other major systemic illnesses at the time of biopsy collection. However, the control group did present with conditions including renovascular disease, pancytopenia, pleurisy, hepatosplenomegaly, inflammatory bowel disease, and gastroesophageal reflux disease. The mean age in the TB-HIV cohort was 37 ± SD years and ranged between 22 and 57 years. The majority of tissue samples in this group were from males (n = 25, 55.6%), and most were identified as African (n = 20, 44.4%), followed by Asian (n = 15, 33.3%) and Caucasian (n = 10, 22.2%). Among the TB-HIV group, the mean CD4 count was 263.6 cells/mm³ with values ranging from 140 to 344 cells/mm³. The demographic profiles of the TB-HIV group are depicted in Table 2.1.

TABLE 3.1: DEMOGRAPHIC CHARACTERISTICS FOR THE TB-HIV AND THE CONTROL GROUP

Characteristics	**TB-HIV group**	**Control group**	**p- value**
CD4 count, cells/mm3	9 ± 73.4	—	N/A
Age, mean ±SD (year range)	37 ± 9.9 (22-57)	39.7 ± 8.2 (27-59)	0.9073
Gender			
Male, n (%)	20 (55.6%)	20 (44.4%)	1.000
Female, n (%)	25 (44.4%)	25(55.6%)	
Race			
African, n (%)	20 (44.4 %)	20, (44.4%)	1.000
Caucasian, n (%)	15, (33.3%)	15, (33.3%)	
Asian, n (%)	10, (22.2 %)	10, (22.2%)	

In the control group, the mean age was slightly higher at 39.7 ± 8.2 years, ranging from 27 to 59 years. Females made up a larger proportion of this group (n = 25, 55.6%) compared to

males (n = 20, 44.4%). Similar to the TB-HIV group, most tissue samples in the control group were from African (n = 20, 44.4%), followed by Caucasian (n = 15, 33.3%) and Asian (n = 10, 22.2%) (Table 3.1).

3.2. Conventional PCR to confirm TB-HIV co-infection

Conventional PCR was utilized to amplify cDNA obtained from 10 selected FFPE tissue samples by targeting the HIV *gag-pol* and *Mtb rpoB* genes, both associated with microbial virulence. Sample selection was based on cDNA purity and yield, as determined by spectrophotometric analysis using a NanoDrop instrument. Successful amplification of the HIV *gag-pol* and *Mtb rpoB* gene regions was observed in cDNA from the TB-HIV co-infected samples (Figure 3.1 and Figure 3.2). The observed amplicon sizes were approximately 120 bp for HIV *gag-pol* (Figure 3.1) and 110 bp for *Mtb rpoB* (Figure 3.2). No amplification was detected in the no-template controls, confirming the absence of DNA contamination.

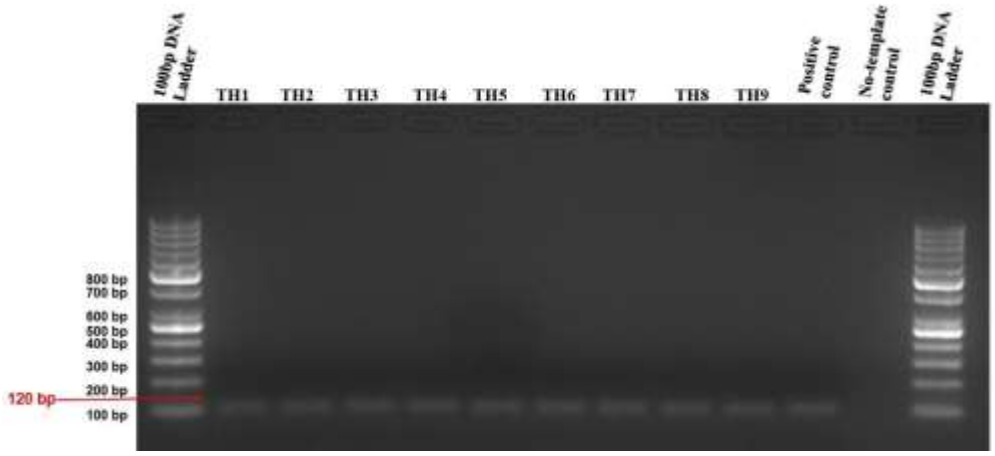


FIGURE 3.1: AMPLIFICATION OF HIV *GAG-POL* GENE BY CONVENTIONAL PCR.

Total RNA was extracted from TB-HIV co-infected individuals (TH1-TH9) and subjected to reverse transcription to produce cDNA. The synthesized cDNA molecules were amplified by conventional PCR using primers specific for the HIV *gag-pol*. Agarose gel electrophoresis revealed the expected PCR products of 120 bp, except in the no-template control.

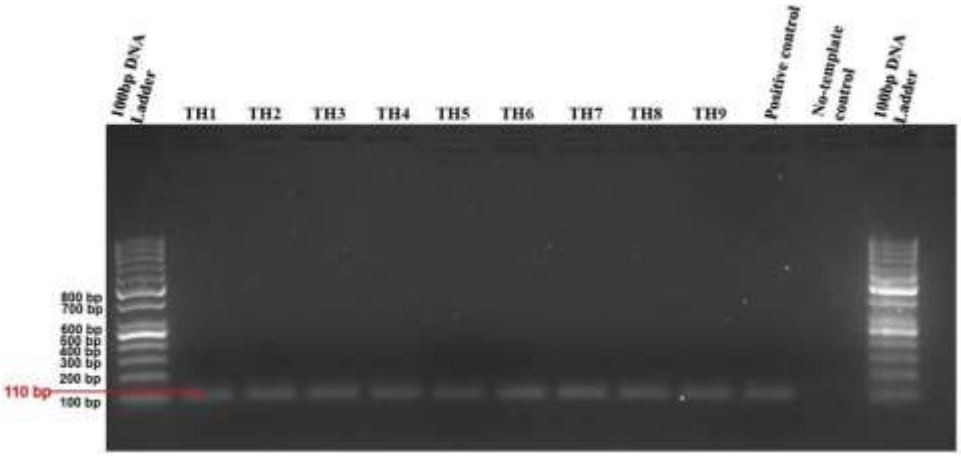


FIGURE 3.2: AMPLIFICATION OF *MTB RPOB* GENE BY CONVENTIONAL PCR.

Total RNA was extracted from TB-HIV co-infected individuals (TH1-TH9) and subjected to reverse transcription to produce cDNA. The synthesized cDNA molecules were amplified by conventional PCR using primers specific for the *Mtb rpoB* gene. Agarose gel electrophoresis revealed the expected PCR products of 110 bp except in the no-template control.

3.3 Sequence and phylogenetic analysis

3.3.1 HIV-1 sequences

The 120 bp HIV *gag-pol* and 110 bp *Mtb rpoB* PCR amplicons were successfully sequenced at Inqaba Biotechnical Industries. The BLAST analysis revealed that the HIV-1 sequences from the ten tissue samples in our study have varying degrees of sequence similarity to the reference strains in the LANL HIV Sequence Database. The majority of sequences (80%, n=8/10) aligned closely with the CN54 strain (accession AX149648), classified as intersubtype 07_BC, originally isolated in China in 1997. These matches exhibited a high percent identity ranging from 93% to 99%, with E-values between 1.00E-20 and 5.00E-02, indicating statistically significant alignments (Table 3.2). Notably, the HIV-1 sequence from tissue sample TH1 showed the highest similarity, with 99% identity and an E-value of 1.00E-20, suggesting a strong match to the reference sequence. Whereas the HIV-1 sequence from tissue sample TH3, despite having a relatively high bit score (103), showed a lower percent identity (93%) and a higher E-value (5.00E-02). This observation may reflect partial alignment or sequence divergence. The remaining two HIV-1 sequences from our study cohort matched subtypes A and C. Specifically, the HIV-1 sequence from tissue sample TH6

matched a subtype A reference from Ghana (MN402732) with 88% identity and a bit score of 108. By contrast, the sequence from tissue sample TH7 aligned with a subtype C reference (DJ044212) with 94% identity and the highest bit score of 112, indicating a strong and statistically significant match (Table 3.2).

TABLE 3.2. SUMMARY OF HIV-1 BLAST RESULTS FOR TEN ISOLATES QUERIED AGAINST THE LANL HIV SEQUENCE DATABASE.

Sample ID	Accession Number	Subtype	Country (year)	Identities	E- value	Score (bits)
TH1	AX149648	07_BC	China (1997)	99%	1,00E-20	102
TH2	AX149648	07_BC	China (1997)	96%	2,00E-18	95
TH3	AX149648	07_BC	China (1997)	93%	5,00E-02	103
TH4	AX149648	07_BC	China (1997)	97%	8,00E-19	96.5
TH5	AX149648	07_BC	China (1997)	96%	2,00E-18	95
TH6	MN402732	A	Ghana (N/A)	88%	2,00E-22	108
TH7	DJ044212	C	N/A	94%	1,00E-23	112
TH8	AX149648	07_BC	China (1997)	95%	4,00E-16	87.5
TH9	AX149648	07_BC	China (1997)	95%	1,00E-16	89
TH10	AX149648	07_BC	China (1997)	95%	1,00E-16	89

N/A – not available

Multiple sequence alignment revealed regions of high conservation among the study HIV-1 sequences, indicating genetic similarity within the cohort (Figure 3.3 and Figure 3.4). Distinct sequence patterns were observed between the HIV-1 reference subtypes from the LANL HIV Sequence Database and the HIV-1 sequences from this study (Figure 3.3). Additionally, multiple sequence alignment with the 10 additional reference HIV-1 sequences retrieved from the NCBI database revealed conserved regions shared between the study HIV-1 sequences and the publicly available HIV-1 sequences from the NCBI database (Figure 3.4).



FIGURE 3.3 MULTIPLE SEQUENCE ALIGNMENT OF THE 10 HIV-1 SEQUENCES FROM THIS STUDY ALONGSIDE REFERENCE SEQUENCES FOR HIV-1 SUBTYPES A, B, AND C OBTAINED FROM THE LANL HIV SEQUENCE DATABASE.

The alignment was performed using ClustalW through the BioEdit Sequence Alignment Editor. Color-coded nucleotides (A = red, T = green, G = blue, C = black) facilitated visual identification of conserved and variable gene regions within the HIV-1 strains.

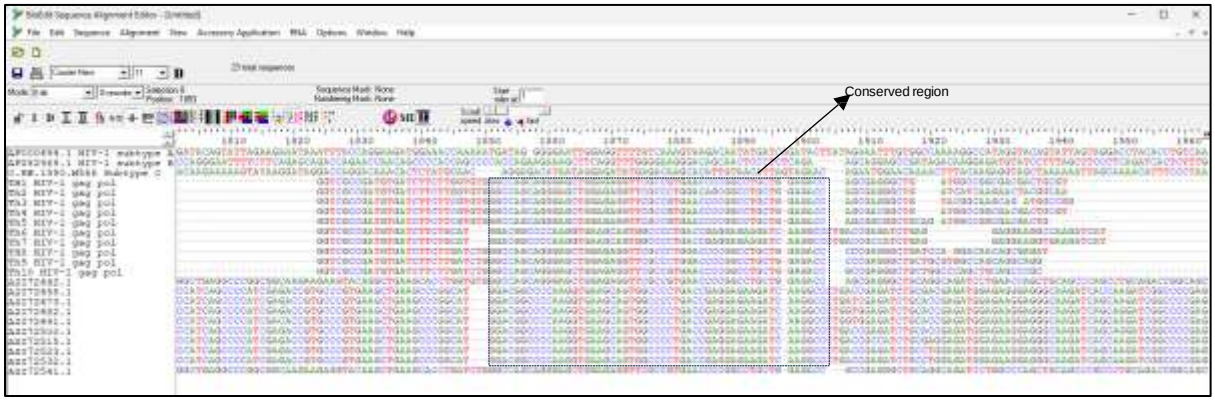


FIGURE 3.4. MULTIPLE SEQUENCE ALIGNMENT OF THE 10 HIV-1 SEQUENCES FROM THIS STUDY ALONGSIDE REFERENCE SEQUENCES FOR HIV-1 SUBTYPES A, B, AND C OBTAINED FROM THE LANL HIV SEQUENCE DATABASE, AS WELL AS 10 HIV-1 SEQUENCES FROM THE NCBI DATABASE.

The alignment was performed using ClustalW through the BioEdit Sequence Alignment Editor. Color-coded nucleotides (A = red, T = green, G = blue, C = black) facilitated visual identification of conserved and variable gene regions of HIV-1 strains.

Phylogenetic analysis assessed the evolutionary relationships between HIV-1 sequences from this study, HIV-1 reference sequences representing subtypes A, B, and C, as well as 10 HIV-1 reference sequences from the NCBI database. The resulting Maximum likelihood tree revealed three distinct clusters. The first cluster contained the three reference sequences

representing subtypes A, B, and C, which are genetically divergent from the study sequences as well as the HIV-1 reference sequences from the NCBI Database (Figure 3.5). Notably, Cluster 2 and Cluster 3 showed a monophyletic relationship with each other, indicating that the sequences within these two clusters share a common ancestor and are more closely related. This monophyletic relationship was supported by a bootstrap value of 96, confirming the reliability of the branching patterns. Specifically, Cluster 2 contained eight HIV-1 sequences from this study, forming a close relationship with each other as well as with two reference HIV-1 sequences (AZI7244.1 and AZI7254.1) from the NCBI database (Figure 3.5). Similarly, HIV-1 sequences from tissue samples TH6 and TH7 formed a close relation with eight reference HIV-1 sequences from the NCBI database in cluster 3. The close monophyletic relationship observed in cluster 3 was strongly supported by a bootstrap value of 84.5 (Figure 3.5).

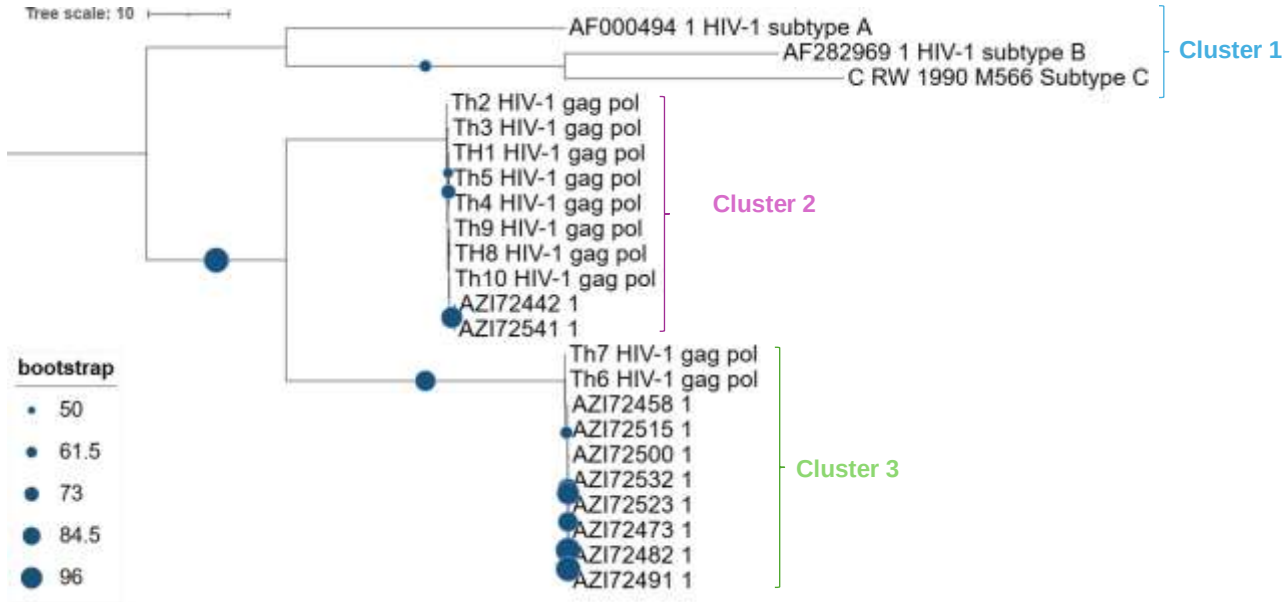


FIGURE 3.5. MAXIMUM LIKELIHOOD TREE CONSTRUCTED USING RAXMLGUI 2.0 WITH A BOOTSTRAPPING STRINGENCY OF 1000.

The nucleotide sequences of 10 HIV-1 sequences from this study, 10 HIV-1 sequences from the NCBI database, and three HIV-1 subtypes A, B, and C sequences from the LANL HIV sequence database were employed for phylogenetic analysis. The sequences were aligned using ClustalW through the BioEdit Sequence Alignment Editor. The phylogenetic tree was rooted at the midpoint, and the branch lengths indicate the genetic distance and are depicted by the bar (0.1). Bootstrap support values, represented by blue circles of varying sizes, ranged from 50 to 96, with larger circles indicating higher confidence in the branching patterns.

3.3.2 *Mtb* sequences

The BLAST results for the *Mtb* sequences are presented in Table 3.2. The majority of the sequences (90%, n=9/10) aligned with the *Mycobacterium tuberculosis* strain CP085590.1, while one sequence (Mtb07) matched the *rpoB* gene sequence for accession number KY087999.1 (Table 3.3). Sequence identity ranged from 88.37% to 100%, with Mtb01 and Mtb03 showing perfect identity (100%) to the reference strain CP085590.1. The highest query coverage was observed in Mtb02 (84%) and Mtb03 (83%), indicating substantial alignment with the reference genome in the NCBI database (Table 3.3).

The lowest identity was recorded for Mtb08 (88.37%), although its query coverage remained relatively high at 72%. Multiple sequence alignment of the *Mtb* sequences, including the nine reference sequences, revealed regions of high conservation among the reference *Mtb* sequences, indicating genetic similarity within these sequences. Moreover, conserved regions and distinct sequence patterns were observed between the *Mtb* sequences obtained in this study (Figure 3.6).

TABLE 3.3. SUMMARY OF *MTB* BLAST RESULTS FOR TEN ISOLATES QUERIED.

Sample ID	Sequence ID	Accession Number	Description	Identity	E- value	query cover
TH1	Mtb01	CP085590.1	*Mycobacterium tuberculosis* strain	100%	9,00E-33	68%
TH2	Mtb02	CP085590.1	*Mycobacterium tuberculosis* strain	98.02%	6,00E-40	84%
TH3	Mtb03	CP085590.1	*Mycobacterium tuberculosis* strain	100%	9,00E-43	83%
TH4	Mtb04	CP085590.1	*Mycobacterium tuberculosis* strain	95.51%	6,00E-30	74%
TH5	Mtb05	CP085590.1	*Mycobacterium tuberculosis* strain	93.48%	3,00E+28	77%
TH6	Mtb06	CP085590.1	*Mycobacterium tuberculosis* strain	90.11%	1,00E-22	76%
TH7	Mtb07	KY087999.1	*Mycobacterium tuberculosis rpoB* gene	98.77%	2,00E-30	68%
TH8	Mtb08	CP085590.1	*Mycobacterium tuberculosis* strain	88.37%	3,00E-18	72%
TH9	Mtb09	CP085590.1	*Mycobacterium tuberculosis* strain	97.56%	2,00E-29	68%
TH10	Mtb10	CP085590.1	*Mycobacterium tuberculosis* strain	92.68%	1,00E-22	68%

Phylogenetic analysis of the *Mtb rpoB* gene sequences revealed two distinct clusters, namely cluster 1 and cluster 2 (Figure 3.7). The first cluster contained five *Mtb* sequences derived from this study. However, this cluster had no bootstrap values supporting the relationship. Nevertheless, within this cluster, *Mtb* sequence Mtb09 and Mtb10 showed a close relationship with a bootstrap value of 93. Moreover, these sequences exhibited a

monophyletic relationship with *Mtb* sequences Mtb07 and Mtb01, with a bootstrap value of 91, supporting the relationship and indicating strong confidence in shared ancestry (Figure 3.7).

The second cluster, supported by a bootstrap value of 56, was the largest and contained five *Mtb* sequences from this study, together with the nine *Mtb* reference sequences from the NCBI database (Figure 3.7). The latter *Mtb* sequences formed a tight cluster with a bootstrap value of 100, supporting their shared ancestry. Furthermore, these sequences formed a monophyletic relationship with Mtb03 with a bootstrap value of 77 to support the relationship (Figure 3.7).



FIGURE 3.6: MULTIPLE SEQUENCE ALIGNMENT OF 10 *MTB* SEQUENCES FROM THIS STUDY ALONGSIDE NINE *MTB* REFERENCE SEQUENCES FROM THE NCBI DATABASE.

The alignment was performed using ClustalW through the BioEdit Sequence Alignment Editor. Color-coded nucleotides (A = red, T = green, G = blue, C = black) facilitated visual identification of conserved and variable gene regions of the *Mtb* strains.

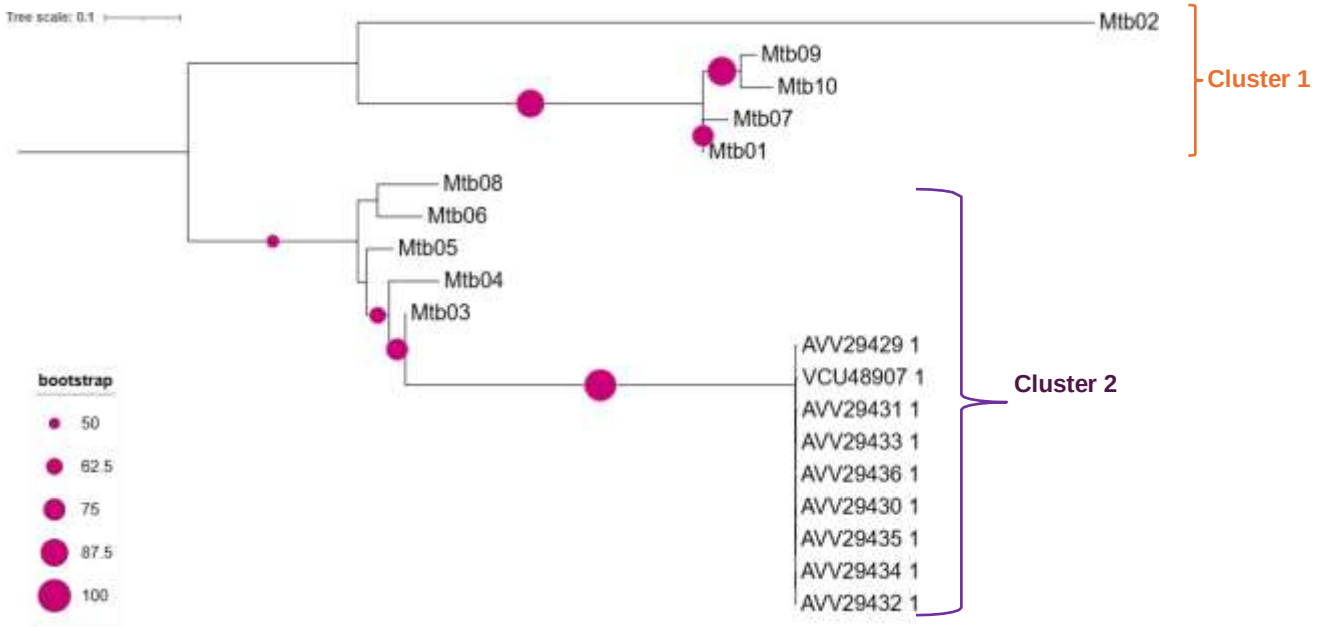
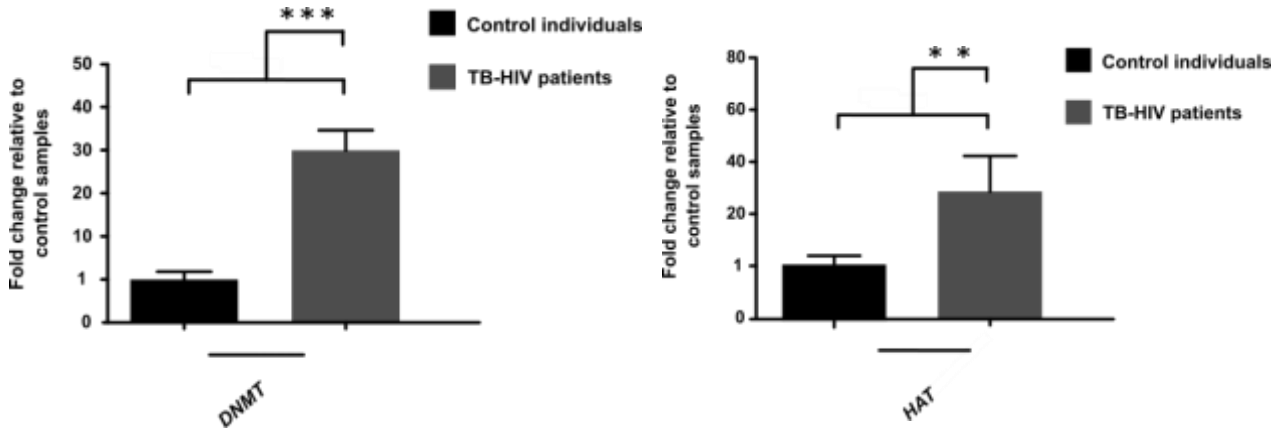


FIGURE 3.7. MAXIMUM LIKELIHOOD TREE CONSTRUCTED USING RAXMLGUI 2.0 WITH A BOOTSTRAPPING STRINGENCY OF 1000.

The nucleotide sequences of 10 *Mtb* sequences from this study and nine *Mtb* reference sequences from the NCBI database were employed for phylogenetic analysis. The sequences were aligned using ClustalW through the BioEdit Sequence Alignment Editor. The phylogenetic tree was rooted at the midpoint, and the branch lengths indicate the genetic distance and are depicted by the bar (0.1). Bootstrap support values, represented by purple circles of varying sizes, ranged from 50 to 100, with larger circles indicating higher confidence in the branching patterns.

3.4. RT-PCR to detect the expression of genes associated with DNA methylation, histone acetylation, and histone methylation.

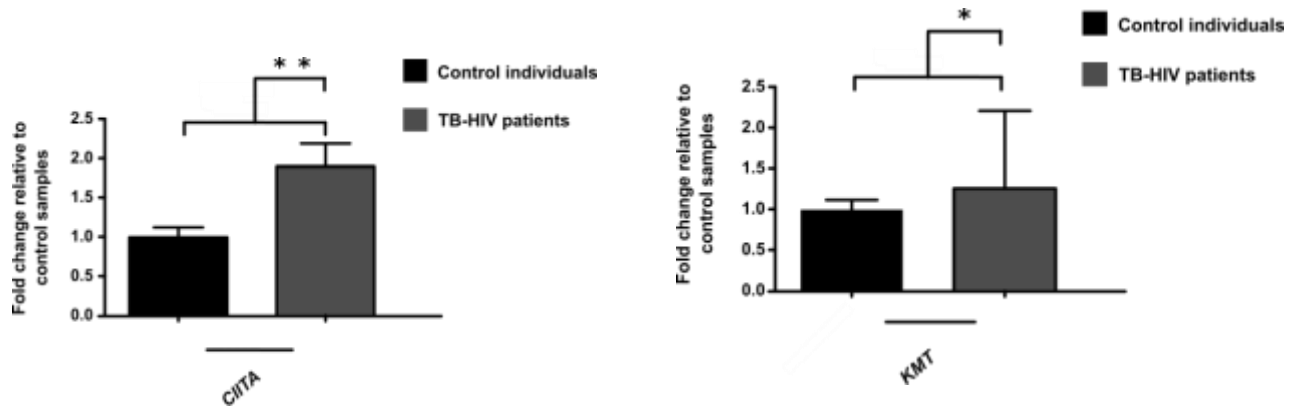
The RT-qPCR analysis revealed significantly elevated expression levels of *DNMT1* and *HAT* genes in the TB-HIV co-infected cohort in comparison to the control cohort (Figure 3.8). Both these genes are key regulators of DNA methylation. Specifically, the *DNMT1* gene was upregulated 30-fold in the TB-HIV co-infected cohort in comparison to the control group with $p<0.01$ (Figure 3.8). Similarly, the *HAT* gene in the TB-HIV cohort was significantly upregulated, by up to 30-fold compared to the control group with $P<0.001$ (Figure 3.8).



FIGURES 3.8. *DNMT1* AND *HAT* GENE EXPRESSION IN THE TB-HIV HIV CO-INFECTED COHORT RELATIVE TO THE CONTROL GROUP.

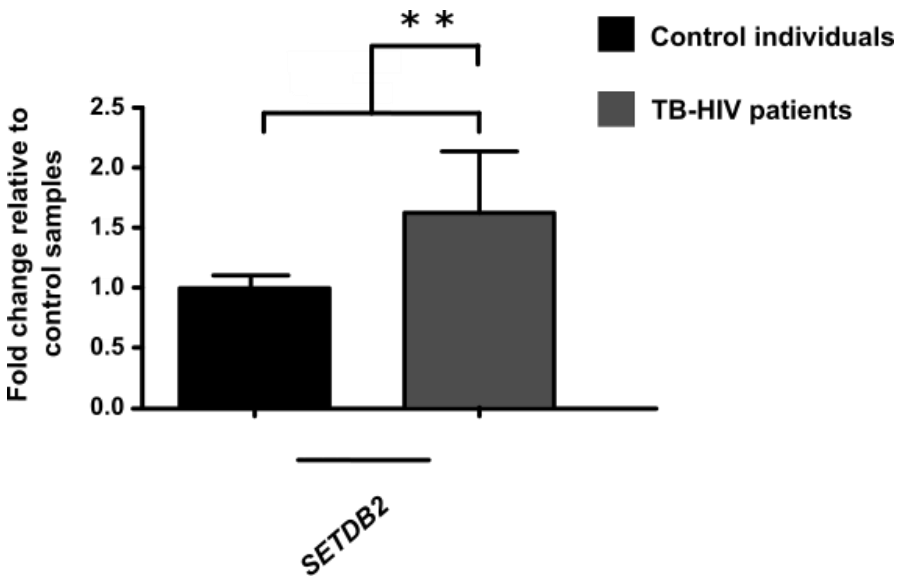
Total RNA was extracted from FFPE specimens retrieved from control subjects and TB-HIV co-infected patients, and 1 µg was used for cDNA synthesis. Target gene amplification and quantification were accomplished by RT-qPCR using primers specific for the *DNMT1* and *HAT* genes. Data were obtained from 90 samples representing control individuals (n=45) and TB-HIV co-infected patients (n=45). Values depict the means ±SEM, and statistical analysis was conducted using the non-parametric t-test contained in the GraphPad Prism software. The values $p \leq 0.05$, $^{**}p \leq 0.01$, and $^{***}p \leq 0.001$ indicated statistical significance between the control and experimental samples. The RT-qPCR data were obtained from two independent experiments, and all replicates were pooled for analysis.

Similarly, there was a significant upregulation of the *CIITA* and *KMT* genes in the TB-HIV cohort relative to the control group (Figure 3.9). These genes play critical roles in histone acetylation. In comparison with control groups, the expression of *CIITA* and *KMT* in the TB-HIV cohort increased by approximately 1.8-fold and 1.3-fold, with p values less than 0.01 and 0.05, respectively (Figure 3.9). A similar trend was also observed for the *SETDB2* gene, which is an important regulator of DNA methylation. This gene was significantly upregulated approximately 1.6-fold in the TB-HIV cohort relative to the control group, with a $p< 0.01$ (Figure 3.10).



FIGURES 3.9. *CIITA* AND *KMT* GENE EXPRESSION IN THE TB-HIV CO-INFECTED COHORT RELATIVE TO THE CONTROL GROUP.

Total RNA was extracted from FFPE specimens retrieved from control subjects and TB-HIV co-infected patients, and 1 µg was used for cDNA synthesis. Target gene amplification and quantification were accomplished by RT-qPCR using primers specific for *CIITA* and *KMT* gene. Data were obtained from 90 samples representing control individuals (n=45) and TB-HIV co-infected patients (n=45). Values depict the means ±SEM, and statistical analysis was conducted using the non-parametric t-test contained in the GraphPad Prism software. The values $p \leq 0.05$, $^{**}p \leq 0.01$, and $^{***}p \leq 0.001$ indicated statistical significance between the control and experimental samples. The data were obtained from two independent experiments, and all replicates were pooled for analysis.



FIGURES 3.10. *SETDB2* GENE EXPRESSION IN THE TB-HIV CO-INFECTED COHORT RELATIVE TO THE CONTROL GROUP.

Total RNA was extracted from FFPE specimens retrieved from control subjects and TB-HIV co-infected patients, and 1 µg was used for cDNA synthesis. Target gene amplification and quantification were accomplished by RT-qPCR using primers specific for the *SETDB2* gene. Data were obtained from 90 samples representing control individuals (n=45) and TB-HIV co-infected patients (n=45). Values depict the means ±SEM, and statistical analysis was conducted using the non-parametric t-test contained in the GraphPad Prism software. The values $p \leq 0.05$, $^{**}p \leq 0.01$, and $^{***}p \leq 0.001$ indicated statistical significance between the control and experimental samples. The RT-qPCR results were collected from two independent experiments, and all replicates were pooled for analysis.

3.5 Association of gene expression with demographics

3.5.1 Correlation of age and gene expression in the TB-HIV co-infected cohort

Spearman's correlation coefficient analysed the association between age and gene expression of epigenetic markers (*DNMT, HAT, KMT, CIITA, and SETDB2*) in the TB-HIV co-infected group. Correlation coefficients (r) were weak and ranged from –0.0347 to 0.2009, with corresponding 95% confidence intervals crossing zero, indicating no consistent direction of association (Figure 3.11 and Table 3.4). None of the correlations reached statistical significance ($p > 0.05$), suggesting that age did not influence the expression levels of the examined epigenetic markers in this cohort (Figure 3.11).

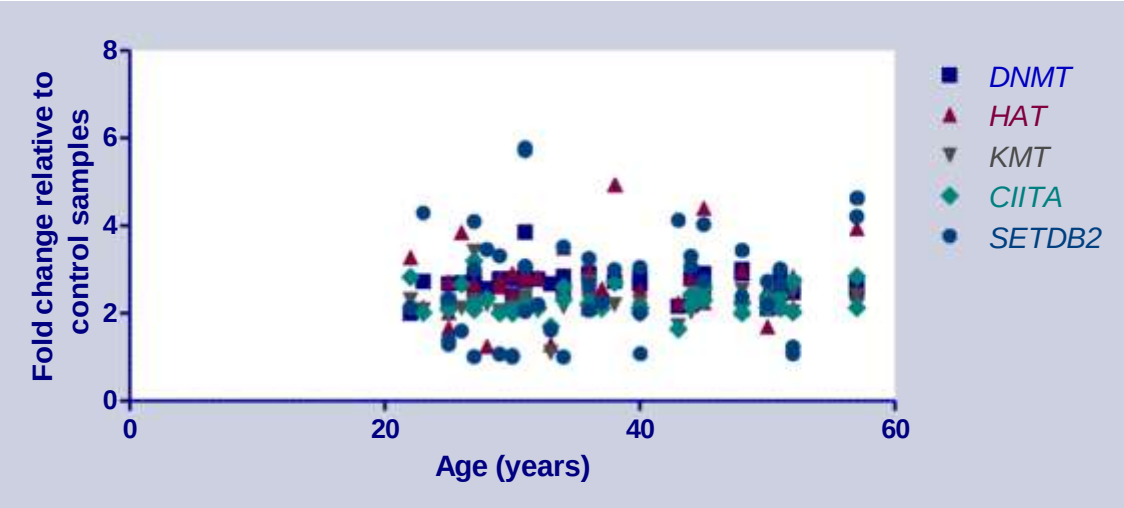


FIGURE 3.11. ASSOCIATION OF AGE WITH THE GENE EXPRESSION OF EPIGENETIC MARKERS, *DNMT*, *HAT*, *KMT*, *CIITA*, AND *SETDB2* IN THE TB-HIV CO-INFECTED COHORT.

The association between gene expression of the respective genes with age was determined using Spearman's rank correlation.

TABLE 3.4. ASSOCIATION OF AGE WITH THE GENE EXPRESSION OF EPIGENETIC MARKERS, DNMT, HAT, KMT, CIITA, AND SETDB2 IN THE TB-HIV CO-INFECTED COHORT.

Parameter	*DNMT*	*HAT*	*KMT*	*CIITA*	*SETDB2*
Number of XY Pairs	45	45	45	45	45
Spearman r	-0,03470	0,002407	0,2009	0,1265	0,1713
95% confidence interval	-0.3330 to 0.2699	-0.2996 to 0.3039	-0.1073 to 0.4740	-0.1822 to 0.4125	-0.1375 to 0.4498
P-value (two-tailed)	0,8210	0,9875	0,1856	0,4076	0,2604
P-value summary	ns	ns	ns	ns	ns

ns- not significant

3.5.2 Association of gene expression with gender in the TB-HIV co-infected cohort.

The Wilcoxon rank-sum test was applied to assess the association between gender and the expression levels of the *DNMT*, *HAT*, *KMT*, *CIITA*, and *SETDB2* genes in the TB-HIV co-infected cohorts. A statistically significant association with gender was detected for the *DNMT* gene, supported by a positive Z-score of 2.46. However, the remaining genes (*DNMT*, *HAT*, and *KMT*) did not show a significant association with gender in the TB-HIV group (Figure 3.12). These results suggest that gender-related differences in gene expression are specifically evident for the *DNMT* gene in the TB-HIV co-infection context but not in the control group (Figure 3.12).

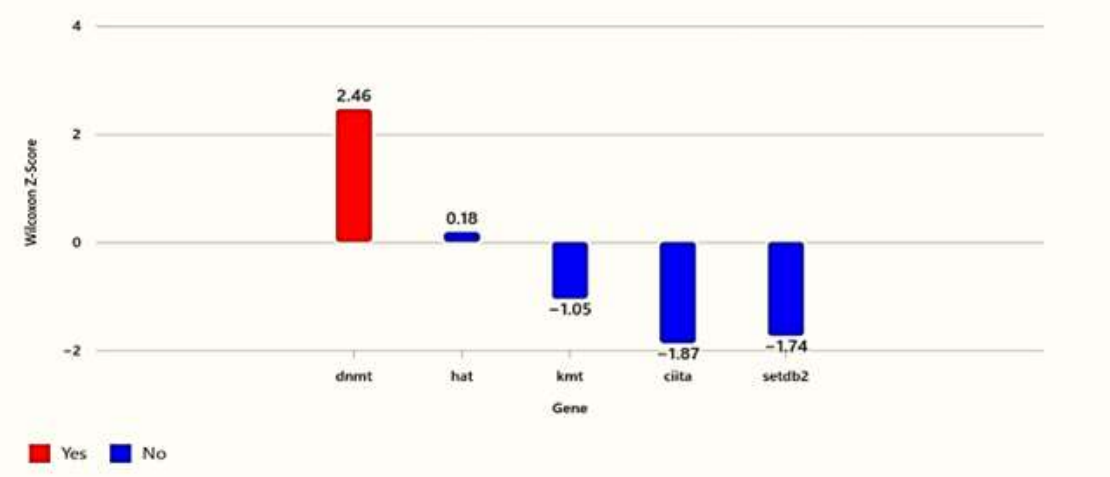


FIGURE 3.12. THE ASSOCIATION BETWEEN GENDER AND EXPRESSION LEVELS OF FIVE GENES BASED ON THE WILCOXON RANK-SUM TEST RESULTS IN THE TB-HIV CO-INFECTED COHORT.

The red bar means that there is an association between the upregulated gene and gender. Whereas the blue bar means that there is no association between the upregulated genes and gender.

3.5.3 Association of gene expression with race

The *CIITA* and *SETDB2* genes show statistically significant differences in expression across races. Specifically, statistically significant associations with race were detected for *CIITA* (χ^2 = 15.168, p = 0.0005) and *SETDB2* (χ^2 = 8.738, p = 0.0127) in the TB-HIV cohort, with African participants contributing the highest rank sums (Table 3.5). For both genes, African individuals had the highest rank sum, suggesting higher expression levels within this racial group compared to the other racial groups (Table 3.5).

TABLE 3.5. ASSOCIATION OF RACE WITH GENE EXPRESSIONS IN CONTROL AND TB-HIV CO-INFECTED GROUPS.

Gene	Cohort	Chi² (with ties)	p-value	Significant (p < 0.05)	Race with the highest rank sum
DNMT	Control	0.000	1.0000	No	African
	TB-HIV	2.053	0.3583	No	Caucasian
HAT	Control	0.000	1.0000	No	African
	TB-HIV	0.428	0.8073	No	Caucasian
KMT	Control	0.000	1.0000	No	African
	TB-HIV	5.169	0.0754	No	African

CIITA	Control	0.000	1.0000	No	African
	TB-HIV	15.168	0.0005	Yes	African
SETDB2	Control	0.360	0.8353	No	African
	TB-HIV	8.738	0.0127	Yes	African

Red colour indicates statistical significance ($p<0.001$)

3.6 H3 multiplex assay to detect epigenetic modification patterns

Figure 3.13 illustrates the comparative levels of H3 histone epigenetic modifications in tissue samples in the control and TB-HIV co-infected groups. Epigenetic activity was quantified using optical density (OD) measurements, with values ranging from 0.0 to 1.5. The control group, represented by black bars, exhibited OD values between 0.0 and 0.5. Whereas, in the TB-HIV co-infected group, OD values for methylation modifications ranged from 0.4 to 0.8. OD450 absorbance values were elevated for H3K4me1 (OD450 $\approx$ 0.75) and H3K27me3 (OD450 $\approx$ 0.78). In contrast, H3K4me3 and H3K9me2 showed reduced OD450 values of approximately 0.45 and 0.42, respectively. Acetylation modifications, represented by blue bars, showed OD values ranging from 0.6 to 0.9. H3K9ac and H3K27ac showed OD450 values of 0.85 and 0.88, respectively. Phosphorylation marks were also upregulated, with H3S10ph and H3S28ph reaching OD450 values of 0.89 and 0.91, respectively.

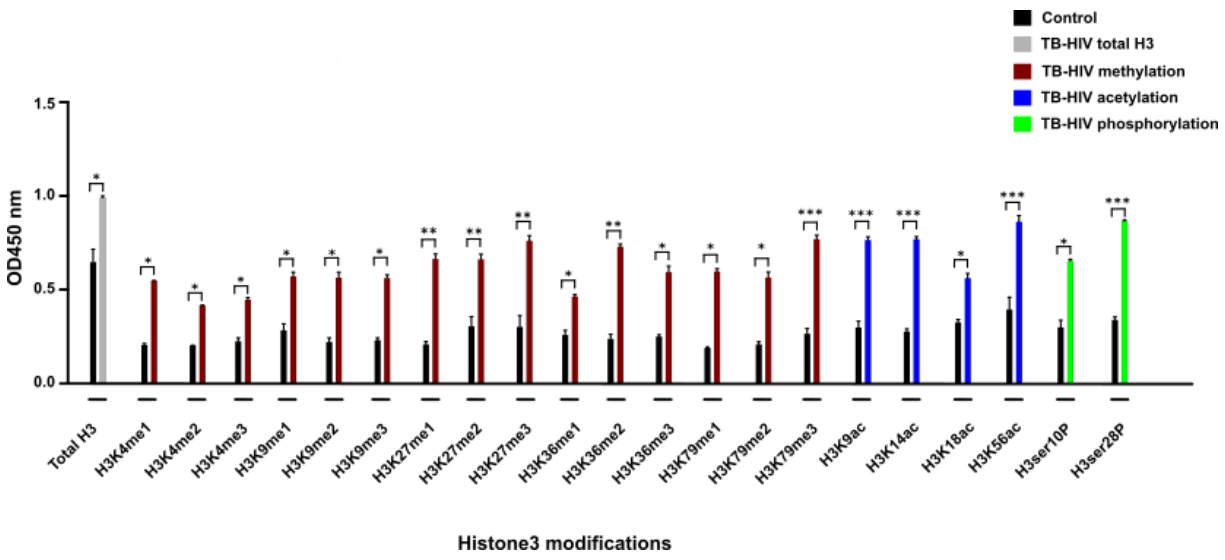


FIGURE 3.13. TARGET PROTEIN PRODUCTION IN TB-HIV CO-INFECTED AND CONTROL GROUPS.

The level of histone acetylation, methylation, and phosphorylation in both study cohorts was determined by the histone H3 modification multiplex assay. Data were collected from the control subjects (n=45) and experimental group (n=45), and values denote the means ±SEM. Statistical significance was determined by applying the non-parametric t-test. The values *$p \leq 0.05$, **$p \leq 0.01$, and ***$p \leq 0.001$ indicated statistical significance between the control and experimental samples. The histone3 (H3) modification multiplex assay data were collected from two independent experiments, and all replicates were pooled for data analysis.

3.7 Correlation of protein markers with demographics

3.7.1 Association of age with protein markers in the TB-HIV co-infected group

In the TB-HIV co-infected cohort, age was weakly associated (r= 0.29; P<0.05) with a marker of methylation (H3K4me2) (Table 3.6, Figure 3.14). There was no significant association between age and markers of acetylation and phosphorylation in this group (Table 3.6, Figure 3.14). The Spearman's correlation coefficient was r= 0.3607 and 0.4067 in the methylation markers, H3K4me1 and H3K79me3, respectively. In addition, the correlation coefficients in the acetylation markers, H3K14 and H3K56, were 0.389 and 0.3224, respectively (Table 3.6, Figure 3.14). The phosphorylated marker, H3K10P, had a coefficient of r = 0.319 (Table 3.6, Figure 3.14).

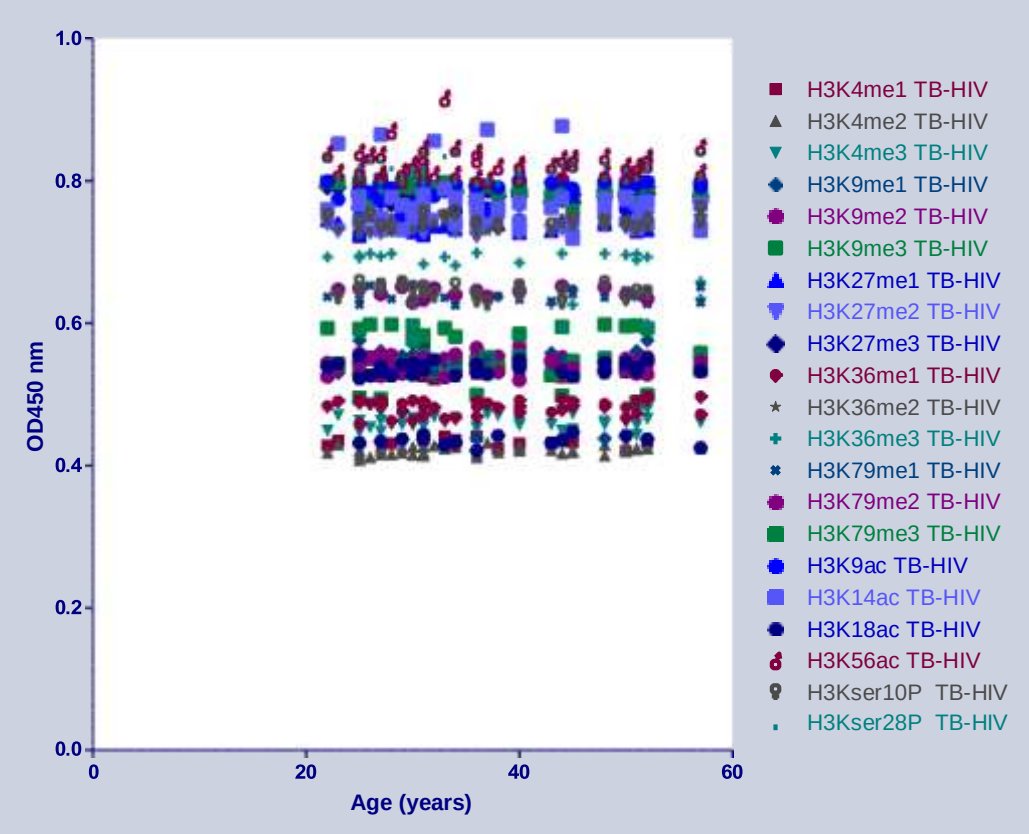


FIGURE 3.14. IMAGE SHOWING THE ASSOCIATION OF AGE, METHYLATION, ACETYLATION, AND PHOSPHORYLATION MARKERS IN THE TB-HIV CO-INFECTED COHORT.

The association between was determined using Spearman's rank correlation.

TABLE 3.6. SPEARMAN'S CORRELATION COEFFICIENTS FOR THE ASSOCIATION OF AGE WITH METHYLATION, ACETYLATION, AND PHOSPHORYLATION MARKERS IN THE TB-HIV CO-INFECTED COHORT.

Parameter	H3K4me1	H3K4me2	H3K4me3	H3K9me1	H3K9me2	H3K9me3	H3K27me1	H3K27me2	H3K27me3	H3K36me1	H3K36me2	H3K36me3	H3K79me1	H3K79me2	H3K79me3	H3K9ac	H3K14ac	H3K18ac	H3K56ac	H3Kser10P	H3Kser28P
Number of XY Pairs	45	45	45	45	45	45	45	45	45	45	45	45	45	45	45	45	45	45	45	45	45
Spearman r	0,08002	0,29 80	0,1084	-0,01409	-0,09799	-0,02798	0,00 2543	0,1315	-0,1397	0,07028	-0,01740	0,1536	0,07273	-0,09232	-0,1405	0,2024	-0,09159	-0,03145	-0,00 2871	0,03322	0,01473
95% confidence interval	-0.2272 to 0.3728	-0.00 4125 to 0.55 03	-0.1999 to 0.3971	-0.3145 to 0.2889	-0.3883 to 0.2100	-0.3270 to 0.2761	-0.2994 to 0.3041	-0.1773 to 0.4167	-0.4236 to 0.1692	-0.2365 to 0.3643	-0.3175 to 0.2858	-0.1553 to 0.4352	-0.2342 to 0.3664	-0.3834 to 0.2154	-0.4243 to 0.1684	-0.1058 to 0.4751	-0.3828 to 0.2161	-0.3301 to 0.2729	-0.3044 to 0.2991	-0.2713 to 0.3316	-0.2883 to 0.3151
P value (two-tailed	0,6013	0,04 68	0,4786	0,9268	0,5219	0,8552	0,9868	0,3891	0,3602	0,6464	0,9097	0,3137	0,6349	0,5464	0,3573	0,1824	0,5496	0,8375	0,9851	0,8285	0,9235

)																						
P-value summary	ns	*	ns	ns	ns	ns	ns	ns	ns	ns	ns	ns	ns	ns	ns	ns	ns	ns	ns	ns	ns	ns

3.7.2 Protein Marker associations with gender and race in the TB-HIV co-infected and Control groups.

Table 3.7 shows the p-values obtained for each histone modification marker when analyzed for associations with gender and race in both the study cohorts (Table 3.7). Markers with p-values < 0.05 were considered statistically significant, indicating a potential association between the specific histone modification and either gender or race. This analysis highlights distinct epigenetic signatures that may differ across demographic variables in both cohorts. In the TB-HIV co-infected cohort, a broader distribution of associations was observed across both gender and race.

Significant gender-based associations were found for several markers, including H3K36me1 ($p = 0.0155$), H3K36me3 ($p = 0.0276$), and H3K56ac ($p = 0.0106$) (Table 3.7). Similarly, race-specific associations were widespread, with highly significant findings for H3K4me1 ($p = 0.0079$), H3K9me1 ($p = 0.0108$), H3K9me3 ($p = 0.0324$), H3K36me3 ($p = 0.0001$), H3K79me1/2/3 ($p \leq 0.0034$), H3K9ac ($p = 0.0001$), H3K14ac ($p = 0.0097$), H3Ser10ph ($p = 0.0001$), and H3Ser28ph ($p = 0.0010$) (Table 3.7). These results suggest that the experimental group had an increase in both gender- and race-specific variability in histone modifications compared to the control group. In the control cohort, several histone modifications showed significant associations with race, while far fewer were linked to gender (Table 3.7).

Notably, strong race-specific associations were observed for H3K4me3, H3K9me1, H3K9me2, H3K9me3, H3K27me1/2/3, H3K36me1/2/3, H3K79me2/3, H3K9ac, H3K14ac, and H3K18ac (all $p < 0.01$). This indicates that histone methylation and acetylation marks in the control group were more strongly influenced by racial background than by gender (Table 3.7). In contrast, gender-specific differences were comparatively limited, with significance observed only for a small subset of markers (e.g., H3K4me1, H3K9me2/3, H3K14ac, H3K56ac; $p < 0.05$) (Table 3.7). Analysis of protein marker associations with demographic variables revealed distinct patterns between the control and experimental groups (Table 3.7).

TABLE 3.7. STATISTICAL ASSOCIATIONS OF HISTONE MODIFICATION MARKERS WITH GENDER AND RACE IN THE TB-HIV CO-INFECTED AND CONTROL GROUPS.

Markers	Control group		Experimental group	
	Gender	Race	Gender	Race
H3K4me1	0.0367	0.7172	0,1666	0,0079
H3K4me2	0.9051	0.0295	0,5368	0,172
H3K4me3	0.6628	0.0001	0,1525	0,0705
H3K9me1	0.6223	0.0001	0,486	0,0108
H3K9me2	0.0990	0.0001	0,3432	0,1073
H3K9me3	0.0990	0.0001	0,9955	0,0324
H3K27me1	0.3854	0.0001	0,9144	0,1394
H3K27me2	0.7045	0.0001	0,8429	0,3699
H3K27me3	0.8431	0.0001	0,3486	0,0871
H3K36me1	0.7300	0.0001	0,0155	0,1811
H3K36me2	0.1430	0.0001	1	0,3095
H3K36me3	0.1813	0.0001	0,0276	0,0001
H3K79me1	0.9955	0.2387	0,3552	0,0001
H3K79me2	0.7461	0.0390	0,0877	0,0001
H3K79me3	0.1562	0.0279	0.9503	0.0034
H3K9ac	0.1633	0.0001	0,3261	0.0001
H3K14ac	0.0793	0.0095	0.6549	0.0097
H3K18ac	0.7046	0.0001	0,773	0,5317
H3K56ac	0.0494	0.6567	0,1063	0,0002
H3Ser10ph	0.5003	0.4608	0,515	0,0001
H3Ser28ph	0.8166	0.2533	0,2346	0.0010

Chapter 4: Discussion

4.1. Conventional PCR, DNA Sequencing, and Phylogenetic Analysis for HIV and TB

The HIV *gag-pol* and *Mtb rpoB* genes were successfully amplified and sequenced from the 10 randomly selected tissue samples from our study cohort, confirming the HIV-TB co-infection. Moreover, there was no amplification in the no-template control, indicating the absence of cross-contamination. Unfortunately, the primers used in this study were originally designed for RT-qPCR, which necessitated short amplicons (<250 bp) for optimal sensitivity and specificity; thus, smaller PCR amplicon sizes were obtained, specifically a 120 bp long fragment for the *gag-pol* gene and a 110 bp long fragment for *rpoB*.

Notably, FFPE samples are known to be degraded and may suffer from extensive cross-linking in formalin, which compromises DNA, RNA, and protein quality, ultimately resulting in smaller DNA fragments (176). Consequently, short amplicons, particularly from conserved regions like the *gag-pol* and *rpoB* genes, may be suboptimal for phylogenetic analysis, resulting in insufficient sequence variability to accurately resolve or infer evolutionary relationships. Nevertheless, the BLAST analysis identified the majority of the *gag-pol* sequences from the tissue samples as HIV-1 subtype 07_BC. This was unexpected as South Africa has one of the highest HIV burdens globally, with subtype C accounting for over 95% of infections (181). The subtype 07_BC is a recombinant form common in China that has descended from subtypes B and C, making it one of the most prevalent HIV-1 strains in Asia (182). The presence of BC recombinant HIV-1 strains has been previously reported in a South African study conducted in the Western Cape Province in 2014, where 4.6% of the study cohorts were infected with the BC recombinant strains, marking the first detection of BC recombinants in South Africa. The authors attributed the presence of these strains to increasing tourism and migration rates to South Africa, which is currently very high (183). While our findings may suggest true subtype diversity in our study cohort, the use of a short 120 bp *gag-pol* fragment likely limited the resolution of the subtype classification, potentially skewing results toward conserved recombinant sequences. Therefore, further analysis using a longer gene fragment or full-genome sequencing is necessary to determine subtype identity accurately. The BLAST analysis further identified the ten *rpoB* gene sequences as those of *Mycobacterium tuberculosis*. This was expected as the tissue samples were from patients diagnosed with HIV-TB coinfection. Phylogenetic analysis corroborated the LANL BLAST results, which revealed sequence similarities between the HIV-1 sequences in cluster 2,

which were genetically distinct from the HIV-1 sequences from tissue samples Th6 and Th7. In contrast, the LANL BLAST results showed that the HIV-1 sequence from tissue samples Th6 and Th7 belong to different subtypes; however, these sequences formed a close relationship in cluster 3, suggesting a common ancestry. Moreover, a monophyletic relationship between HIV-1 sequences in clusters 2 and 3 indicates that these HIV-1 sequences share a common ancestor and are more closely related to each other. Likewise, the *Mtb* sequences showed close relations, suggesting that they diverged from a common ancestor. It is worth noting that, in phylogenetic studies, longer gene fragments are generally preferred as they provide a greater number of informative sites, which enhances the resolution and reliability of evolutionary relationships (177). Therefore, the short *gag-pol* and *rpoB* gene fragments obtained in this study may have lacked sufficient sequence variability to resolve HIV-1 subtypes or infer evolutionary relationships accurately between the HIV and *Mtb* sequences.

4.2 Epigenetic Modifications in the TB-HIV Co-Infected Tissue Samples

The dynamics between DNA methylation and gene expression play a role in the progression of infectious diseases such as HIV-1 and TB. Findings from this study provide valuable insights into the DNA methylation patterns, consistent with previous investigations that demonstrated the correlation between significant upregulation of the *DNMT* gene catalyzing methylation and infection with HIV-1 (114,120). Furthermore, our findings regarding DNA methylation patterns in TB-HIV infections validate previous investigations that highlighted the effect of significant DNA methylation on the immune response and particularly demonstrated that TB infection results in methylation of specific CpG sites within the TLR2 promoter, leading to downregulation of the TLR2 gene in NK cells and monocytes of individuals with active pulmonary TB (121). Our study further corroborated a prior investigation that assessed the DNA methylation patterns of TB patients and revealed that hypermethylation of genes involved in signalling pathways (such as TNF/NF-kB and IFN-y) are associated with a weaker immune responsiveness to the infection (122). Given the extensive lack of studies examining DNA methylation using FFPE tissue samples, our findings validate the impact of DNA methylation in TB-HIV infection. While our findings agree with the stated prior investigations, our DNA methylation results were inconsistent with data reported by Marimani et al. (2020), who observed a lower methylation profile in the

TB-HIV co-infected cohort relative to the healthy subjects (102). Therefore, in light of speculation, the incongruency in the results may be due to factors like drug resistance in their TB-HIV cohort. Therefore, further studies are needed to explore the underlying causes behind this discrepancy.

Lysine Methyltransferase (SETDB2) is a protein that regulates gene expression by catalyzing methylation at Histone3 (H3) and Lysine 9, and its function is particularly involved in transcriptional silencing (123). Therefore, the elevated expression of this gene, as indicated by our results (Figure a-e), as well as the increased H3K9 methylation (Figure 3.2; Table 4.1), suggests that during co-infection with TB-HIV, there is significant transcriptional silencing, potentially deactivating key genes implicated in crucial immune defences, thus contributing to the progression of the infection. These findings corroborate a study by Maricato et al. (2015), which also demonstrated that infected blood cells exhibit increased expression of the gene, thus highlighting a direct correlation between HIV infection and expression of the *SETDB2* gene (123). Therefore, our findings underscore the importance of further investigations into the *SETDB2* transcriptional silencing in TB-HIV co-infected patients, as there is an extensive lack of studies in this area.

Lysine Methyltransferase (KMT) is also an important regulator of methylation at various lysine residues, and our findings suggest that upregulation of the *KMT* gene in the TB-HIV co-infected patients is associated with progression of the disease due to suppression of the immune response. Despite the extensive lack of studies examining *KMT* expression in the context of TB and HIV, an investigation by Pegans et al., (2010) supports our findings, as it demonstrated that lysine methyltransferase (Set 7/9- KMT7) enhances transcription of HIV by monomethylating the viral Tat protein (127). Additionally, the significant correlation between *KMT* expression and HIV transcription suggests *KMT* as a potential target for the development of novel therapeutics against HIV.

Previous studies have identified age-related CpG methylation changes, indicating that aging influences the methylation profile. In addition, race has also been shown to affect DNA methylation, suggesting that the age and racial background of TB-HIV co-infected patients may contribute to methylation patterns, independent of infection status (178,179). Interestingly, age showed no significant association with epigenetic gene expression observed among the five genes in our TB-HIV co-infected cohort, suggesting that infection-related stimuli exert a stronger influence than chronological aging in shaping epigenetic landscapes

within this TB-HIV cohort. However, Race emerged as a stronger determinant of epigenetic gene expression of *CIITA* and *SETDB2*, with African participants exhibiting higher expression of *CIITA* and *SETDB2* genes. Surprisingly, the effect of Gender was limited, with a significant association observed only for *DNMT1* gene expression, pointing to possible sex-specific differences in DNA methylation regulation under TB-HIV co-infection. A prior investigation has proved that there is an association between gender and epigenetic regulation, suggesting that females and males may exhibit variable methylation patterns (180), which may result in varied gene expression outcomes.

4.3 Histone modification patterns

Histone acetylation is a crucial biological process that modifies chromatin structure and accessibility to transcriptional mediators. The enzyme HAT plays a significant role in this process by modulating access of the transcriptional mediators to the chromatin structure and promoters, influencing the expression of genes (104). Acetylation at these specific positions: H3K9, H3K14, H3K18, and H3K56 was observed (Figure 3.2), and it is typically associated with gene activation, which generally demonstrates increased access to the chromatin, thus leading to significant expression of genes (105,145-147). Our results demonstrated elevated expression of the *HAT* gene in TB-HIV co-infection. This finding is in agreement with earlier investigations that reported elevated expression of *HAT* in HIV positive patients following *Mtb* infection (124). These valuable findings in relation to the *HAT* gene expression highlight the potential importance of exploring further the link between histone acetylation and immune dysfunction in the context of TB, HIV co-infection. Moreover, *CIITA*, another modulator of histone acetylation, encodes the class II transactivator protein. This study shed light on a noteworthy observation: the *CIITA* gene exhibits extensive upregulation in the TB-HIV co-infected cohort relative to the uninfected control cohort, suggesting that this biological phenomenon promotes the progression of the infection and the disease. Notably, these findings align with earlier investigations conducted by Porter et al., (2010), which emphasize the impact of *CIITA* expression on facilitating the attachment of the HIV-1 virus to CD4 cells, leading to progressive depletion of the cells and compromised immunological response, thereby favouring persistence of the HIV infection (125). Furthermore, Porter et al., (2010) also demonstrated the precise effect of the *CIITA* gene in facilitating the cytoplasmic processing of Gag-pol protein in HIV-1, thereby enhancing the infectivity of the virions in

CIITA-expressing cells. These remarkable findings provide compelling evidence of the critical role *CIITA* plays in the pathogenesis of HIV in TB-HIV co-infection.

Phosphorylation is a posttranscriptional mechanism that involves the addition of phosphate groups to various histone residues, catalysed by a kinase enzyme, affecting chromatin accessibility and gene expression depending on the histone residue (109). In our findings, phosphorylation at histone residues Serine 10 and 28 was observed (Figure 3.2). In molecular biology, phosphorylation at serine 10 and 28 plays a crucial role in activating immediate early genes, which are triggered in response to a wide variety of stimuli, and sets into motion a cascade of subsequent gene expressions and cellular responses (110,111). The findings in our study validate that phosphorylation is induced in response to TB-HIV co-infection and also corroborate the results by Marimani et al., (2020), which indicate elevated phosphorylation status in the TB-HIV co-infected cohort (102). Our results align with and build upon prior investigations that demonstrated a protective phosphorylation profile in the host after infection with HIV or TB (112,113). However, while phosphorylation is often protective, a study conducted by Lochab et al., (2020) suggests that *Mtb* exploits host ATM kinases for its survival by inducing DNA damage, specifically double-stranded breaks and activating the ATM kinase through the SecA2 pathway; thus, enhancing the persistence of *Mtb* and progression of tuberculosis infection (114). Moreover, it has been suggested that P38 kinase, involved in phosphorylation, is also utilized by HIV as a survival strategy through activation of the P38 pathway, which is essential for replication of the virus (115). The notable discrepancies in findings may be attributed to significantly compromised immunity, as *Mtb* and HIV can potentially interfere with immune signalling pathways, including those related to ATM and P38 kinases (116). Importantly, our gene expression results were confirmed by the Histone H3 modification multiplex assay. Likewise, this data revealed a sharp increase in the degree of protein acetylation, methylation, and phosphorylation in the TB-HIV contingent relative to the non-TB-HIV control cluster. This vast variation in the degree of protein acetylation, methylation, and phosphorylation may potentially influence protein production levels, function, and catalytic activity. Deficiencies in protein function and catalytic activity, particularly in key enzymes involved in host immunity, may result in a negative impact on both the innate and adaptive immune responses.

The H3 protein modifications were further analyzed for associations with age, gender, and race in the TB-HIV co-infected cohort. Notably, several markers showed statistically significant associations ($p < 0.05$) in the control group, indicating potential relevance in

epigenetic differentiation across gender or racial groups. Specifically, H3K4me1 and H3K56ac were significantly associated with gender. Whereas most of the markers were associated with race, with only five markers not significantly associated with race, including all the phosphorylated markers and one of the acetylation markers. The remaining markers were not statistically significant, suggesting limited or no association. These findings provide insight into the epigenetic landscape of H3 modifications within the control cohort. In the TB-HIV co-infected cohort, most epigenetic markers did not show statistically significant differences between males and females. However, H3K36me1 and H3K36me3 showed significant gender-based differences, with p-values of 0.0155 and 0.0276, respectively. These findings suggest that methylation at these sites may be influenced by gender in the context of TB-HIV coinfection. Other markers such as H3K4me1, H3K4me3, and H3K79me2 approached significance ($p < 0.2$), indicating potential gender-related trends that may warrant further investigation.

Race appeared to have a more pronounced effect on epigenetic variation in the control group. Several markers showed highly significant differences across racial groups, including H3K36me3, H3K79me1, H3K79me2, H3K56ac, H3KSer10P, and H3KSer28P, all with p-values ≤ 0.001. These results suggest strong racial influences on histone modifications, potentially reflecting underlying genetic or environmental factors. Markers such as H3K4me1, H3K9me1, H3K9me3, and H3K14ac also showed significant racial differences ($p < 0.05$), reinforcing the idea that race may be a key variable in epigenetic regulation within this cohort. Compared to the control group, the TB-HIV co-infected group showed an overall decrease in the number of markers that were associated with gender and race. This supports the fact that in the TB-HIV co-infected group, epigenetic changes are less influenced by age, gender, and race.

In conclusion, while gender-related differences in epigenetic markers were limited to a few specific sites, race emerged as a more influential factor, with multiple markers showing statistically significant variation. These findings highlight the importance of considering demographic variables in epigenetic studies, especially in disease contexts like TB-HIV co-infection. Therefore, further research could explore the biological mechanisms driving these differences and their implications for disease progression or treatment response.

While the study successfully demonstrated the impact of epigenetic modifications on gene expression in the TB-HIV co-infected cohort, it was not without limitations. A critical limitation was the choice of the control group used in the study. Specifically, the study compared TB-HIV co-infected tissue samples to uninfected controls, without including HIV-only or TB-only cohorts. This limits the ability to associate the observed epigenetic changes to either pathogen individually or to their synergistic interaction, as both pathogens are known to induce epigenetic modifications independently (152-161). Specifically, HIV infection has been reported to increase the expression of DNA methyltransferases, alter histone acetylation, and modulate host gene expression through viral proteins such as Tat (167-169). Viral proteins like Tat, Nef, and Rev stimulate DNMT1 promoter activity, altering host methylation patterns (160,170). Moreover, HIV induces aberrant methylation in host genes, particularly those involved in immune response, viral restriction, and inflammation (171). Similarly, TB infection can induce histone methylation, DNA methylation, and chromatin remodelling in macrophages and dendritic cell, contributing to immune evasion and persistence (172). Moreover, *Mtb* infection has been reported to induce IFN-γ production by T and NK cells, which activates the JAK-STAT1 pathway and upregulates the *CIITA* gene (172,173). Research indicates that *Mtb* manipulates chromatin structure and histone modifications at specific promoter regions to hinder the effective transcription of key genes, including the *CIITA* gene, thereby impairing the host's immune response and facilitating persistent infection (174,175). Therefore, without HIV-only and TB-only control groups, it is not possible to determine whether the epigenetic changes in *DNMT1*, *HAT*, *CIITA*, *KMT*, and *SETDB2* gene expression observed in our study were driven by HIV, TB, or their synergistic interaction. Future studies will include (1) HIV-infected tissue samples without TB, (2) TB-infected tissue samples without HIV, and (3) HIV-TB uninfected controls to better understand the individual and combined epigenetic modifications driven by TB-HIV.

Another notable limitation of this study is the lack of matching for co-morbidities and underlying conditions between the experimental and control cohorts. The HIV-TB co-infected cohort included individuals with additional clinical conditions such as Kaposi sarcoma, palatal ulcers, erythema induratum, lupus panniculitis, and necrotizing granulomas. In contrast, the control group comprised individuals without a documented history of cancer, hypertension, diabetes, allergies, or other major systemic illnesses at the time of biopsy collection. However, the control group did present with conditions including renovascular disease, pancytopenia, pleurisy, hepatosplenomegaly, inflammatory bowel disease, and

gastroesophageal reflux disease. The co-morbidities and underlying conditions present in both the study cohorts may have independently influenced epigenetic regulation noted in this study, thereby confounding the interpretation of the observed differences in epigenetic marker expression. Notably, the presence of Kaposi sarcoma in the TB-HIV co-infected cohort may have introduced a significant confounding factor (162). Campbell et al. (2020) reported that Kaposi's sarcoma-associated herpesvirus actively manipulates host epigenetic mechanisms to maintain viral latency and promote oncogenesis. These virus-induced changes, including DNA methylation, histone modifications, and noncoding RNA activity, may contribute to the elevated epigenetic marker expression observed in our study (Campbell et al, 2020). Similarly, the presence of lupus panniculitis in the TB-HIV co-infected cohort may have also introduced a confounding impact, as systemic lupus erythematosus is known to involve widespread epigenetic dysregulation. Specifically, aberrant DNA methylation, histone modification, and noncoding RNA activity in immune cells may contribute to the elevated epigenetic marker expression observed in our study (163). In addition, immune reconstitution inflammatory syndrome (IRIS) in patients recently initiated on ART, malignancies, and other opportunistic or chronic infections not accounted for in the study may have further contributed to the elevated epigenetic marker expression in the HIV/TB cohort. Other key factors that may potentially play a role in regulating gene expression include length of time on HIV-TB therapy, virulence of the infecting HIV-TB pathogen and the presence of other unreported life-threatening clinical conditions. In addition, adhering to a treatment plan that includes TB and HIV therapy may lead to epigenetic dysregulation and further deterioration of the immune system. Other limitations include the lack of whole genome acetylation, methylation and phosphorylation data. Whole genome sequencing allows detection of other gene regions associated with phosphorylation, acetylation and methylation. Detection of these candidate genes may provide new insights for understanding of the molecular mechanisms involved in gene regulation, aberrant protein production levels and the impact of these target genes in modulating the host's immune response. Notably, subsequent projects will utilize detailed clinical data sheets containing patient CD4 counts, viral load, bacterial load, duration on TB-HIV therapy, name of TB or HIV drugs, and other crucial patient clinical information. This will yield a comprehensive clinical profile for both the experimental and control cohorts and will promote data accuracy, reliability, and reproducibility.

Chapter 5: Conclusion

In light of the increasing burden of HIV and TB co-infection across sub-Saharan Africa and globally, this study provides novel insights and makes important contributions to the underexplored field of epigenetics in infectious diseases, particularly within the African context. The demographic analysis confirmed that the TB-HIV cohort was well-matched to controls, although significant immunosuppression was evident in the patient group. Molecular confirmation and phylogenetic analyses established the presence of HIV *gag-pol* and *Mtb rpoB* genes, with HIV sequences predominantly clustering with intersubtype 07_BC and *Mtb* sequences showing strong identity to reference strains. These findings highlight the genetic diversity of circulating pathogens within this population. At the level of gene expression, TB-HIV co-infection was shown to significantly upregulate key epigenetic regulators, notably *DNMT1* and *HAT*, with expression patterns influenced by demographic factors such as gender and race.

Furthermore, histone modification profiling revealed extensive chromatin remodeling, characterized by altered methylation, acetylation, and phosphorylation states, suggesting a complex interplay between infection, immune suppression, and host epigenetic regulation. Importantly, demographic associations indicated that race and gender significantly shaped both gene expression and histone modification outcomes, underscoring the need for context-specific investigations in diverse populations. Taken together, these findings extend current knowledge by showing that HIV-TB co-infection not only disrupts immune pathways but also induces profound epigenetic reprogramming, which may contribute to disease progression and variability in clinical outcomes. This work emphasizes the importance of integrating epigenetic perspectives into HIV and TB research and provides a foundation for future studies aimed at identifying potential biomarkers and therapeutic targets in affected populations.

Chapter 6: Appendices

Ethics Clearance Certificates

UNIVERSITY OF THE WITWATERSRAND JOHANNESBURG

HUMAN RESEARCH ETHICS COMMITTEE (MEDICAL)

Office of the Deputy Vice-Chancellor (Research and Innovation)

TO: Mr K Mamabolo; Dr P Magangane; Ms T Duze
School of Pathology
Department of Anatomical Pathology
Medical School
University

E-mail: 1053014@students.wits.ac.za

CC: Supervisor: Dr M Marimani
<Musa.Marimani@wits.ac.za>
and <HREC-Medical Research Office@wits.ac.za>

FROM: Mr Iain Burns
Human Research Ethics Committee (Medical)
Tel: 011 717 1252

E-mail: Iain.Burns@wits.ac.za

DATE: 2022/07/05

REF: R14/49

PROTOCOL NO: **M220614** (This is your ethics application reference number. Please quote it in all enquiries, oral or written, relating to this study.)

PROJECT TITLE: *Epigenetic regulation profile in healthy and TB-HIV infected patients*

Please find attached the Clearance Certificate for the above project. I hope it goes well and that an article in a recognized publication comes out of it. This will reflect well on your professional standing and contribute to Government funding of the University.

MSWorks2000/Iain0007/Clearscan.wps

UNIVERSITY OF THE WITWATERSRAND JOHANNESBURG

R49 Mr K Mamabolo; Dr P Magangane; Ms T Duze

HUMAN RESEARCH ETHICS COMMITTEE (MEDICAL)
CLEARANCE CERTIFICATE NO. M220614

NAME: (Principal Investigator)	Mr K Mamabolo; Dr P Magangane; Ms T Duze
DEPARTMENT:	School of Pathology Department of Anatomical Pathology Medical School University
PROJECT TITLE:	*Epigenetic regulation profile in healthy and TB-HIV infected patients*
DATE CONSIDERED:	Ad hoc
DECISION:	Approved unconditionally
CONDITIONS:	
NOTE:	If contact information regarding student study participants is required, please contact the Registrar's office - <Nicoleen.Potgieter@wits.ac.za>
SUPERVISOR:	Dr M Marimani
APPROVED BY:	CB Penny Dr CB Penny, Chairperson, HREC (Medical)
DATE OF APPROVAL:	2022/07/05

This Clearance Certificate is valid for 5 years from the date of approval. An extension may be applied for.

DECLARATION OF INVESTIGATORS

To be completed in duplicate and **ONE COPY** returned to the Research Office secretariat on the 3rd floor, Phillip Tobias Building, Parktown, University of the Witwatersrand, Johannesburg.

I/we fully understand the conditions under which I am/we are authorized to carry out the above-mentioned research and I/we undertake to ensure compliance with these conditions. Should any departure be contemplated from the research protocol as approved, I/we undertake to submit details to the Committee. **I agree to submit a yearly progress report**. When a funder requires annual re-certification, the application date will be one year after the date when the study was initially reviewed. In this case, the study was initially reviewed in **June** and therefore reports and re-certification will be due in the month of **June** each year. Unreported changes to the study may invalidate the clearance given by the HREC (Medical).

K Mamabolo
Signature of Principal Investigator

07 July 2022
Date

Approval letter to access virology results

NATIONAL HEALTH LABORATORY SERVICE

NATIONAL HEALTH LABORATORY SERVICE
Practice number: 5200296

UNIVERSITY OF THE WITWATERSRAND JOHANNESBURG

University of the Witwatersrand, School of Pathology

DEPARTMENT OF VIROLOGY

19 May 2022

To Whom it may concern

APPROVAL TO ACCESS VIROLOGY RESULTS ON TRACKCARE

This letter serves as approval for Mr Katlego Mamabolo's request to access Department of Virology, Charlotte Maxeke Johannesburg Academic Hospital (CMJAH) results for the purpose of his MSc study entitled "Epigenetic regulation profile in healthy and TB-HIV infected patients" which will be conducted in the Department of Anatomical Pathology, CMJAH/Wits. This permission specifically relates to access of HIV results of study participants which will be anonymised as per study proposal in order to maintain patient confidentiality. These results will be used to address the following study objectives: (i) "To evaluate the expression of *DNMT1*, *SETDB2* and *KMT* genes involved in methylation in healthy and TB-HIV co-infected human FFPE tissue samples by reverse transcription quantitative polymerase chain reaction (RT-qPCR)" and (ii) "To examine the expression profile of *CIITA* and *HAT* genes implicated in histone acetylation in TB-HIV co-infected and uninfected human biopsies by RT-qPCR".

We expect that due recognition will be given to the department in peer-reviewed publications as relevant when data are used.

Kind regards

Dr Florette Treurnicht
HoD
Virology
National Health Laboratory Service
and the University of the Witwatersrand
7 York Road, Parktown
Tel: 011 489 8853 | Fax: xxx xxx xxxx | Cell: 071 609 5200
florette.treurnicht@nhls.ac.za ; florette.treurnicht@wits.ac.za

Chapter 7: References

1. Kumar V, Abbas AK, Aster JC, Perkins JA, editors. Robbins Basic Pathology. Tenth edition. Philadelphia, Pennsylvania: Elsevier; 2018. 935 p.

2. Santiago ML, Range F, Keele BF, Li Y, Bailes E, Bibollet-Ruche F, et al. Simian Immunodeficiency Virus Infection in Free-Ranging Sooty Mangabeys (Cercocebus atys atys) from the Taï Forest, Côte d'Ivoire: Implications for the Origin of Epidemic Human Immunodeficiency Virus Type 2. *Journal of Virology*. 2005;(**79**):12515–27. Doi: 10.1128/JVI.79.19.12515-12527.2005

3. Zulfiqar HF, Javed A, Sumbal, Afroze B, Ali Q, Akbar K, et al. HIV Diagnosis and Treatment through Advanced Technologies. *Frontiers in Public Health* 2017;(**5**):32. Doi: 10.3389/fpubh.2017.00032

4. Bbosa N, Kaleebu P, Ssemwanga D. HIV subtype diversity worldwide. *Current Opinions in HIV and AIDS*. 2019;(**3**):153–60. Doi: 10.1097/COH.0000000000000534

5. Reis MNG, Guimarães ML, Bello G, Stefani MMA. Identification of New HIV-1 Circulating Recombinant Forms CRF81_cpx and CRF99_BF1 in Central Western Brazil and of Unique BF1 Recombinant Forms. *Frontier in Microbiology*.,2019;(**10**):97. Doi: 10.3389/fmicb.2019.00097

6. Rossi E, Meuser ME, Cunanan CJ, Cocklin S. Structure, Function, and Interactions of the HIV-1 Capsid Protein. *Life*.2021;(**11**):100. Doi: 10.3390/life11020100

7. Sakuragi J ichi. Morphogenesis of the Infectious HIV-1 Virion. *Front Microbiol*. 2011;2:Available from: http://journal.frontiersin.org/article/10.3389/fmicb.2011.00242/abstract

8. German Advisory Committee Blood (Arbeitskreis Blut), Subgroup 'Assessment of Pathogens Transmissible by Blood'. Human Immunodeficiency Virus (HIV). *Transfusion Medicine and Hemotherapy*. 2016;(**43**):203–22. Doi: 10.1159/000445852

9. Molla AA, Gelagay AA. Risky sexual practice and associated factors among HIV positive adults attending anti-retroviral treatment clinic at Gondar University Referral Hospital, Northwest Ethiopia. *PLOS ONE*. 2017;(**3**):e0174267. Doi: https://doi.org/10.1371/journal.pone.0174267

10. Ball LJ, Puka K, Speechley M, Wong R, Hallam B, Wiener JC, et al. Sharing of Injection Drug Preparation Equipment Is Associated with HIV Infection: A Cross-sectional Study. *Journal of Acquired Immune Deficiency Syndrome*. 2019(**4**):99–103. Doi: 10.1097/QAI.0000000000002062

11. Akindipe T, Abiodun L, Adebajo S, Lawal R, Rataemane S. From addiction to infection: managing drug abuse in the context of HIV/AIDS in Africa. *African Journal of Reproductive Health*. 2014; (**3**):47–54.

12. Mackesy-Amiti M Akindipe T, Abiodun L, Adebajo S, Lawal R, Rataemane S. From addiction to infection: managing drug abuse in the context of HIV/AIDS in Africa. African *Journal of Reproductive Health*. 2014;(**3**):47–54

13. Hemophilia and HIV | Indiana Hemophilia & Thrombosis Center [Internet]. [cited 2024 May 9]. Available from: https://www.ihtc.org/hemophilia-HIV

14. Redd AD, Collinson-Streng A, Martens C, Ricklefs S, Mullis CE, Manucci J, et al. Identification of HIV Superinfection in Seroconcordant Couples in Rakai, Uganda, by Use of Next-Generation Deep Sequencing. *Journal of Clinical Microbiology*. 2011;(**49**):2859–67. Doi: https://doi.org/10.1128/jcm.00804-11

15. van der Kuyl AC, Kozaczynska K, Ariën KK, Gali Y, Balázs VR, Dekker SJ, et al. Analysis of infectious virus clones from two HIV-1 superinfection cases suggests that the primary strains have lower fitness. *Retrovirology*. 2010;(**7**):60. Doi: https://doi.org/10.1186/1742-4690-7-60

16. Hallett TB, Aberle-Grasse J, Bello G, Boulos LM, Cayemittes MPA, Cheluget B, et al Declines in HIV prevalence can be associated with changing sexual behaviour in Uganda, urban Kenya, Zimbabwe, and urban Haiti. *Sexually Transmitted Infections*. 2006;(**82**):1–8. Doi: https://doi.org/10.1136/sti.2005.016014

17. Wilkins T. HIV 1: epidemiology, pathophysiology and transmission. *The Lancet*. 2020 ;(**368**): 489-504. Doi: 10.1016/S0140-6736(06)69157-5

18. Jasinska AJ, Pandrea I, Apetrei C. CCR5 as a Coreceptor for Human Immunodeficiency Virus and Simian Immunodeficiency Viruses: A Prototypic Love-Hate Affair. *Frontiers in Immunology*. 2022 ;(**13**):835994. Doi: https://doi.org/10.3389/fimmu.2022.835994

19. Hokello J, Tyagi K, Owor RO, Sharma AL, Bhushan A, Daniel R, et al. New Insights into HIV Life Cycle, Th1/Th2 Shift during HIV Infection and Preferential Virus Infection of Th2 Cells: Implications of Early HIV Treatment Initiation and Care. *Life*. 2024;(**14**):104. Doi: 10.3390/life14010104

20. Wang WK, Chen MY, Chuang CY, Jeang KT, Huang LM. Molecular biology of human immunodeficiency virus type 1. *Journal of Microbiology, Immunology and Infection*;(33):131–40.

21. Freed EO. HIV-1 replication. *Somatic Cell and Molecular Genetics*. 2001;(**26**):13-33. Doi: https://doi.org/10.1023/A:1021070512287

22. Kirchhoff F. HIV Life Cycle: Overview. *Springer New York*; 2013. p. 1–9. Doi: 10.1007/978-1-4614-9610-6_60-1

23. Vandormael A, De Oliveira T, Tanser F, Bärnighausen T, Herbeck JT. High percentage of undiagnosed HIV cases within a hyperendemic South African community: a population-based study. *Journal of Epidemiology and Community Health*. 2018;(**72**):168–72. Doi: 10.1136/jech-2017-209713

24. Zuma K, Simbayi L, Zungu N, Moyo S, Marinda E, Jooste S, et al. The HIV Epidemic in South Africa: Key Findings from 2017 National Population-Based Survey. *International Journal of Environmental Research and Public Health*. 2022;(**19**):8125. Doi: 10.3390/ijerph19138125

25. Bystryak S, Acharya C. Detection of HIV-1 p24 antigen in patients with varying degrees of viremia using an ELISA with a photochemical signal amplification system. *Clinica Chimica Acta*. 2016;(**456**):128–36. Doi: 10.1016/j.cca.2016.02.022

26. Johnson C, Baggaley R, Forsythe S, van Rooyen H, Ford N, Napierala Mavedzenge S, et al. Realizing the Potential for HIV Self-Testing. *AIDS and Behavior*. 2014;(**18**):391–5. Doi: 10.1007/s10461-014-0832-x

27. Witzel TC, Rodger AJ. New initiatives to develop self-testing for HIV. *Current Opinion in Infectious Disease*. 2017;(**30**):50. Doi: 10.1097/QCO.0000000000000336

28. Figueroa C, Johnson C, Verster A, Baggaley R. Attitudes and Acceptability on HIV Self-testing Among Key Populations: A Literature Review. *AIDS and Behavior*. 2015;(19):1949–65. Doi: 10.1007/s10461-015-1097-8

29. Lippman SA, Périssé ARS, Veloso VG, Sullivan PS, Buchbinder S, Sineath RC, et al. Acceptability of self-conducted home-based HIV testing among men who have sex with men in Brazil: data from an on-line survey. *Cadernos de Saúde Pública*. 2014;(**30**):724–34. Doi: 10.1590/0102-311x00008913

30. Lippman SA, Moran L, Sevelius J, Castillo LS, Ventura A, Treves-Kagan S, et al. Acceptability and Feasibility of HIV Self-Testing Among Transgender Women in San Francisco: A Mixed Methods Pilot Study. *AIDS and Behavior*. 2016;(**20**):928–38. Doi: https://doi.org/10.1007/s10461-015-1236-2

31. Mhango M, Chitungo I, Dzinamarira T. COVID-19 lockdowns: impact on facility-based HIV testing and the case for the scaling up of home-based testing services in sub-Saharan Africa. *AIDS and Behavior*. 2020;(**24**):3014–6. Doi: 10.1007/s10461-020-02939-6

32. Dovel K, Shaba F, Offorjebe OA, Balakasi K, Nyirenda M, Phiri K, et al. Effect of facility- based HIV self-testing on uptake of testing among outpatients in Malawi: a cluster-randomised trial. *Lancet Global Health*. 2020;(**8**):e276–87. Doi: 10.1016/S2214-109X(19)30534-0

33. Bhatt B, Jindal H, Sk S, Malik JS, Sangwan K, Resident J. Vaccination in HIV positive adults: Need to address. *Human Vaccines and Immunotherapeutic*. 2014;(**10**):3011–2. Doi: 10.4161/21645515.2014.971645

34. UNAIDS data 2020 [Internet]. [cited 2023 Jan 31]. Available from: https://www.unaids.org/en/resources/documents/2020/unaids-data

35. Paterson D, Swindells S, Mohr J, Brester M, Vergis E, Squier C, et al. Adherence to protease inhibitor therapy and outcomes in patients with HIV infection. *Annals of internal medicine*. 2000;(**133**):21-30. Doi: 10.7326/0003-4819-133-1-200007040-00025

36. Chesney MA. Factors Affecting Adherence to Antiretroviral Therapy. *Clinical Infectious Diseases*. 2000;(**30**): 171–176. Doi: 10.1086/313849.

37. Barillari G. The Anti-Angiogenic Effects of Anti-Human Immunodeficiency Virus Drugs. *Frontiers in Oncology*. 2020;(**10**):806. Doi: 10.3389/fonc.2020.00806

38. Prozorov AA, Danilenko VN. *Mycobacteria* of the tuberculosis complex: Genomics, molecular epidemiology, and evolution trends. *Biology Bulletin Review*. 2011;(**1**):483–495. Doi: 10.1134/S2079086411060065

39. Bai RJ, Dai LL, Wu H. Advances and challenges in antiretroviral therapy for acquired immunodeficiency syndrome. *Chinese Medical Journal*. 2020;(**133**):2775–7. Doi: 10.1097/CM9.0000000000001226

40. Bailon L, Mothe B, Berman L, Brander C. Novel Approaches Towards a Functional Cure of HIV/AIDS. *Drugs*. 2020;(**80**):859–868. Doi: 10.1007/s40265-020-01322-y

41. Shan L, Deng K, Shroff NS, Durand CM, Rabi SAlireza, Yang HC, et al. Stimulation of HIV-1- Specific Cytolytic T Lymphocytes Facilitates Elimination of Latent Viral Reservoir after Virus Reactivation. *Immunity*. 2012 ;(**36**):491–501. Doi: 10.1016/j.immuni.2012.01.014

42. Deeks SG. Shock and kill. *Nature*. 2012;(**487**):439–440. Doi: 10.1038/487439a

43. Vargas B, Sluis-Cremer N. Toward a Functional Cure for HIV-1 Infection: The Block and Lock Therapeutic Approach. *Frontiers in Virology*. 2022;(**2**):917941. Doi: https://doi.org/10.3389/fviro.2022.917941

44. Darcis G, Van Driessche B, Van Lint C. Preclinical shock strategies to reactivate latent HIV-1: *an update*. *Current Opinions in HIV AIDS*. 2016;(**11**):388–93. Doi: 10.1097/COH.0000000000000288

45. Hütter G, Nowak D, Mossner M, Ganepola S, Müßig A, Allers K, et al. Long-Term Control of HIV by CCR5 Delta32/Delta32 Stem-Cell Transplantation. *The New England Journal of Medine*. 2009;(**360**):692–698. Doi: 10.1056/NEJMoa0802905

46. Gupta RK, Peppa D, Hill AL, Gálvez C, Salgado M, Pace M, et al. Evidence for HIV-1 cure after CCR5Δ32/Δ32 allogeneic haemopoietic stem-cell transplantation 30 months post analytical treatment interruption: a case report. *The Lancet HIV*. 2020;(**7**):340–347. Doi: 10.1016/S2352-3018(20)30069-2

47. Arnold C. Molecular evolution of *Mycobacterium tuberculosis*. *Clinical Microbiology and Infection*. 2007;(**13**):120–128. Doi: 10.1111/j.1469-0691.2006.01637.x

48. Jordi V, Gary P. Evolution of microbial pathogens. *Clinical Infectious Diseases*. 2007;(**44**):313- 314. Doi: 10.1086/508881.

49. Brosch R, Gordon SV, Marmiesse M, Brodin P, Buchrieser C, Eiglmeier K, et al. A new evolutionary scenario for the *Mycobacterium tuberculosis* complex. *Proceedings of the National Academy of Sciences of the United States of America*. 2002;(**99**):3684–3689. Doi: 10.1073/pnas.052548299

50. Carroll KC, Hobden JA, Miller S, Morse SA, Mietzner TA, Detrick B, et al. In: Jawetz, Melnick, & Adelberg's Medical Microbiology, 27e [Internet]. New York, NY: McGraw-Hill Education; 2019 [cited 2024 May 4]. Available from: accessmedicine.mhmedical.com/content.aspx?aid=1114731852

51. Farnia P, Farnia P, Ghanavi J, Zhavnerko G, Poleschuyk N, Velayati A. A review on the shape changes in pathogenic bacteria with emphasis on *Mycobacterium tuberculosis*. *Biomedical and Biotechnology Research Journal*. 2018;(**2**):242. Doi: 10.4103/bbrj.bbrj_86_18

52. Velayati AA, Farnia P. Diversity in Cell Shape of *Mycobacterium tuberculosis*. In: Atlas of *Myobacterium Tuberculosis* [Internet]. Elsevier; 2017 [cited 2024 May 4]. p. 71–99. Available from: https://linkinghub.elsevier.com/retrieve/pii/B9780128038086000037

53. Turner RD, Chiu C, Churchyard GJ, Esmail H, Lewinsohn DM, Gandhi NR, et al. Tuberculosis Infectiousness and Host Susceptibility. *Journal of Infectious Diseases*. 2017; (**216**):636–643. Doi: 10.1093/infdis/jix361

54. Bhunia SK, Sarkar M, Banerjee A, Giri B. An update on pathogenesis and management of tuberculosis with special reference to drug resistance. *Asian Pacific Journal of Tropical Disease*. 2015;(**5**):673–86. Doi: 10.1016/S2222-1808(15)60912-4

55. Maertzdorf J, Tönnies M, Lozza L, Schommer-Leitner S, Mollenkopf H, Bauer TT, et al. *Mycobacterium tuberculosis* Invasion of the Human Lung: First Contact. *Frontiers in Immunology*. 2018;(**9**):1346. Doi: 10.3389/fimmu.2018.01346

56. Pisu D, Huang L, Grenier JK, Russell DG. Dual RNA-Seq of *Mtb*-Infected Macrophages *In Vivo* Reveals Ontologically Distinct Host-Pathogen Interactions. *Cell Reports*. 2020;(**30**):335-350. Doi: 10.1016/j.celrep.2019.12.033

57. Silwal P, Paik S, Kim JK, Yoshimori T, Jo EK. Regulatory Mechanisms of Autophagy-Targeted Antimicrobial Therapeutics Against *Mycobacterial* Infection. *Frontiers in Cellular and Infection Microbiology*. 2021;(**11**):633360. Doi: 10.3389/fcimb.2021.633360

58. Zulauf KE, Sullivan JT, Braunstein M. The SecA2 pathway of Mycobacterium tuberculosis exports effectors that work in concert to arrest phagosome and autophagosome maturation. *PLOS Pathogens*.2018;(**14**):e1007011. Doi: https://doi.org/10.1371/journal.ppat.1007011

59. Chai Q, Wang L, Liu CH, Ge B. New insights into the evasion of host innate immunity by *Mycobacterium tuberculosis*. *Cellular and Molecular Immunology*. 2020;(**17**):901–13. Doi: 10.1038/s41423-020-0502-z

60. Yan W, Zheng Y, Dou C, Zhang G, Arnaout T, Cheng W. The pathogenic mechanism of *Mycobacterium tuberculosis*: implication for new drug development. *Molecular Biomedicine*. 2022;(**3**):48. Doi: 10.1186/s43556-022-00106-y

61. Kolloli A, Singh P, Subbian S. Granulomatous Response to *Mycobacterium tuberculosis* Infection. Understanding the Host Immune Response Against *Mycobacterium tuberculosis* Infection. *Frontiers in Pediatrics*. 2019;(**7**):350. Doi: 10.3389/fped.2019.00350

62. Salgame P. MMPs in tuberculosis: granuloma creators and tissue destroyers. *Journal of Clinical Investigation*. 2011;(**121**):1686–8. Doi: 10.1172/JCI57423

63. World Health Organization. Global tuberculosis report 2013. World Health Organization; 2013.

64. Fellay J, Shianna KV, Ge D, Colombo S, Ledergerber B, Weale M, et al. A Whole-Genome Association Study of Major Determinants for Host Control of HIV-1. *Science*. 2007;(**317**):944-947.Doi: 10.1126/science.1143767

65. Fellay J, Ge D, Shianna KV, Colombo S, Ledergerber B, Cirulli ET, et al. Common Genetic Variation and the Control of HIV-1 in Humans. *Plos Genetics*. 2009;(**5**):e1000791. Doi: 10.1371/journal.pgen.1000791

66. Pelak K, Goldstein DB, Walley NM, Fellay J, Ge D, Shianna KV, et al. Host Determinants of HIV- 1 Control in African Americans. *Journal of Infectious Diseases*. 2010;(**201**):1141–1149. Doi: 10.1086/651382

67. Catano G, Kulkarni H, He W, Marconi VC, Agan BK, Landrum M, et al. HIV-1 Disease-Influencing Effects Associated with ZNRD1, HCP5 and HLA-C Alleles Are Attributable Mainly to Either HLA-A10 or HLA-B*57 Alleles. *Plos One*. 2008;(**3**):e3636. Doi: 10.1371/journal.pone.0003636

68. Questions and Answers About Tuberculosis | TB | CDC [Internet]. 2023 [cited 2024 May 9]. Available from: https://www.cdc.gov/tb/publications/faqs/tb-qa.htm

69. Lu C, Wu J, Wang H, Wang S, Diao N, Wang F, et al. Novel Biomarkers Distinguishing Active Tuberculosis from Latent Infection Identified by Gene Expression Profile of Peripheral Blood Mononuclear Cells. *PLoS ONE*. 2011;(**6**):e24290. Doi 10.1371/journal.pone.0024290

70. Wu B, Huang C, Kato-Maeda M, Hopewell PC, Daley CL, Krensky AM, et al. Messenger RNA Expression of IL-8, FOXP3, and IL-12β Differentiates Latent Tuberculosis Infection from Disease. *Journal of Immunology*. 2007;(**178**):3688–94. Doi: 10.4049/jimmunol.178.6.3688

71. Lee SW, Wu LSH, Huang GM, Huang KY, Lee TY, Weng JTY. Gene expression profiling identifies candidate biomarkers for active and latent tuberculosis. *BMC Bioinformatics*. 2016;(**17**):S3: Doi: 10.1186/s12859-015-0848-x

72. Lucya V. Prevention of Tuberculosis: Literature Review. *KnE Life Sci*. 2021;630–4. Doi: 10.18502/kls. v6i1.8663

73. Abubakar I, Pimpin L, Ariti C, Beynon R, Mangtani P, Sterne JAC, et al. Systematic review and meta-analysis of the current evidence on the duration of protection by Bacillus Calmette-Guérin vaccination against tuberculosis. *Health Technology Assessment*. 2013(**17**). Doi: http://dx.doi.org/10.3310/hta17370 1–vi

74. Mangtani P, Nguipdop-Djomo P, Keogh RH, Trinder L, Smith PG, Fine PE, et al. Observational study to estimate the changes in the effectiveness of Bacillus Calmette-Guérin (BCG) vaccination with time since vaccination for preventing tuberculosis in the UK. *Health Technology Assessment.* 2017; (**21**):1–54, Doi: http://dx.doi. org/10.3310/hta21390.

75. Tanner R, Villarreal-Ramos B, Vordermeier HM, McShane H. The Humoral Immune Response to BCG Vaccination. *Frontiers in Immunology*. 2019;(**10**):1317. Doi: 10.3389/fimmu.2019.01317

76. Moetemed MS, ALakkad A, Abdalla HA. Evaluating the effectiveness of first-Line anti-tuberculosis in Al Dhafra Hospitals. *Journal of Drug Delivery and Therapeutics*. 2023;(**13**):91–5. Doi: https://doi.org/10.22270/jddt.v13i8.5939

77. Wei-jie Z. Study the Interactions of Second or Third Line Anti-tuberculosis Drugs *in Vitro*. *China Pharm* [Internet]. 2012 [cited 2024 May 1]; Available from: https://www.semanticscholar.org/paper/Study-the-Interactions-of-Second-or-Third-Line-in-Wei-jie/d7dfaf83e1d6c70445b4a8f6646534964d250615

78. Nguyen TVA, Cao TBT, Akkerman OW, Tiberi S, Vu DH, Alffenaar JWC. Bedaquiline as part of combination therapy in adults with pulmonary multi-drug resistant tuberculosis. *ExpertReview of Clinical Pharmacology*.2016;(**9**):1025–37. Doi: 10.1080/17512433.2016.1200462

79. Heyckendorf J, Olaru ID, Ruhwald M, Lange C. Getting Personal Perspectives on Individualized Treatment Duration in Multidrug-Resistant and Extensively Drug-Resistant Tuberculosis. *American Journal of Respiratory and Critical Care Medicine*. 2014;(**190**):374-83. Doi: 10.1164/rccm.201402-0363PP

80. Hiruy H, Rogers Z, Mbowane C, Adamson J, Ngotho L, Karim F, et al. Subtherapeutic concentrations of first-line anti-TB drugs in South African children treated according to current guidelines: the PHATISA study. *Journal of Antimicrobial Chemotherapy*. 2015;(**70**):1115–23. Doi: 10.1093/jac/dku478

81. Marimani M, Ahmad A, Duse A. The role of epigenetics, bacterial and host factors in progression of *Mycobacterium tuberculosis* infection. *Tuberculosis*. 2018;(**113**):200–214. Doi: 0.1016/j.tube.2018.10.009

82. Caminero JA, Sotgiu G, Zumla A, Migliori GB. Best drug treatment for multidrug-resistant and extensively drug-resistant tuberculosis. *Lancet Infectious Diseases*. 2010;(**10**):621–9. Doi: 10.1016/S1473-3099(10)70139-0

83. Novikov VE, Usacheva NE, Myakisheva TV. Modern approaches to pharmacotherapy of tuberculosis infection in children. *Research Results in Pharmacology*. 2021;(**7**):47–53. Doi: 10.3897/rrpharmacology.7.66627

84. Prasad R, Singh A, Gupta N. Adverse drug reactions in tuberculosis and management. *Indian Journal of Tuberculosis*. 2019;(**66**):520–532. Doi: 10.1016/j.ijtb.2019.11.005

85. Kraemer JD, Cabrera OA, Singh JA, Depp TB, Gostin LO. Public health measures to control tuberculosis in low-income countries: ethics and human rights considerations. International. *Journal of Tuberculosis and Lung Disease*. 2011;(**15**):19–24. Doi: 10.5588/ijtld.10.0412

86. Martinez-Martinez YB, Huante MB, Files M, Gelman BB, Endsley M, Endsley JJ. HIV compromises Th17 and Th22 immunity in a humanized mouse model of Tuberculosis and HIV co-infection. *Journal of Immunology*. 2022 ;(**208**):16-58. Doi: 10.4049/jimmunol.208.Supp.58.16

87. Pooranagangadevi N, Padmapriyadarsini C. Treatment of Tuberculosis and the Drug Interactions Associated With HIV-TB Co-Infection Treatment. *Frontiers in Tropical Diseases*. 2022;(**3**):834013. Doi: https://doi.org/10.3389/fitd.2022.834013

88. Leite DI, De Castro Bazan Moura S, Da Conceição Avelino Dias M, Costa CCP, Machado GP, Pimentel LCF, et al. A Review of the Development of Multitarget Molecules against HIV-TBcoinfection pathogens. *Molecules*. 2023;(**28**):3342. Doi: https://doi.org/10.3390/molecules28083342

89. Wodelo W, Wampande E, Andama A, Kateete D, Ssekatawa K. Polymorphisms in Immune Genes and Their Association with Tuberculosis Susceptibility: An Analysis of the African Population. *Application of Clinical Genetics*. 2024; (**17**):33–46. Doi: 10.2147/TACG.S457395

90. de Sá NBR, Ribeiro-Alves M, da Silva TP, Pilotto JH, Rolla VC, Giacoia-Gripp CBW, et al. Clinical and genetic markers associated with tuberculosis, HIV-1 infection, and TB/HIV-immune reconstitution inflammatory syndrome outcomes. *BMC Infectious Diseases*. 2020;(**20**):59. Doi: 10.1186/s12879-020-4786-5

91. Thami PK, Choga W, Mulisa DD, Dandara C, Shevchenko AK, Leteane MM, et al. Whole Genome Rare-Variant Association Study of HIV-1 Progression in a Southern African Population. *medRxiv*; 2020 [cited 2024 May 12]. p. 2020.12.16.20248307. Available from: https://www.medrxiv.org/content/10.1101/2020.12.16.20248307v1

92. Kaur G, Mehra N. Genetic determinants of HIV-1 infection and progression to AIDS: susceptibility to HIV infection. *Tissue Antigens*. 2009;(**73**):289–301. Doi:

https://doi.org/10.1111/j.1399-0039.2009.01220.x

93. Compaore TR, Ouattara AK, Baguiya A, Traore L, Zoure AA, Ouedraogo HG, et al. APOBEC3G Role on HIV Infection in Africa: A Systematic Review. *American Journal of Molecular Biology*. 2024;(**14**):25–42. Doi: 10.4236/ajmb.2024.141003

94. Kamba K, Nagata T, Katahira M. Catalytic Analysis of APOBEC3G Involving Real-Time NMR Spectroscopy Reveals Nucleic Acid Determinants for Deamination. Menéndez-Arias L. *PLOS ONE*. 2015;(**10**):e0124142. Doi: https://doi.org/10.1371/journal.pone.0124142

95. Mabaso M, Maseko G, Sewpaul R, Naidoo I, Jooste S, Takatshana S, et al. Trends and correlates of HIV prevalence among adolescents in South Africa: evidence from the 2008, 2012 and 2017 South African National HIV Prevalence, Incidence and Behaviour surveys. *AIDS Research and Therapy*. 2021;(**18**):97. Doi: https://doi.org/10.1186/s12981-021-00422-3

96. Worku MG, Teshale AB, Tesema GA. Prevalence and associated factors of HIV testing among young (15–24) women in eastern Africa: a multilevel analysis of demographic health survey data (2008-2018). *Archives of Public Health*. 2022;(**80**):117. Doi: https://doi.org/10.1186/s13690-022-00879-2

97. Rossi D. SAMHD1: a new gene for CLL. *Blood*. 2014;(**123**):951–2. Doi: https://doi.org/10.1182/blood-2013-12-545384

98. Liberatore RA, Bieniasz PD. Tetherin is a key effector of the antiretroviral activity of type I interferon in vitro and in vivo. *Proceedings of the National Academy of Sciences of the United States of America*. 2011;(**108**): Doi: https://doi.org/10.1073/pnas.1113694108

99. Lawn SD, Harries AD, Williams BG, Chaisson RE, Losina E, De Cock KM, et al. Antiretroviral therapy and the control of HIV-associated tuberculosis. Will ART do it? *International Journal of Tuberculosis and Lung Disease*. 2011;(**15**):571–81. Doi: 10.5588/ijtld.10.0483.

100. Kanwal R, Gupta K, Gupta S. Cancer Epigenetics: An Introduction. *Methods in Molecular Biology*.2015;(**1238**):3-25. Doi: 10.1007/978-1-4939-1804-1_1

101. Chaturvedi P, Tyagi SC. Epigenetic mechanisms underlying cardiac degeneration and regeneration. *International Journal of Cardiology*. 2014;(**173**):1–11. Doi: https://doi.org/10.1016/j.ijcard.2014.02.008

102. Marimani M, Ahmad A, Stacey S, Duse A. Examining the levels of acetylation, DNA methylation and phosphorylation in HIV-1 positive and multidrug-resistant TB-HIV patients. *Journal of Global Antimicrobial Resistance*. 2020;(**23**):232–242. Doi: https://doi.org/10.1016/j.jgar.2020.09.023

103. Venkatesh I, Makky K. Teaching epigenetic regulation of gene expression is critical in 21st-century science education: Key concepts & teaching strategies. *The American Biology Teacher*. 2020;82(**6**):372–80. Doi: https://doi.org/10.1525/abt.2020.82.6.372

104. Wang Z, Zang C, Cui K, Schones DE, Barski A, Peng W, et al. Genome-wide mapping of HATs and HDACs reveals distinct functions in active and inactive genes. *Cell*. 2009;(**138**):1019–138. Doi: 10.1016/j.cell.2009.06.049

105. Cell Signaling Technology [Internet]. [cited 2023 Oct 9]. Epigenetic Writers and Erasers of Histone H3. Available from: https://www.cellsignal.com/pathways/epigenetic-histone-h3-pathway

106. González-Ramírez M, Ballaré C, Mugianesi F, Beringer M, Santanach A, Blanco E, et al. Differential contribution to gene expression prediction of histone modifications at enhancers or promoters. Zang C. *PLoS Computational Biology*. 2021;(**17**):e1009368. Doi: https://doi.org/10.1371/journal.pcbi.1009368

107. Chang A, Liu L, Ashby JM, Wu D, Chen Y, O'Neill SS, et al. Data from Recruitment of KMT2C/MLL3 to DNA Damage Sites Mediates DNA Damage Responses and Regulates PARP Inhibitor Sensitivity in Cancer [Internet]. *American Association for Cancer Research*. 2023 [cited 2024 Jun 8]. Available from: https://aacr.figshare.com/collections/Data_from_Recruitment_of_KMT2C_MLL3_to_DNA_Damage_Sites_Mediates_DNA_Damage_Responses_and_Regulates_PARP_Inhibitor_Sensitivity_in_Cancer/6513634/1

108. Cocozza S, Akhtar MostM, Miele G, Monticelli A. CpG Islands Undermethylation in Human Genomic Regions under Selective Pressure. Toland AE, *PLoS ONE*. 2011;(**6**):e23156. Doi: https://doi.org/10.1371/journal.pone.0023156

109. Rossetto D, Avvakumov N, Côté J. Histone phosphorylation: A chromatin modification involved in diverse nuclear events. *Epigenetics*. 2012;(**7**):1098–108. Doi: https://doi.org/10.4161/epi.21975

110. Soloaga A, Thomson S, Wiggin GR, Rampersaud N, Dyson MH, Hazzalin CA, et al. MSK2 and MSK1 mediate the mitogen-and stress-induced phosphorylation of histone H3 and HMG-14. *Semi-monthly peer-reviewed scientific journal*. 2003;(**22**):2788–2797. Doi: https://doi.org/10.1093/emboj/cdg273

111. Hazzalin CA, Mahadevan LC. MAPK-regulated transcription: a continuously variable gene switch? *Nature Review Molecular Cell Biology*. 2002;(**3**):30–40. Doi: 10.1038/nrm715

112. White TE, Brandariz-Nuñez A, Valle-Casuso JC, Amie S, Nguyen LA, Kim B, et al. The Retroviral Restriction Ability of SAMHD1, but Not Its Deoxynucleotide Triphosphohydrolase Activity, Is Regulated by Phosphorylation. *Cell Host and Microbe.* 2013;(**13**):441–451. Doi: 10.1016/j.chom.2013.03.005

113. Bach H, Papavinasasundaram KG, Wong D, Hmama Z, Av-Gay Y. Mycobacterium tuberculosis Virulence Is Mediated by PtpA Dephosphorylation of Human Vacuolar Protein Sorting 33B. *Cell Host and Microbe*. 2008;(**3**):316–322. Doi: 10.1016/j.chom.2008.03.008

114. Lochab S, Singh Y, Sengupta S, Nandicoori VK. Mycobacterium tuberculosis exploits host ATM kinase for survival advantage through SecA2 secretome. *eLife*. 2020;(**9**):e51466. Doi: 10.7554/eLife.51466

115. Muthumani K, Wadsworth SA, Dayes NS, Hwang DS, Choo AY, Abeysinghe HR, et al. Suppression of HIV-1 viral replication and cellular pathogenesis by a novel p38/JNK kinase inhibitor. *AIDS.* 2004;(**18**):739-748. Doi: 10.1097/00002030-200403260-00004

116. Furler RL, Uittenbogaart CH. Signaling through the P38 and ERK pathways: a common link between HIV replication and the immune response. *Immunology Research*. 2010;(**48**):99–109. Doi: 10.1007/s12026-010-8170-1

117. León Machado JA, Steimle V. The MHC Class II Transactivator CIITA: Not (Quite) the Odd-One-Out Anymore among NLR Proteins. *International Journal of Molecular Sciences.* 2021;(**22**):1074. Doi: 10.3390/ijms22031074

118. Obiri-Yeboah D, Pappoe F, Baidoo I, Arthur F, Hayfron-Benjamin A, Essien-Baidoo S, et al. Immunologic and virological response to ART among HIV infected individuals at a tertiary hospital in Ghana. *BMC Infectious Diseases*. 2018;(**18**):230. Doi: 10.1186/s12879-018-3142-5

119. Sinha P, Srivastava GN, Tripathi R, Mishra MN, Anupurba S. Detection of mutations in the rpoB gene of rifampicin-resistant *Mycobacterium tuberculosis* strains inhibiting wild type probe hybridization in the MTBDR plus assay by DNA sequencing directly from clinical specimens. *BMC Microbiology*. 2020;(**20**):284. Doi:10.1186/s12866-020-01967-5

120. Mikovits JA, Young HA, Vertino P, Issa JPJ, Pitha PM, Turcoski-Corrales S, et al. Infection with Human Immunodeficiency Virus Type 1 Upregulates DNA Methyltransferase, Resulting in *De Novo* Methylation of the Gamma Interferon (IFN-γ) Promoter and Subsequent Downregulation of IFN-γ Production. *Molecular and Cellular Biology.* 1998;(**18**):5166–5177. Doi: 10.1128/mcb.18.9.5166

121. Qin W, Scicluna BP, Van Der Poll T. The Role of Host Cell DNA Methylation in the Immune Response to Bacterial Infection. *Frontiers in Immunology*. 2021;(**12**):696280. Doi:10.3389/fimmu.2021.696280

122. DiNardo AR, Rajapakshe K, Nishiguchi T, Grimm SL, Mtetwa G, Dlamini Q, et al. DNA hypermethylation during tuberculosis dampens host immune responsiveness. *Journal of Clinical Investigation*. 2020;(**130**):3113–3123. Doi: 10.1172/JCI134622

123. Maricato JT, Furtado MN, Takenaka MC, Nunes ERM, Fincatti P, Meliso FM, et al. Epigenetic Modulations in Activated Cells Early after HIV-1 Infection and their Possible Functional Consequences. *Plos One*. 2015;(**10**):e0119234. Doi: 10.1371/journal.pone.0119234

124. Espíndola MS, Soares LS, Galvão-Lima LJ, Zambuzi FA, Cacemiro MC, Brauer VS, et al. Epigenetic alterations are associated with monocyte immune dysfunctions in HIV-1 infection. *Scientific Reports*. 2018; (**8**):5505. Doi: 10.1038/s41598-018-23841-1

125. Porter KA, Kelley LN, Nekorchuk MD, Jones JH, Hahn AB, De Noronha CMC, et al.

CIITA Enhances HIV-1 Attachment to $CD4^+$ T Cells leading to Enhanced Infection and Cell Depletion. *Journal of Immunology*. 2010;(**185**):6480–6488. Doi: 10.4049/jimmunol.1000830

126. Porter KA, Kelley LN, George A, Harton JA, Duus KM. Class II Transactivator (CIITA) Enhances Cytoplasmic Processing of HIV-1 Pr55Gag. *Plos One*. 2010;(**5**):e11304. Doi: 10.1371/journal.pone.0011304

127. Pagans S, Kauder SE, Kaehlcke K, Sakane N, Schroeder S, Dormeyer W, et al. The Cellular Lysine Methyltransferase Set7/9-KMT7 Binds HIV-1 TAR RNA, Monomethylates the Viral Transactivator Tat, and Enhances HIV Transcription. *Cell Host and Microbe*. 2010;(**7**):234–244. Doi: 10.1016/j.chom.2010.02.005

128. Thuy LHA, Thuan LD, Phuong TK. DNA Hypermethylation in Breast Cancer. In: Pham PV, editor. Breast Cancer - From Biology to Medicine [Internet]. InTech; 2017 [cited 2024 May 16]. Available from: http://www.intechopen.com/books/breast-cancer-from-biology-to-medicine/dna-hypermethylation-in-breast-cancer

129. Shin JE, Cho Y. Epigenetic regulation of axon regeneration after neural injury. *Molecules and Cells*. 2017;(**40**):10-16. Doi: 10.14348/molcells.2017.2311

130. Gaspar-Maia A, Alajem A, Polesso F, Sridharan R, Mason MJ, Heidersbach A, et al. Chd1 regulates open chromatin and pluripotency of embryonic stem cells. *Nature*. 2009;(**460**):863–868. Doi: 10.1038/nature08212

131. Mo A, Mukamel EA, Davis FP, Luo C, Henry GL, Picard S, et al. Epigenomic signatures of neuronal diversity in the mammalian brain. *Neuron*. 2015;(**86**):1369–1384. Doi: 10.1016/j.neuron.2015.05.018

132. Khare SP, Habib F, Sharma R, Gadewal N, Gupta S, Galande S. Histome--a relational knowledgebase of human histone proteins and histone modifying enzymes. *Nucleic Acids Research*. 2012;(**40**):337-42. Doi: 10.1093/nar/gkr1125

133. Zhou X, Chen H, Li J, Shi Y, Zhuang S, Liu N. The Role and Mechanism of Lysine Methyltransferase and Arginine Methyltransferase in Kidney Diseases. *Frontier in Pharmacology*. 2022;(**13**). Doi: 10.3389/fphar.2022.885527

134. Wood K, Tellier M, Murphy S. DOT1L and H3K79 Methylation in Transcription and Genomic Stability. *Biomolecules.* 2018;(**8**):11. Doi: 10.3390/biom8010011

135. Buitrago D, Labrador M, Arcon JP, Lema R, Flores O, Esteve-Codina A, *et al*. Impact of DNA methylation on 3D genome structure. *Nature Communications*. 2021;(**12**):3243. Doi: 10.1038/s41467- 021-23142-8

136. Jiang C, Pugh BF. Nucleosome positioning and gene regulation: advances through genomics. *Nature Reviews Genetics*. 2009;(**10**):161–172. Doi: 10.1038/nrg2522

137. Kulis M, Queirós AC, Beekman R, Martín-Subero JI. Intragenic DNA methylation in transcriptional regulation, normal differentiation and cancer. *Elsevier*. 2013;(**1829**):1161–1174. Doi: 10.1016/j.bbagrm.2013.08.001

138. Suzuki MM, Bird A. DNA methylation landscapes: provocative insights from epigenomics. *Nature Reviews Genetics*. 2008;(**9**):465–476. Doi: 10.1038/nrg2341

139. Thompson PJ, Macfarlan TS, Lorincz MC. Long Terminal Repeats: From Parasitic Elements to Building Blocks of the Transcriptional Regulatory Repertoire. *Molecular Cell*. 2016;(**62**):766–776. Doi: 10.1016/j.molcel.2016.03.029

140. Jones PA. Functions of DNA methylation: islands, start sites, gene bodies and beyond. *Nature Reviews Genetics*. 2012;(**13**):484–492. Doi: 10.1038/nrg3230

141. Stein CM, Benchek P, Bartlett J, Igo RP, Sobota RS, Chervenak K, *et al*. Methylome-wide analysis reveals epigenetic marks associated with resistance to tuberculosis in HIV-infected individuals from East Africa. *Infectious Diseases*.2021;(**224**):695-704. Doi: 10.1093/infdis/jiaa785

142. Fang JY, Mikovits JA, Bagni R, Petrow-Sadowski CL, Ruscetti FW. Infection of Lymphoid Cells by Integration-Defective Human Immunodeficiency Virus Type 1 Increases *De Novo* Methylation. *Journal of Virology*. 2001;(**75**):9753–61. Doi: 10.1128/JVI.75.20.9753-9761.2001

143. Chen YC, Hsiao CC, Chen CJ, Chao TY, Leung SY, Liu SF, *et al.* Aberrant Toll-like receptor 2 promoter methylation in blood cells from patients with pulmonary tuberculosis. *Journal of Infection*. 2014;(**69**):546–57. Doi: 10.1016/j.jinf.2014.08.014

144. Brown JA, Amir M, Zeng MY. Chapter 9 - Epigenetic modifications and regulation in infection. In: Boosani CS, Goswami R, editors. *Epigenetics in Organ Specific Disorders* [Internet]. Academic Press; 2023. p. 181–209. Available from: https://www.sciencedirect.com/science/article/pii/B9780128239315000025

145. Williams SK, Truong D, Tyler JK. Acetylation in the globular core of histone H3 on lysine-56 promotes chromatin disassembly during transcriptional activation. *Proceedings of the National l Academy of Sciences of the United States of America*. 2008;(**105**):9000–5. Doi: 10.1073/pnas.0800057105 119

146. Karmodiya K, Krebs AR, Oulad-Abdelghani M, Kimura H, Tora L. H3K9 and H3K14 acetylation co-occur at many gene regulatory elements, while H3K14ac marks a subset of inactive inducible promoters in mouse embryonic stem cells. *BMC Genomics*. 2012(**13**):424. Doi: 10.1186/1471-2164-13-424

147. Xie W, Song C, Young NL, Sperling AS, Xu F, Sridharan R, *et al*. Histone H3 Lysine 56 Acetylation Is Linked to the Core Transcriptional Network in Human Embryonic Stem Cells. *Molecular Cell*. 2009**(33**):417–27. Doi: 10.1016/j.molcel.2009.02.004

148. Ziehl-Neelsen Technique-AFB Staining. Microbe Online [Internet].Available from: https://microbeonline.com/ziehl-neelsen-technique-principle-procedure-reporting/

149. Mokobi F. Ziehl-Neelsen Staining- Principle and Procedure with Results [Internet]. 2022. Available from: https://microbenotes.com/ziehl-neelsen-staining/

150. Mokobi F. Ziehl-Neelsen Staining- Principle and Procedure with Results [Internet]. 2022. Available from: https://microbenotes.com/ziehl-neelsen-staining/

151. Sutthent R, Gaudart N, Chokpaibulkit K, Tanliang N, Kanoksinsombath C, Chaisilwatana P. p24 Antigen Detection Assay Modified with a Booster Step for Diagnosis and Monitoring of Human Immunodeficiency Virus Type 1 Infection. *Journal of Clinical Microbiology*. 2003;(**41**):1016–22. Doi: 10.1128/JCM.41.3.1016-1022.2003

152. Hornbeck PV. Enzyme-Linked Immunosorbent Assays. *Current Protocols in Immunology*. 2015;(**110**):211-2123. Doi: 10.1002/0471142735.im0201s110

152. Arumugam T, Ramphal U, Adimulam T, Chinniah R, Ramsuran V. Deciphering DNA Methylation in HIV Infection. *Frontiers in Immunology*. 2021;(**12**):795121. Doi: https://doi.org/10.3389/fimmu.2021.795121

153. Chen L, Zhang S, Pan X, Hu X, Zhang YH, Yuan F, et al. HIV infection alters the human epigenetic landscape. *Gene Therapy*. 2019;(1–2):29–39. Doi: 10.1038/s41434-018-0051-6

154. Rodríguez-Agustín A, Ayala-Suárez R, Díez-Fuertes F, Maleno MJ, De Villasante I, Merkel A, et al. Intracellular HIV-1 Tat regulator induces epigenetic changes in the DNA methylation landscape. *Frontiers in Immunology*. 2025;(**16**):1532692. Doi: https://doi.org/10.3389/fimmu.2025.1532692

155. Lu F, Zankharia U, Vladimirova O, Yi Y, Collman RG, Lieberman PM. Epigenetic Landscape of HIV-1 Infection in Primary Human Macrophage. Silvestri G. *Journal of Virology*. 2022;(**96**):e00162-22. Doi: 10.1128/jvi.00162-22.

156. Arumugam T, Ramphal U, Adimulam T, Chinniah R, Ramsuran V. Deciphering DNA Methylation in HIV Infection. *Frontiers in Immunology*. 2021;(**12**):795121. Doi: 10.3389/fimmu.2021.795121

157. Thomas SS, Abhinand K, Menon AM, Nair BG, Kumar GB, Arun KB, et al. Epigenetic Mechanisms Induced by *Mycobacterium tuberculosis* to Promote Its Survival in the Host. *International Journal of Molecular Science*. 2024;(**25**):11801. Doi: 10.3390/ijms252111801

158. Madden K, El Hamra R, Berton S, Felker J, Alvarez GG, Blais A, et al. *Mycobacterium tuberculosis* infection triggers epigenetic changes that are enriched in a type I IFN signature. *microLife*. 2023(**4**):uqad006. Doi: 10.1093/femsml/uqad006

159. Saghir SA, Ansari RA. *HLA* gene variations and mycotoxin toxicity: Four case reports. *Mycotoxin Research*. 2024;(**40**):159–73. Doi: 10.1007/s12550-023-00517-y

160. Sachan RSK, Mistry V, Dholaria M, Rana A, Devgon I, Ali I, et al. Overcoming Mycobacterium tuberculosis Drug Resistance: Novel Medications and Repositioning Strategies. *ACS Omega*. 2023;(**8**):32244–57. Doi: 10.1021/acsomega.3c02563

161. Thomas SS, Abhinand K, Menon AM, Nair BG, Kumar GB, Arun KB, et al. Epigenetic Mechanisms Induced by *Mycobacterium tuberculosis* to Promote Its Survival in the Host. *International Journal of Molecular Sciences*. 2024;(**25**):11801. Doi: 10.3390/ijms252111801

162. Campbell M, Yang WS, Yeh WW, Kao CH, Chang PC. Epigenetic Regulation of Kaposi's Sarcoma-Associated Herpesvirus Latency. *Frontiers in Microbiology*. 2020;(**11**):850. Doi: https://doi.org/10.3389/fmicb.2020.00850

163. Araki Y, Mimura T. Epigenetic Dysregulation in the Pathogenesis of Systemic Lupus Erythematosus. *International Journal of Molecular Sciences*. 2024; (**25**):1019. Doi: 10.3390/ijms25021019

164. BIOEDIT-sequence editing program. Available from: https://www.ii.uib.no/~xianjund/exams/Bio332/frames/bioedit_codon.htm

165. Edler D, Klein J, Antonelli A, Silvestro D. raxmlGUI 2.0: A graphical interface and toolkit for phylogenetic analyses using RAxML. Matschiner M. *Methods in Ecology and Evolution*. 2021;(**12**):373–7. Doi: https://doi.org/10.1111/2041-210X.13512

166. Letunic I, Bork P. Interactive Tree of Life (iTOL) v6: recent updates to the phylogenetic tree display and annotation tool. *Nucleic Acids Research*. 2024;(**52**):78–82. Doi: 10.1093/nar/gkae268

167. Chen L, Zhang S, Pan X, Hu X, Zhang YH, Yuan F, et al. HIV infection alters the human epigenetic landscape. *Gene Therapy*. 2019;(**26**):29–39. Doi:https://doi.org/10.1038/s41434-018-0051-6

168. Rodríguez-Agustín A, Ayala-Suárez R, Díez-Fuertes F, Maleno MJ, De Villasante I, Merkel A, et al. Intracellular HIV-1 Tat regulator induces epigenetic changes in the DNA methylation landscape. *Frontiers in Immunology*. 2025;(**16**):1532692. Doi: 10.3389/fimmu.2025.1532692

169. Lu F, Zankharia U, Vladimirova O, Yi Y, Collman RG, Lieberman PM. Epigenetic Landscape of HIV-1 Infection in Primary Human Macrophage. Silvestri G. *Journal of Virology*. 2022;(**96**):00162-22. Doi: 10.1128/jvi.00162-22

170. Kikuchi, A., Onoda, H., Yamaguchi, K. et al. Structural basis for activation of DNMT1. *Nature Communications*. (13) 2022:7130. Doi: https://doi.org/10.1038/s41467-022-34779-4

171. Kannan Y, Entwistle LJ, Pelly VS, Perez-Lloret J, Walker AW, Ley SC, et al. TPL-2 restricts Ccl24-dependent immunity to Heligmosomoides polygyrus. *PLoS Pathogens* 2017(**13**):e1006536. Doi: https://doi.org/10.1371/journal.ppat.1006536

172. Thomas SS, Abhinand K, Menon AM, Nair BG, Kumar GB, Arun KB, et al. Epigenetic Mechanisms Induced by Mycobacterium tuberculosis to Promote Its Survival in the Host. *International Journal of Molecular Sciences*. 2024;(**25**):11801. Doi: https://doi.org/10.3390/ijms252111801

173. Katrina Madden, Rayan El Hamra, Stefania Berton, Jake Felker, Gonzalo G Alvarez, Alexandre Blais, Jim Sun, Mycobacterium tuberculosis infection triggers epigenetic changes that are enriched in a type I IFN signature, *microLife*, 2023;(**4**):uqad006. Doi: https://doi.org/10.1093/femsml/uqad006

174. Saghir, S.A., Ansari, R.A. *HLA* gene variations and mycotoxin toxicity: Four case reports. *Mycotoxin Research* 2024;(**40**):159–173. https://doi.org/10.1007/s12550-023-00517-y

175. Sachan RSK, Mistry V, Dholaria M, Rana A, Devgon I, Ali I, Iqbal J, Eldin SM, Mohammad Said Al-Tawaha AR, Bawazeer S, Dutta J, Karnwal A. Overcoming Mycobacterium tuberculosis Drug Resistance: Novel Medications and Repositioning Strategies. *ACS Omega*. 2023; (**8**):32244-32257. Doi: 10.1021/acsomega.3c02563

176. Dressler, F.F., Schoenfeld, J., Revyakina, O. *et al.* Systematic evaluation and optimization of protein extraction parameters in diagnostic FFPE specimens. *Clin Proteom*. 2022(**19)**:10. https://doi.org/10.1186/s12014-022-09346-0

177. Soltis, D. E., & Soltis, P. S. Choosing an Approach and an Appropriate Gene for Phylogenetic Analysis. Molecular Systematics of Plants II: DNA Sequencing (pp. 1–42). Kluwer Academic Publishers, Massachusetts. (1998). Doi: https://doi.org/10.1007/978-1-4615-5419-6_1

178. Rickabaugh TM, Baxter RM, Sehl M, Sinsheimer JS, Hultin PM, Hultin LE, et al. Acceleration of Age-Associated Methylation Patterns in HIV-1-Infected Adults. Conneely K, editor. *PLoS ONE*. 2015;(**10**):e0119201. Doi: 10.1371/journal.pone.0119201

179. Tajuddin SM, Hernandez DG, Chen BH, Noren Hooten N, Mode NA, Nalls MA, et al. Novel age-associated DNA methylation changes and epigenetic age acceleration in middle-aged African Americans and whites. *Clinical Epigenetics*. 2019;(**11**):119. Doi: 10.1186/s13148-019-0722-1

180. Liu J, Morgan M, Hutchison K, Calhoun VD. A Study of the Influence of Sex on Genome Wide Methylation. *PLoS ONE*. 2010(**4**):e10028. https://doi.org/10.1371/journal.pone.0010028